Theme 1: AGR, Magnox and Exotic Spent Fuels

Theme Leads: Tom Scott and David Read

Universities of Bristol & Surrey

DISTINCTIVE THEMATIC MEETING
17th October, 2017
Penrith

Research Councils UK Energy For a Low Carbon Future

DISTINCTIVE

Aims and Objectives

Aim:
To provide technical underpinning of management options for the UK's AGR, Magnox and Exotic Spent Fuels

Objectives:
1. Understand evolution of Magnox and exotic SF during recovery from aqueous storage, drying and repackaging
2. Develop spectroscopic methods for improved determination of SF dissolution and corrosion rates in water.
3. Determine optimum drying conditions for AGR fuels and subsequent surface reactivity and alteration of unclad UO_2 in dry storage
4. Determine consequences of radiation damage in SF, cladding and other waste forms for safe long term storage
5. Determine suitable waste management options for spent carbide fuels

Research Councils UK Energy For a Low Carbon Future

DISTINCTIVE

Interconnected study

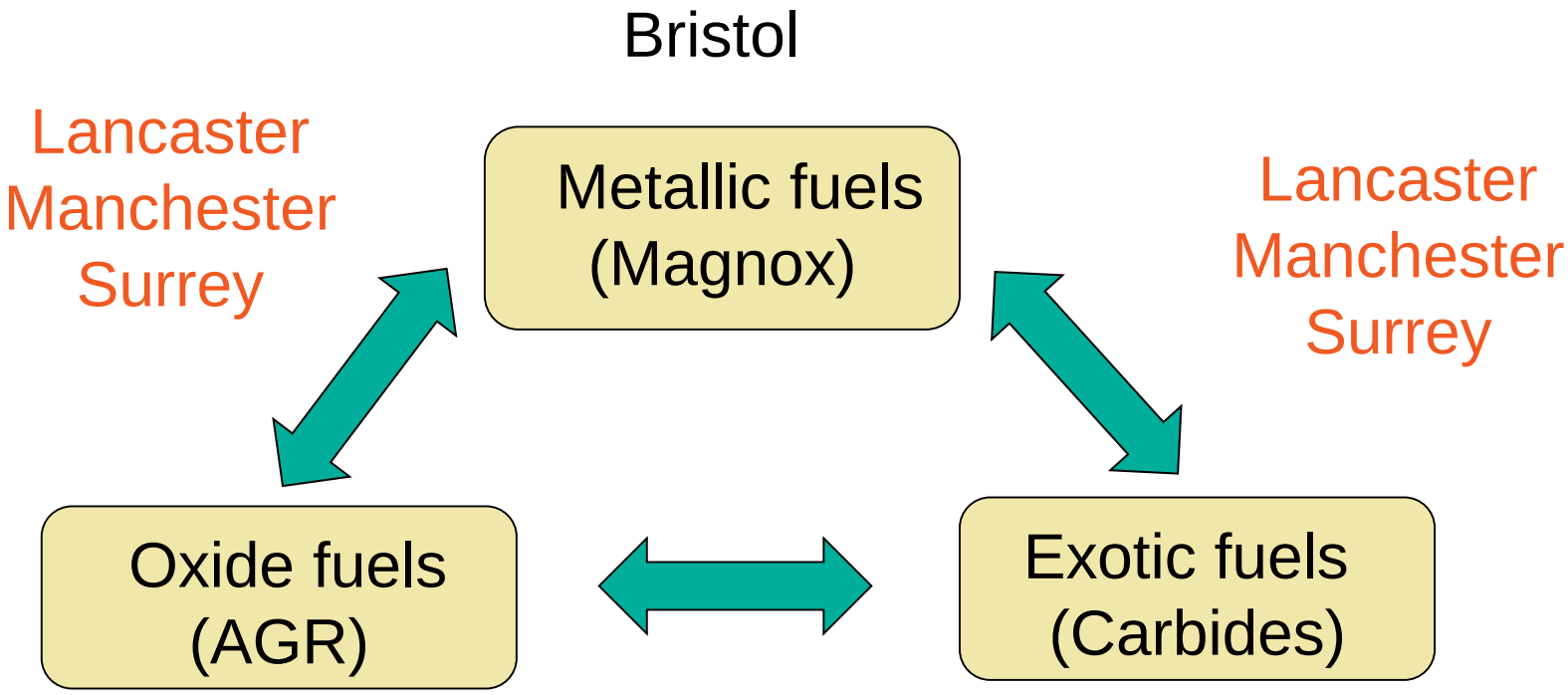

Research Councils UK Energy For a Low Carbon Future

DISTINCTIVE

Challenges

- If NDA's option is interim storage (~60y), assuming GDF in 2075
- Increasing & evolving inventory of SF
- Risks associated with long-term wet storage of AGR SF
- Also risks with transition & dry storage
- Magnox SF in Sellafield ponds needs retrieval and repackaging

Additionally

- End point is unknown
  - Timescale
  - Location
  - Design

- Important that decisions taken now don't compromise future options

Research Councils UK Energy For a Low Carbon Future

DISTINCTIVE

Beyond Distinctive

Goals of Theme 1:

- Develop mechanistic understanding of the processes affecting SF evolution

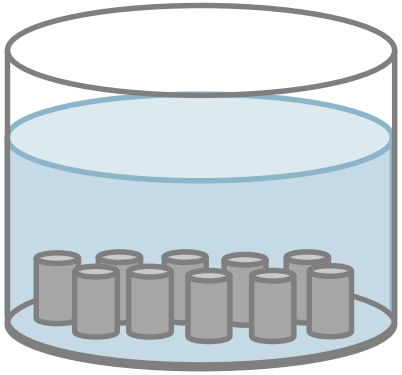

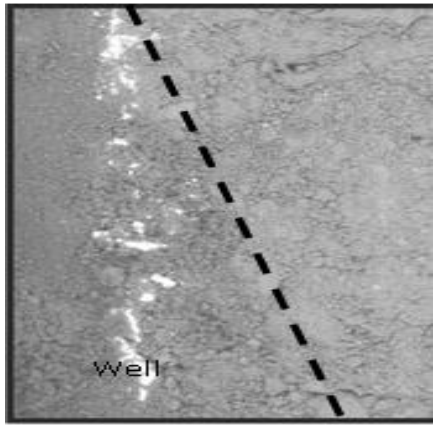

Empirical ⟶ Phenomenological ⟶ Mechanistic

Research Councils UK Energy For a Low Carbon Future

DISTINCTIVE

Beyond Distinctive

Goals of Theme 1:

- Develop an internationally respected and integrated team of experimentalists, theoreticians and modellers capable of tackling SF waste management problems

- Highly capable & growing science base
- State of the art facilities
- Well integrated programme for multidisciplinary cross-working across academic institutes (UK & Overseas)
- Effective collaboration with industry

Research Councils UK Energy For a Low Carbon Future

DISTINCTIVE

Interface Analysis Centre
Materials research for Energy Engineering and the Environment

Investigation of uranium corrosion in liquid H_2O environments under (initial) vacuum contained conditions

Antonios Banos

DISTINCTIVE Meeting – Penrith, Cumbria

October 17th 2017

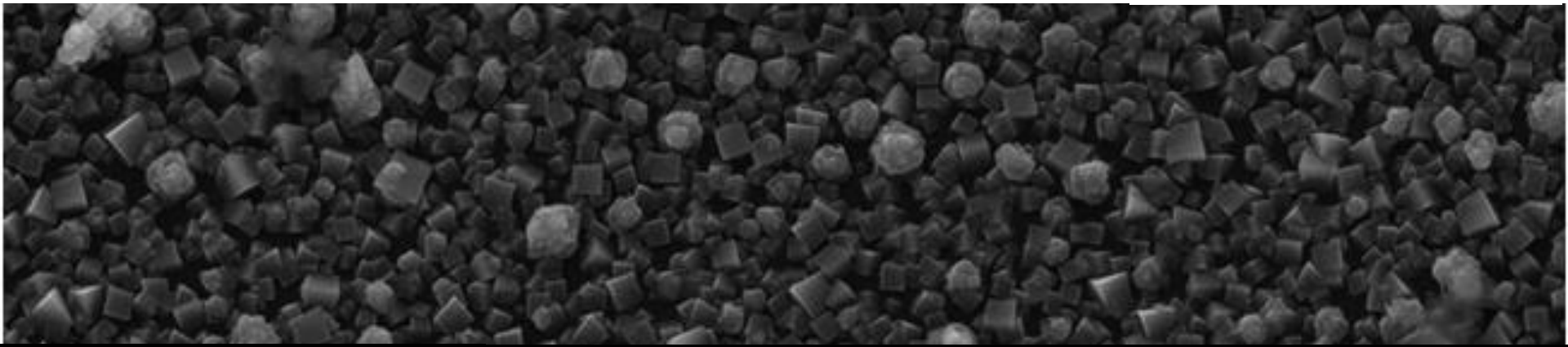

[#]Interface Analysis Centre, University of Bristol,

The Challenge

Figure 1: Aerial view of the pile fuel storage pond (PFSP) in Sellafield, UK.

Figure 2: Aerial view of the first-generation Magnox storage pond (FGMSP) in Sellafield, UK.

Figure 3: The pile fuel cladding silo (PFCS) in Sellafield.

Figure 4: The Magnox swarf storage silo (MSSS) facility in Sellafield, UK.

[#]Interface Analysis Centre, University of Bristol,

The Problem

The video is showing the reaction of freshly-made UH_3 (~ 0.9 g of initial U mass) with 800 mbar of air.

#Interface Analysis Centre, University of Bristol,

The experiments of this work

- Mimic the corrosion conditions under a contained environment (extreme event of H_2 trapping).
- Non-irradiated natural U (Magnox-U) immersed in distilled liquid water.
- Temperature regimes (25, 45, 55, 70 °C).
- Initial vacuum contained conditions.
- 10 samples were examined. Each condition analysed multiple times with varying reaction times.

The aim

- To evaluate the kinetics of the U + $H_2O_{(l)}$ system under various temperature conditions.
- To characterise the post-reacted sample surfaces by analysing the arising gas and solid corrosion products of uranium corrosion.
- To identify if UH_3 is produced for each experimental reaction condition.
- To quantify (if possible) the amount of UH_3, if present in the system.

#Interface Analysis Centre, University of Bristol,

Experimental set-up and procedure

Figure 5: Photographic image of the reaction pot set-up used in this work.

- Reaction water: 3x freeze-evacuate-thaw cycle.
- Uranium: Mechanically abraded to P2500 (~8 µm).
- Ceramic crucible was used to contain the water and the immersed sample.
- (Right end of set-up): Pressure-current transmitter with analogue output.
- (Left end of set-up): Free end to connect to the gas control rig.

Post reaction examination:

- Reacted uranium surface: FIB, SIMS, XRD and TPD combined with RGA analysis.
- Reaction water: pH measurements.

#Interface Analysis Centre, University of Bristol,

Results

Reaction rate determination (H_2 generation)

Sample	Reaction time (hours)	Reaction rate 1st regime (mgU.cm^{-2}.h^{-1})	Reaction rate 2nd regime (mgU.cm^{-2}.h^{-1})	Reaction rate 3rd regime (mgU.cm^{-2}.h^{-1})	Average reaction rate (mgU.cm^{-2}.h^{-1})
W25L	1147.7	n/a	0.0204 ± 0.0006	0.005 ± 0.00005	0.0107
W25L2	978.4	n/a	0.0096 ± 0.00005	n/a	0.0086
W45S	126	0.0185 ± 00005	0.0274 ± 0.0002	n/a	0.0262
W45L	1621.6	0.0043 ± 0.0007	0.0137 ± 0.0004	0.0243 ± 0.00009	0.0215
W45L2	1046	n/a	0.0102 ± 0.0001	n/a	0.0098
W55S	345	0.0276 ± 0.0005	0.0149 ± 0.0001	0.0095 ± 0.00004	0.0148
W55S2	397.2	n/a	0.0791 ± 0.0001	n/a	0.0799
W55L	1618.2	n/a	0.0638 ± 0.00008	0.0517 ± 0.0003	0.0612
W70S	329	0.1035 ± 0.0006	0.1359 ± 0.0002	0.0986 ± 0.0003	0.1166
W70S2	436.3	0.0773 ± 0.0017	0.1084 ± 0.0019	0.0971 ± 0.001	0.0996

'W': Liquid water
Middle numbers: Temperature of reaction
'S' and 'L': Short and long reaction time period

#Interface Analysis Centre, University of Bristol,

Results

Reaction rate - Representative reaction slope

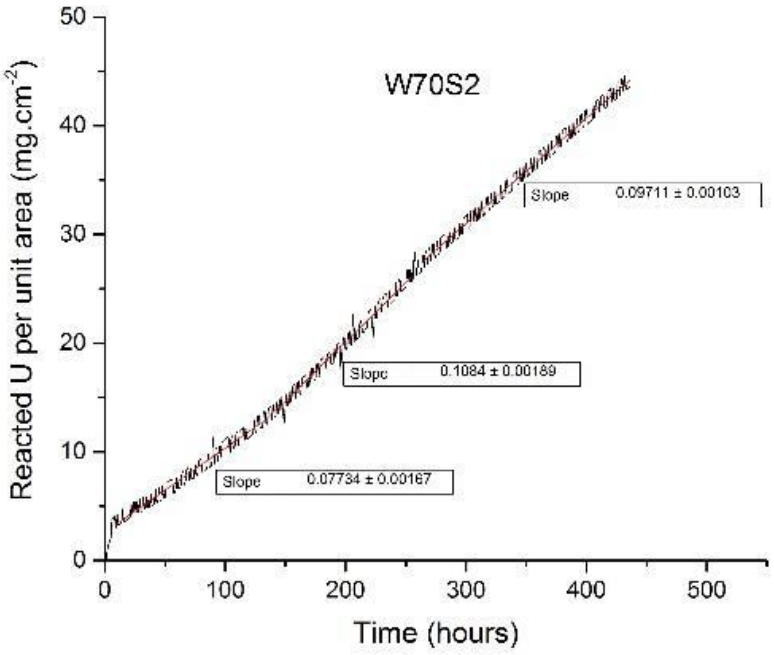

Figure 6: Corrosion progress of uranium immersed in liquid water (in mgU.cm^{-2}), over reaction time (hours) for sample W70S2.

#Interface Analysis Centre, University of Bristol,

Results

FIB analysis - Reaction rate determination - Oxide thickness measurements

Sample	Average oxide thickness (µm)	Reaction rate derived from average oxide thickness measurements ($mgU.cm^{-2}.h^{-1}$)	Reaction rate derived from H_2 generation ($mgU.cm^{-2}.h^{-1}$)
W25L	12.76	0.0107	0.0106
W25L2	1.87	0.0011*	0.0086
W45S	3.71	0.0285	0.0262
W45L	62.02	0.037	0.0215
W55S	14.81	0.0415	0.0148
W55L	166.02	0.0992	0.0612
W70S	91.76	0.2697	0.1166
W70S2	61.09	0.1354	0.0996

*W25L2 oxide flaked off leading to significantly smaller average thickness

- Higher reaction rate kinetics derived from oxide thickness measurements (FIB analysis) in comparison to H_2 generation analysis.
- H_2 deficiency in the gas phase!

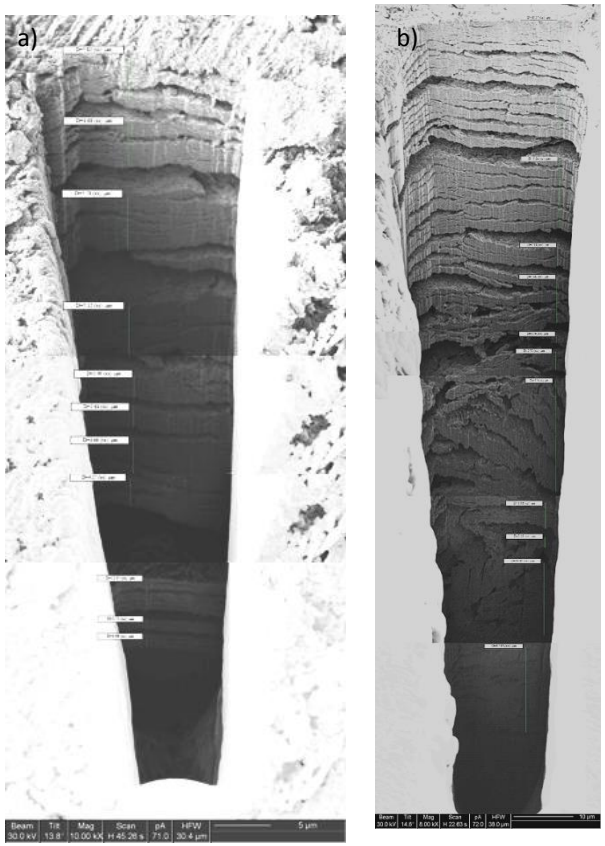

Figure 7: Focused ion beam (FIB) milling images of representative cross-sectional views for samples (a) W45L and (b) W70S

#Interface Analysis Centre, University of Bristol,

Results
Reaction water pH measurements

Sample	pH of water at average temperature of reaction	pH of reactant water at average temperature of reaction	Difference in concentration of H^+ between original and reactant water ($mole.lt^{-1}$)	Difference in H_2 in reactant water (mmol)	Working/ reaction volume (cm^3)	Pressure increase if excess H_2 diffused out to the gas phase (mbar)
W25L	6.85	Not measured	n/a	n/a	n/a	n/a
W25L2	6.85	6.13	5.98E-07	1.2E-06	84.81	0.0004
W45S	6.57	Not measured	n/a	n/a	n/a	n/a
W45L	6.53	6	6.98E-07	1.4E-06	84.77	0.0004
W45L2	6.55	6.18	3.87E-07	7.75E-07	84.80	0.0002
W55S	6.45	5.96	7.37E-07	1.47E-06	84.61	0.0005
W55S2	6.44	6.07	4.89E-07	9.78E-07	80.91	0.0003
W55L	6.45	6.12	4E-07	7.992E-07	84.76	0.0003
W70S	6.29	5.75	1.27E-06	2.54E-06	180.05	0.0004
W70S2	6.3	6	5.08E-07	1.02E-06	84.62	0.0003

- If generated hydrogen remained dissolved in the water (in the form of H^+ ions), then it would be expected that the pH of the water would drop.
- pH indeed dropped but only inconsiderably!

#Interface Analysis Centre, University of Bristol,

Results

SIMS analysis

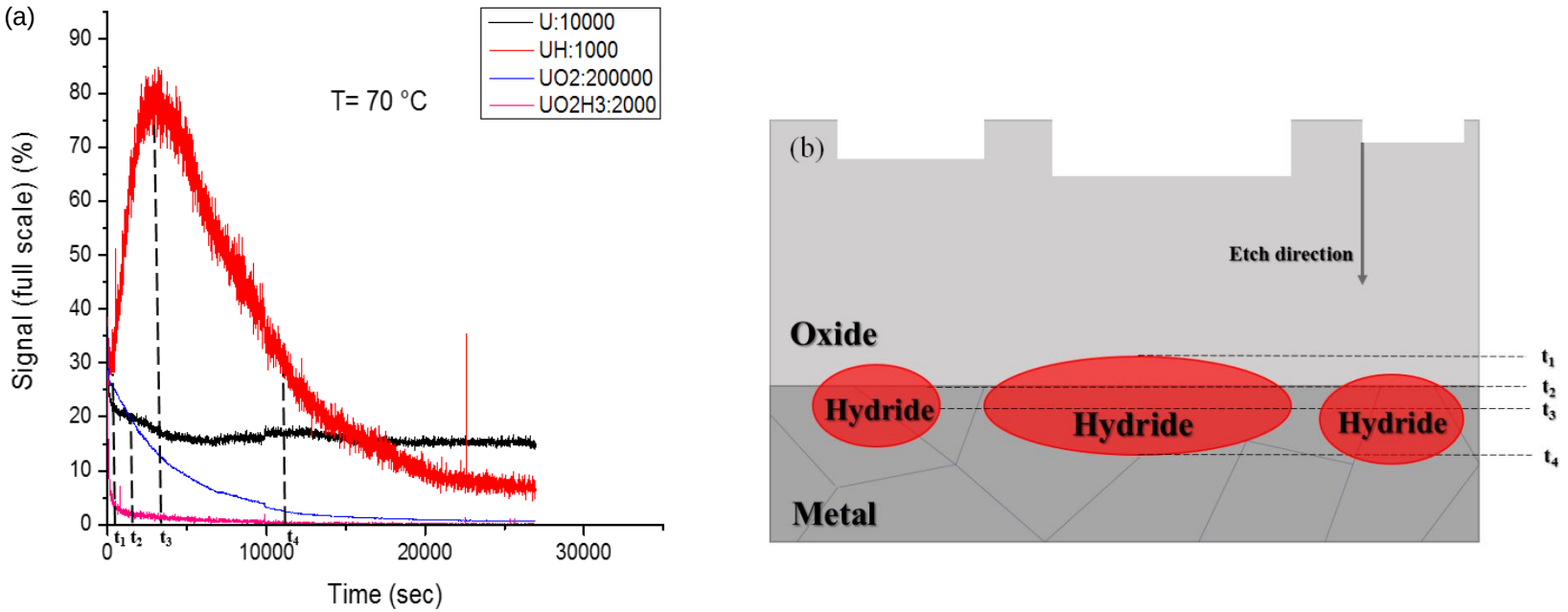

Figure 8: Showing on (a) Mass ion depth profiling for uranium oxidised in liquid water at 70 °C. Ga^+ primary ion beam, 25 keV, 3 nA positive ion mode, 45 ° angle of incidence and (b) a 2D schematic of the cross-sectional view of the same sample taking into account the data from (a). From the graph and 2D illustration, an almost linear increase in the UH signal (red line) may be observed, reaching its maximum value at the metal oxide interface (in the graph, where the blue and black curves intersect). UOH, UOH_3, UO_2H, UO_2H_2 and UO_2H_3 clusters were also traced at and/or near the gas-oxide interface indicating a H_2-rich oxide.

#Interface Analysis Centre, University of Bristol,

Results
XRD analysis

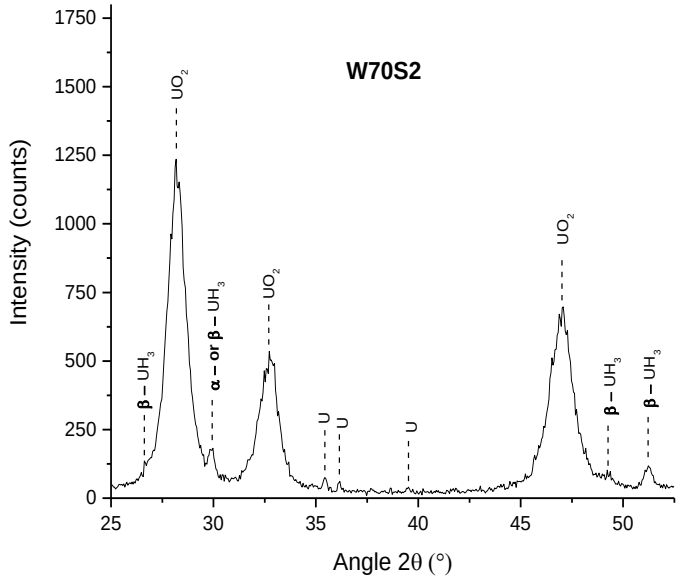

Figure 9: Raw X-ray diffraction (XRD) spectra for sample W70S2. The analyses were performed with a Cu-Kα source at 8 keV, between 25 ° and 52.5 ° angle 2θ, 0.05 step and 5 sec dwell time.

- UH_3 peaks are observed in the spectra.

#Interface Analysis Centre, University of Bristol,

Results

TPD – RGA analysis

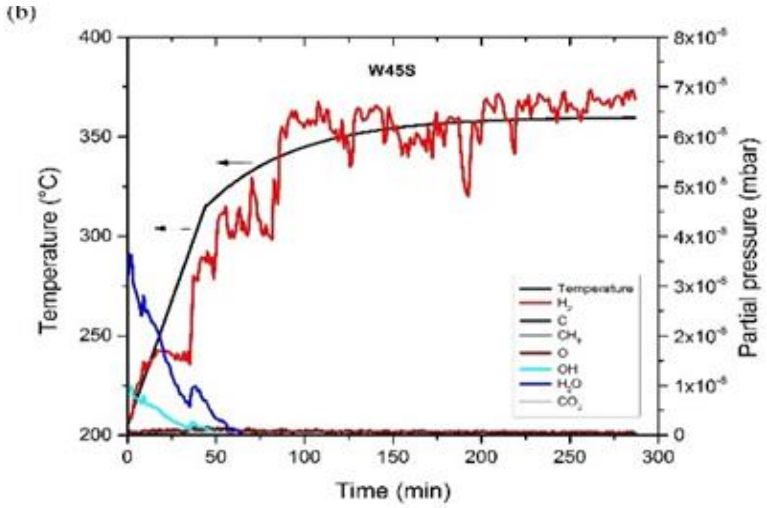

Figure 10: Residual gas analysis (RGA) profiles of the evolved gases for decomposition of reacted uranium between 200 - 450 °C for W45S.

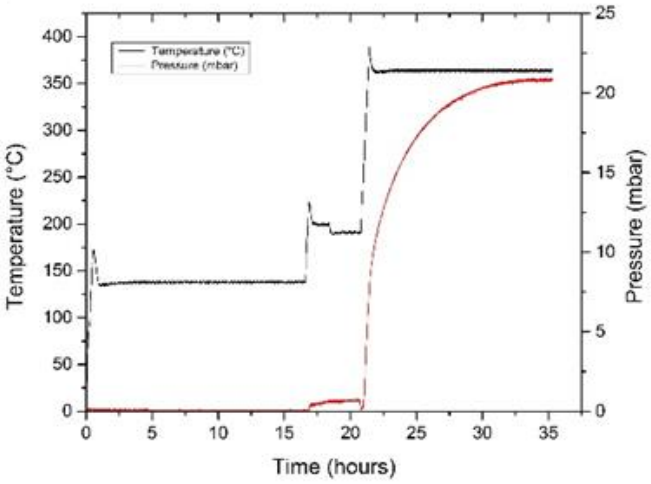

Figure 11: Pressure and temperature vs. time plot from the thermal process (sample degassing) of W45L.

Thermal process: ***Step 1*** (~130 °C, dynamic vacuum) → ***Step 2*** (~200 - 230 °C, isolated volume) → Vacuum → ***Step 3*** (370 - 420 °C, isolated volume). ***(Based on Danon et al.)***

- At ***Step 2*** a mixture of various gases dominated by H_2O, OH^- and H_2 is produced.
- **Only H_2** is degassed during the final stage of the thermal process.

A. Danon, J. Koresh, M. Mintz, Temperature programmed desorption characterization of oxidized uranium surfaces: Relation to some gas-uranium reactions, Langmuir, 15(18):5913-5920, 1999.

#Interface Analysis Centre, University of Bristol,

Results
Quantification of water-formed UH_3

Sample	Reaction time (hours)	Final T of decomposition (K)	Pressure increase due to UH_3 decomposition (mbar)	mmol of inter-layer hydride	mmol of bulk UH_3	mmol of UO_2	Percentage ratio of UH_3 to overall solid corrosion products (%)
W45S	126	632.8	8.2	8.2E-05	0.0086	0.05	14.6
W45L	1621.6	638.6	20.9	4.4E-05	0.0549	0.281	16.3
W45L2	1046	671	7.2	3.8E-05	0.0174	0.0714	19.6
W55S	345	626.7	8.9	8.1E-05	0.0098	0.0815	10.7
W55S2	397.2	672.1	1.9	4.1E-05	0.0037	0.2354	1.6
W55L	1618.2	676.3	11.3	4.6E-05	0.0274	0.8492	3.1
W70S	329	613	10.8	8.7E-05	0.0124	0.6154	2
W70S2	436.3	673.1	13.2	8.3E-05	0.031	0.6696	4.4

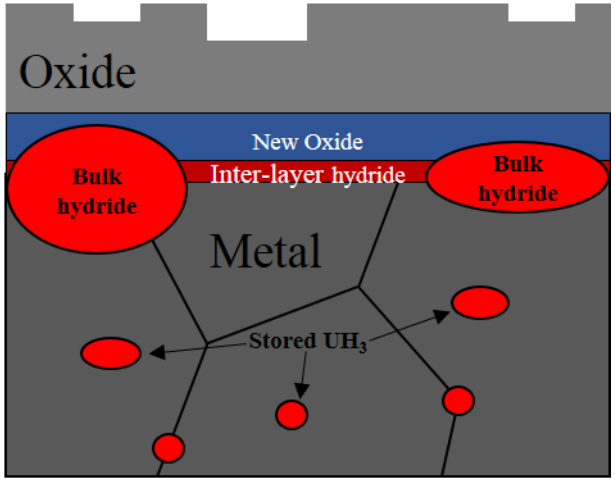

Figure 12: Types of hydrides present on water-corroded uranium metal under contained conditions.

$$n_{bulk\ UH3} = n_{overall\ UH3} - n_{stored\ UH3} - n_{inter\text{-}layer\ UH3}$$

#Interface Analysis Centre, University of Bristol,

Summary - Discussion

- Bulk-UH_3 forms at the metal-oxide interface, on the majority of the samples. Limited UH_3 formation for the samples corroding at 25 °C.
- The relative amount of UH_3 to the overall solid corrosion products was determined for each sample and a percentage ratio was derived. It was found that lower temperature reaction conditions yielded higher UH_3 proportions. However, the absolute UH_3 quantities are markedly higher on the higher temperature samples.
- Considerably slower corrosion kinetics (H_2 generation method) in comparison to the literature.
- The activation energy (E_α) was measured at 50 $kJ.mole^{-1}$.
- Through pressure generation (rate plots) and post-examination analysis (bulk-UH_3 formation) it was suggested that over a critical threshold headspace pressure (calculated to be ~500 mbar): either (a) H_2 evolution is partially suppressed by the headspace pressure or (b) there is a consumption of H_2 gas from the headspace concurrent with new gas being released by continued metal corrosion. It is believed that both these processes lead to enhanced 'bulk' UH_3 formation in the system.

[#]Interface Analysis Centre, University of Bristol,

Thank you!

[#]Interface Analysis Centre, University of Bristol,

The Behaviour of Advanced Gas Reactor Simulated Spent Nuclear Fuels in Wet Interim Storage Conditions

17/10/2017

Elizabeth Howett

Supervisors: Prof Colin Boxall, Dr Richard Wilbraham and Dr David Hambley (NNL)

Contents

- Introduction
- Cyclic voltammetry and OCPs of uranium dioxide and SIMFUELs in:
  - 0.5M Na_2SO_4
  - Simulant pond water
- Electrochemical impedance spectroscopy and Mott Schottky analysis
- Conclusions and further work

PhD Project Incentive and Objectives

- Fuel has been successfully stored for period of 10-20yrs however may extend to 100yrs
- Cladding can be breached due to stress corrosion cracking or damaged during dismantling
- Evolution of the cladding and fuel surfaces on exposure to pond water are considered corrosion processes
- Assess the validity of extended storage periods without extra containment

Materials and experimental conditions

- Pond water chemistry: pH≈11.4

Na^+	Ca^+	Cl^-	SO_4^{2-}	K^+	OH^-
5.4mM	2μM	30μM	2μM	5μM	Balance

- AGR SIMFUEL sample composition:

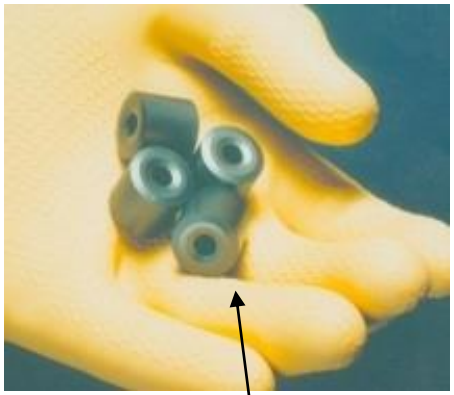

AGR fuel pellets

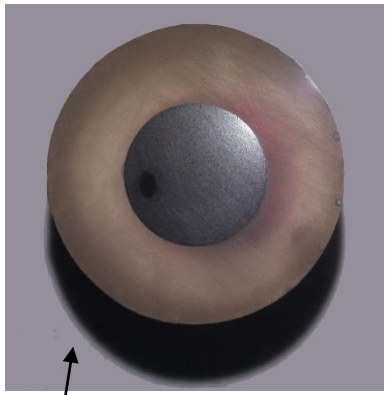

UO_2 electrode

	25 GWd/tU	43 GWd/tU
UO_2	95.705	92.748
Nd_2O_3	0.761	1.284
ZrO_2	0.793	1.276
MoO_3	0.614	1.027
RuO_2	0.512	0.892
$BaCo_3$	0.328	0.576
CeO_2	0.297	0.499
PdO	0.195	0.425
Rh_2O_3	0.080	0.115
La_2O_3	0.156	0.256
SrO	0.081	0.126
Y_2O_3	0.095	0.149
Cs_2CO_3	0.311	0.495
TeO_2	0.073	0.130

Electrochemical behaviour in 0.5M Na_2SO_4, pH≈5.6

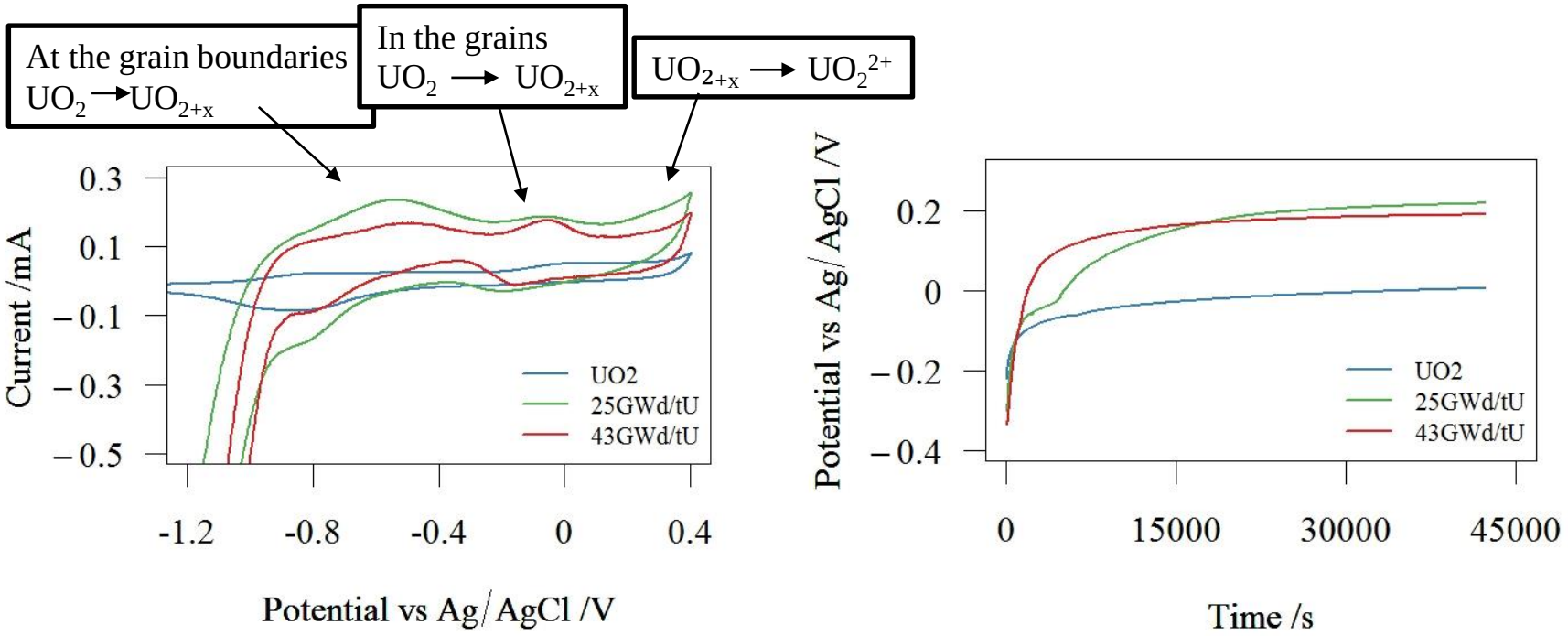

Figure 1: Electrochemical behaviour in 0.5M Na_2SO_4, cyclic voltammetry (left) and open circuit potentials (right)

- Addition of lower valent species increases conductivity
- Fluorite lattice stabilized by further doping
- OCP lies in region were dissolution begins to occur

Electrochemistry in simulant pond water, pH ≈11.4

Comparison to Na_2SO_4:

- Suppression of the dissolution as UO_2^{2+}
- Decrease in the OCP, potential now lies in a region where an oxide layer is developing on the surface

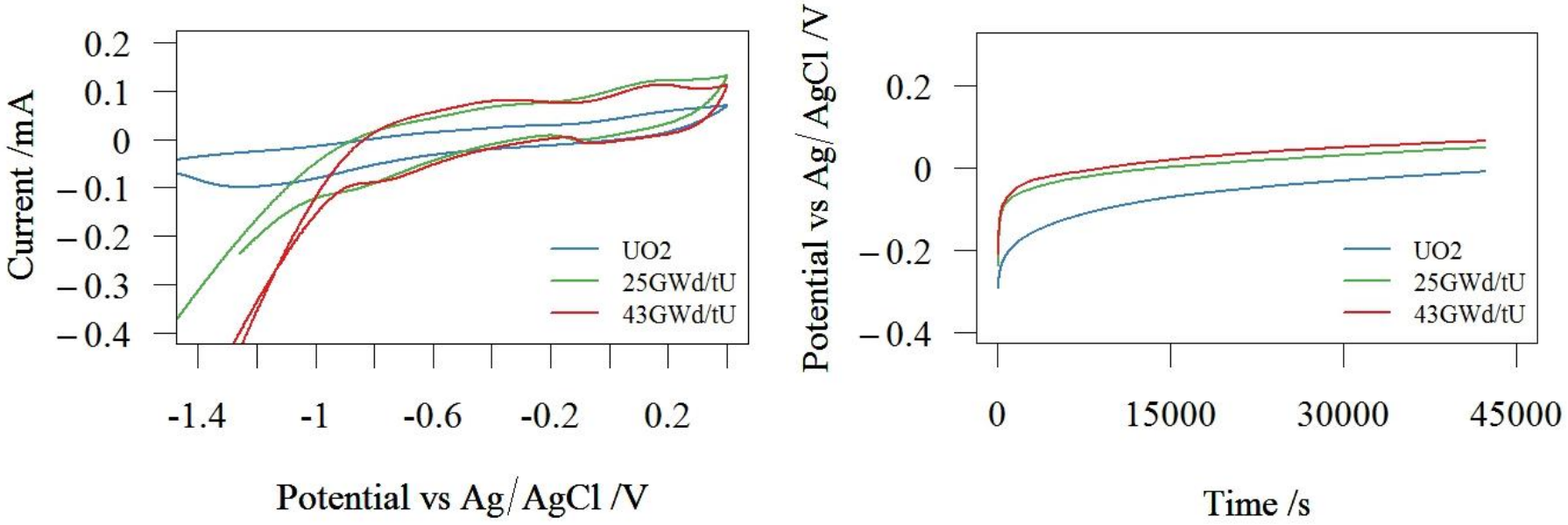

Figure 2: Electrochemical behaviour in simulant pond water, cyclic voltammetry (left) and open circuit potentials (right)

Uranium Dioxide Pourbaix diagrams

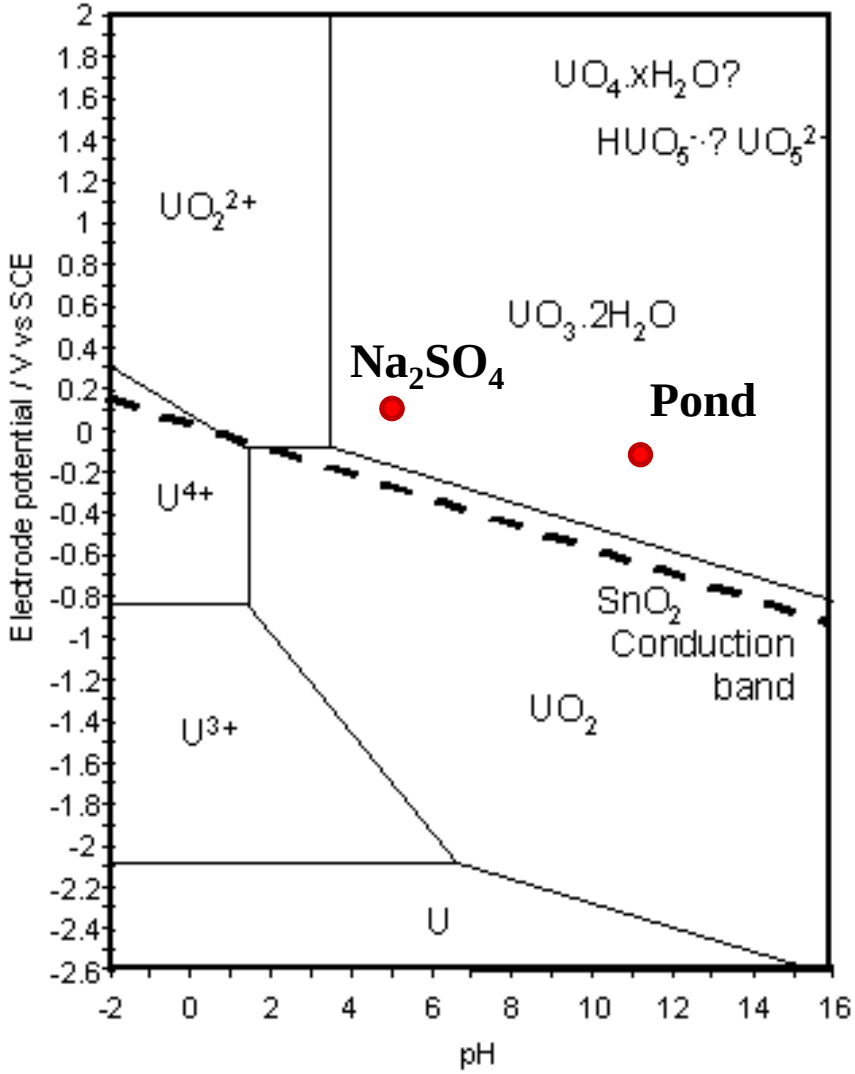

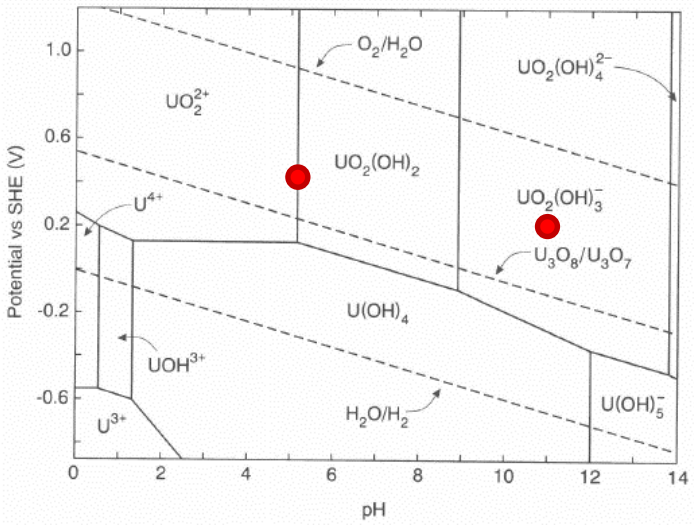

Electrochemical impedance spectroscopy (EIS)

- Measure of the resistance and capacitance developed on the electrode system due to the formation of an oxide layer on the electrode surface
- A small sinusoidal potential is applied to the working electrode and the frequency is scanned between 100,000 and 0.1Hz
- Nyquist plots – show the frequency response of the system, give information on the stability of a system. It is a plot of the real versus imaginary components of the impedance
- Equivalent circuit models are used to extract information on the resistance and capacitance of a system from the Nyquist plot

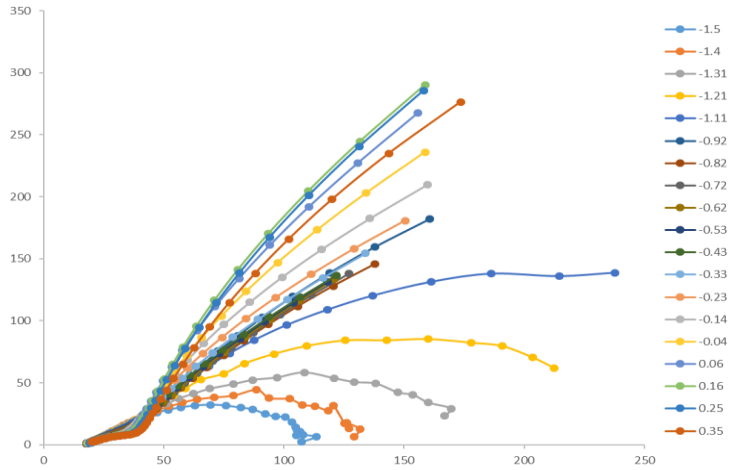

Figure 3: Example of a Nyquist plot for 25GWd/tU in Na_2SO_4

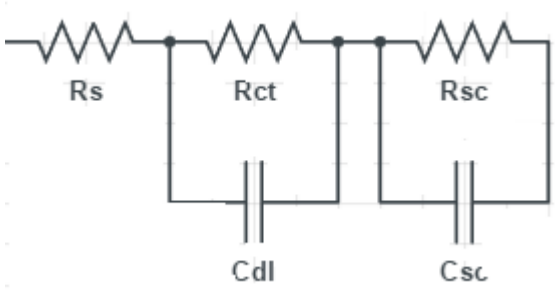

Figure 4: Electrical equivalent circuit model used to represent an electrochemical interface undergoing corrosion

Mott Schottky plots for semiconductors

- Uranium dioxide has semiconductor properties
- Semiconductor electrolyte interface has an associated charge area known as space charge layer
- There is an apparent capacitance associated with the space charge layer
- Mott Schottky equation: $\frac{1}{C^2} = \frac{2}{\varepsilon\varepsilon_0 A^2 q N_D}\left(-E + E_{FB} + \frac{kT}{q}\right)$

Mott Schottky plots in Na_2SO_4

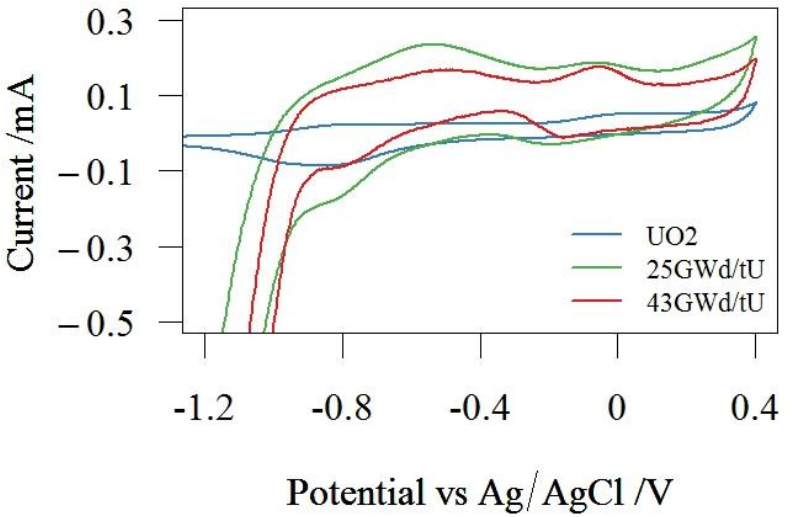

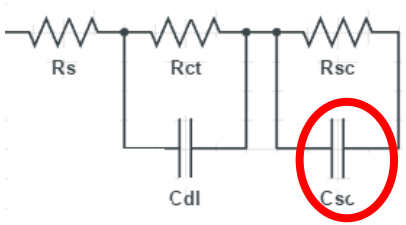

N-type semiconductors have a positive slope whereas p-type semiconductors have a negative slope

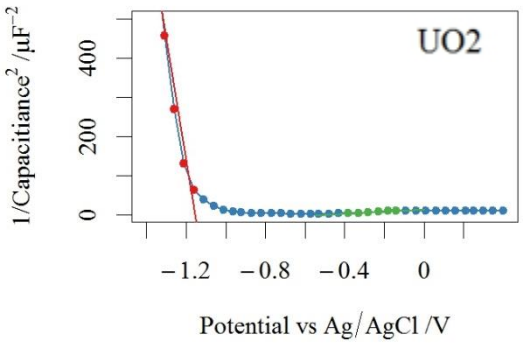

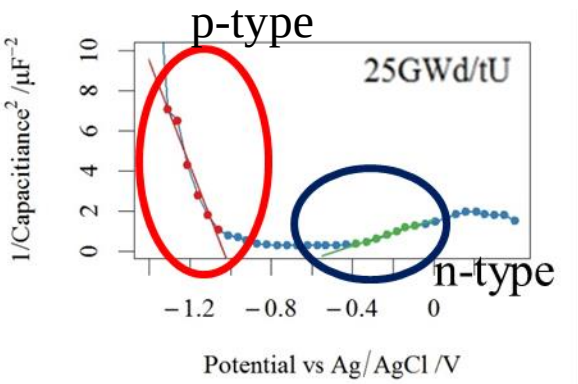

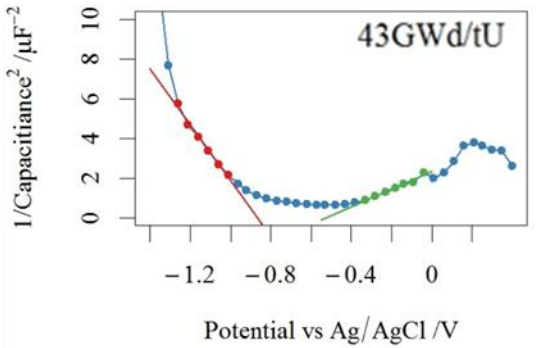

$$\frac{1}{C^2} = \frac{2}{\varepsilon\varepsilon_0 A^2 q N_D}\left(-E + E_{FB} + \frac{kT}{q}\right)$$

Mott Schottky plots in Na_2SO_4

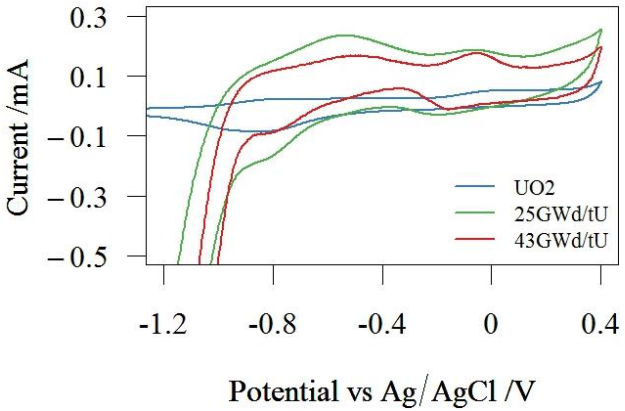

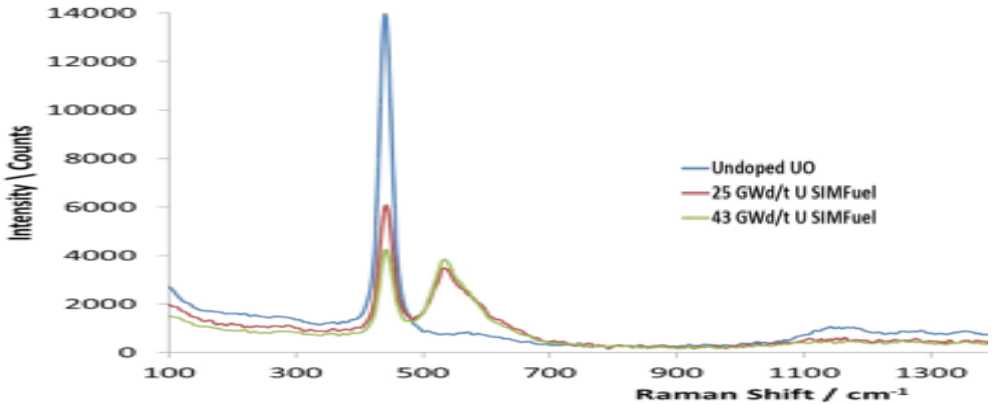

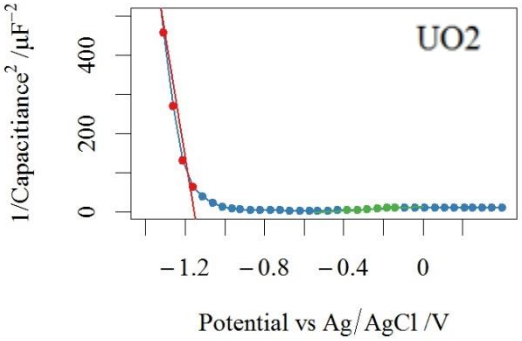

p-type

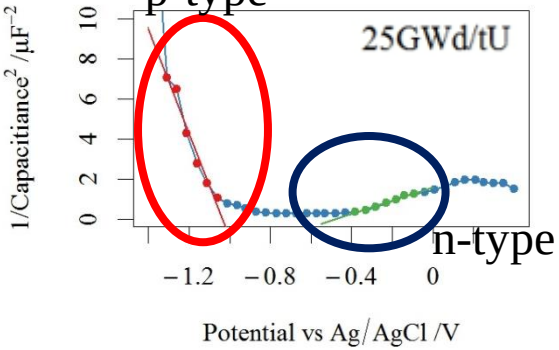

n-type

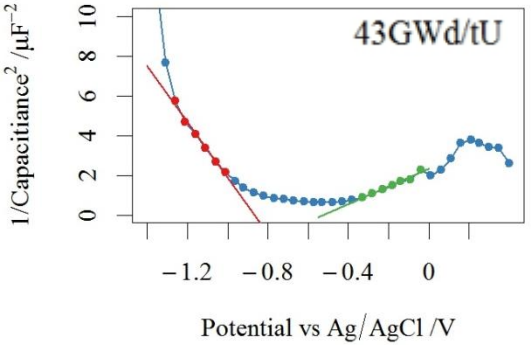

$$\frac{1}{C^2} = \frac{2}{\varepsilon\varepsilon_0 A^2 q N_D}\left(-E + E_{FB} + \frac{kT}{q}\right)$$

Mott Schottky plots in Na_2SO_4

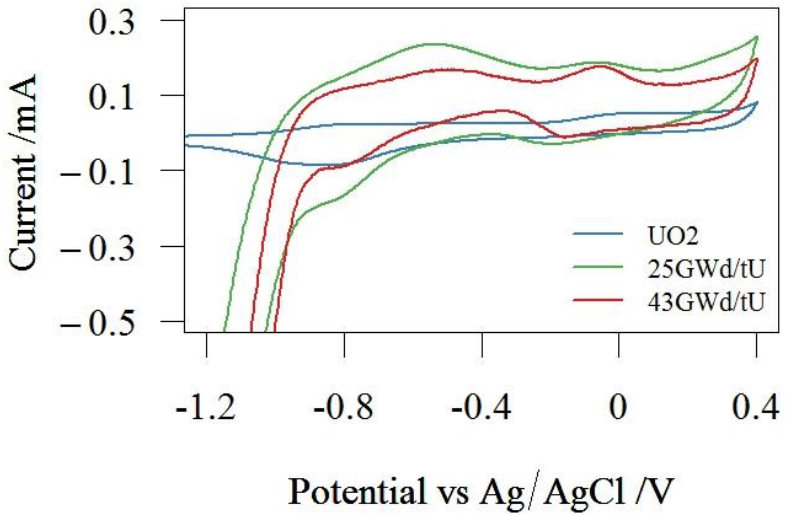

	N_D /m^{-3}	E_{FB}/V vs Ag/AgCl
	p-type	
UO_2	3.02e23	-1.2
25 GWd/tU	3.78e25	-1.06
43 GWd/tU	6.82e25	-0.9
	n-type	
UO_2	3.51e25	-0.52
25 GWd/tU	2.76e26	-0.5
43 GWd/tU	2.43e26	-0.55

$$\frac{1}{C^2} = \frac{2}{\varepsilon\varepsilon_0 A^2 q N_D}\left(-E + E_{FB} + \frac{kT}{q}\right)$$

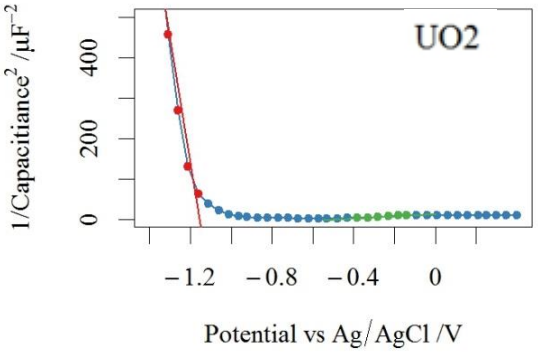

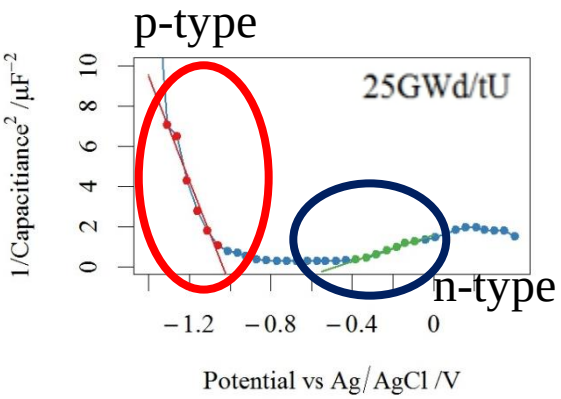

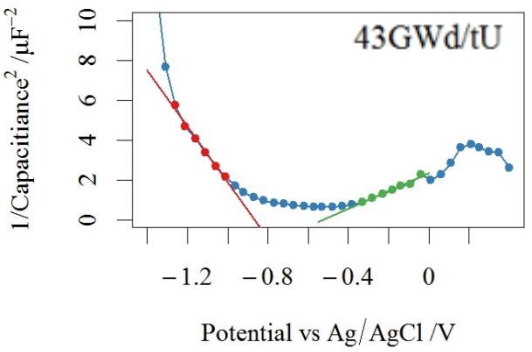

Need for the use of an inert electrolyte in EIS tests

- A problem arises due to the IR drop at the electrode surface in resistive solutions
- Problem is fixed by adding a high concentration of inert electrolyte

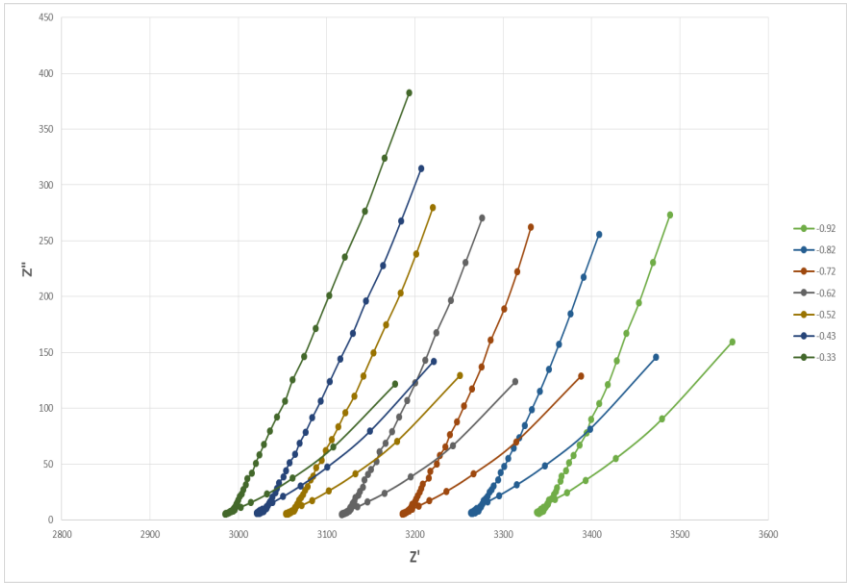

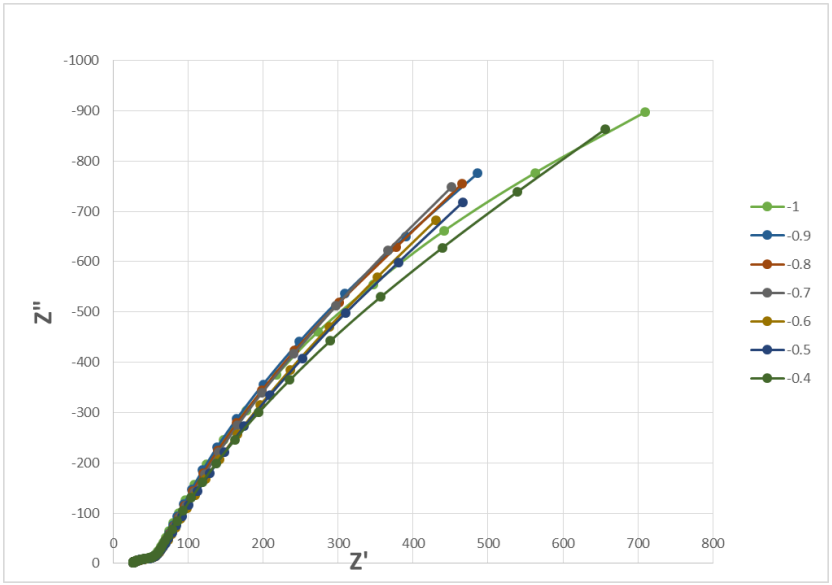

Left: Nyquist plot for 25GWd/tU in simulant pond water, pH≈ 11.4
Right: Nyquist plot for 43GWd/tU in simulant pond + 0.5M Na_2SO_4, pH≈ 11.4

Mott Schottky plots in simulant pond water

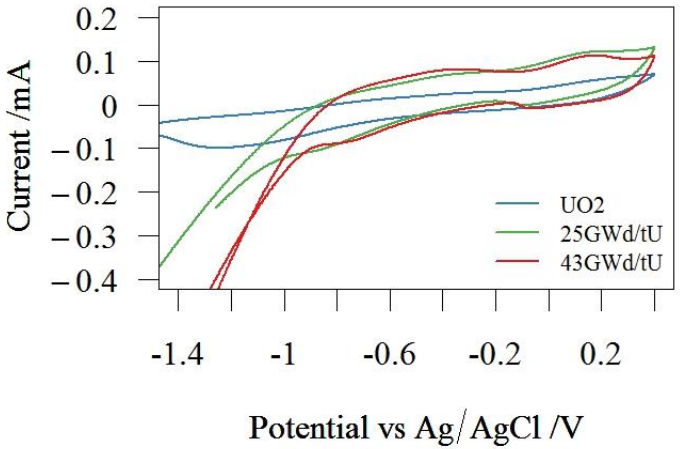

	N_D /m^{-3}	E_{FB}/V vs Ag/AgCl
	p-type	
UO_2	5.62e23	-1.24
25 GWd/tU	1.99e26	-0.77
43 GWd/tU	1.94e26	-0.74
	n-type	
UO_2	2.49e25	-0.45
25 GWd/tU	1.09e26	-0.56
43 GWd/tU	1.05e26	-0.57

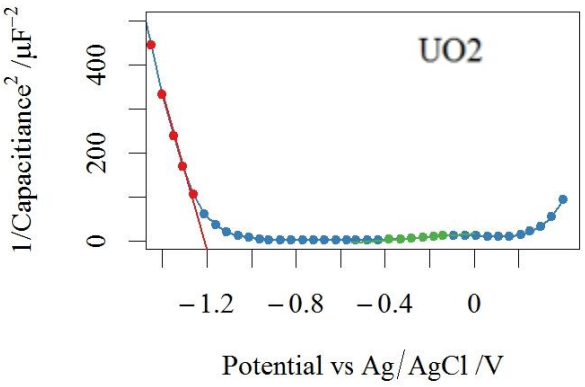

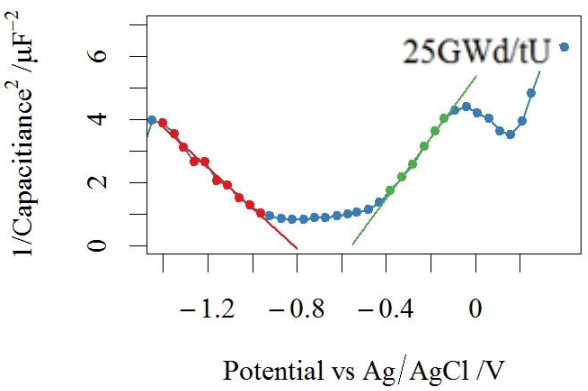

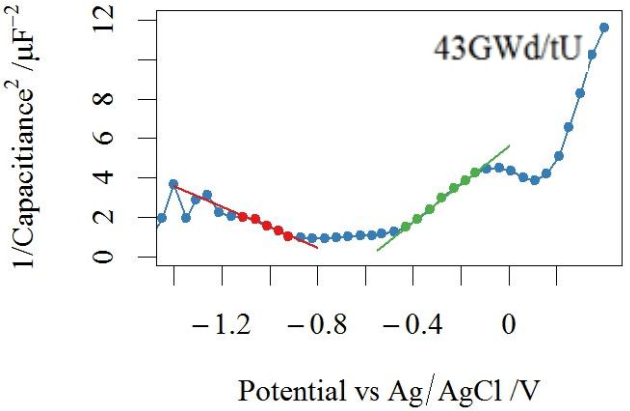

Effect of Grain Size

43GWd/tU, 2.95±1.3 μm

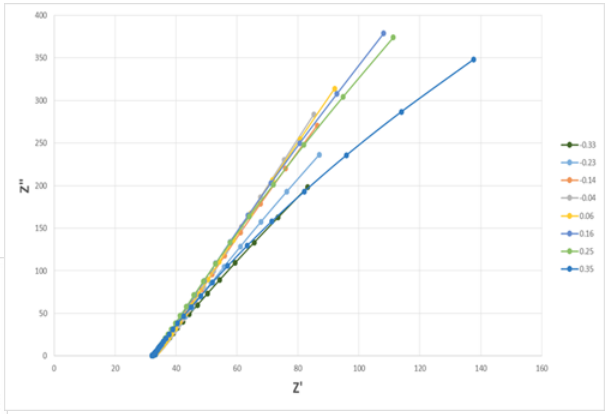

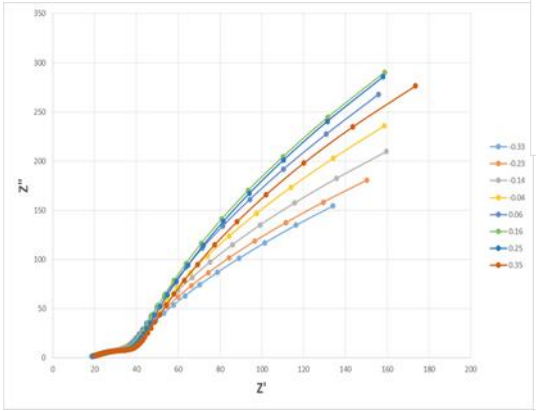

25GWd/tU, 4.21±0.59 μm

UO_2, 9.70±2.3 μm

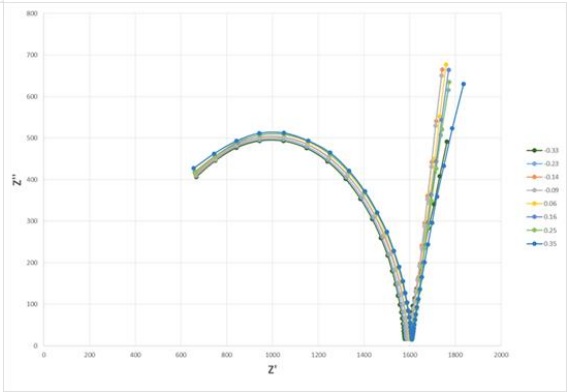

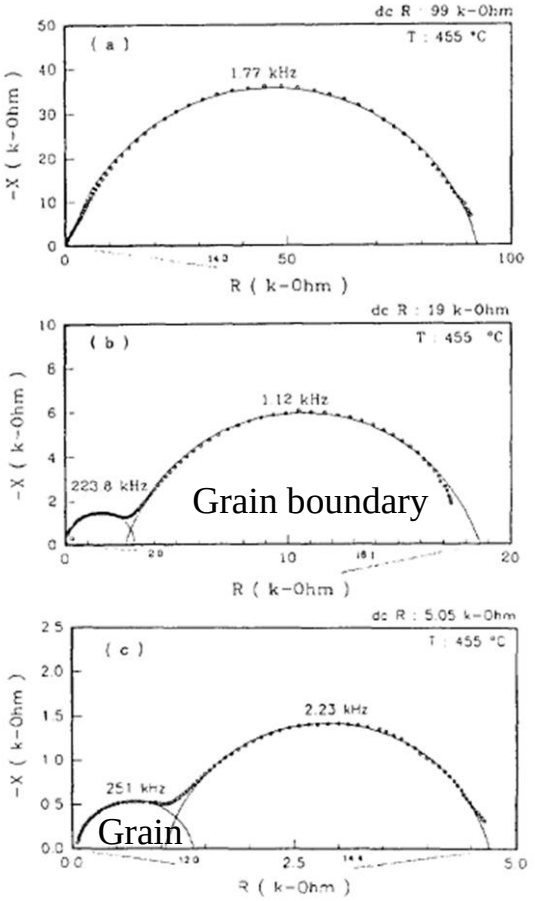

Figure 3. Complex impedance diagrams of undoped $BaTiO_3$ ceramics with various average grain sizes at 455℃ : (a) 1.0 μm, (b) 8.2 μm, and (c) 20 μm.

Conclusions

- In dosed storage pond water at pH ≈11.4 dissolution of the uranium dioxide matrix is suppressed
- Doping uranium dioxide increases the p-type character, driven by the increase in x-value and the insertion of lanthanides into the matrix
- At the potentials interest, in terms of corrosion susceptibility in pond water, an n-type system occurs as the surface transforms to cuboctrahedral U_4O_9
- EIS experiments may be effected by the grain size difference between the SIMFUELs and the pure UO_2, thus understanding the fundamentals of film growth for real SNF it may be more beneficial to look at the EIS behaviour of pure UO_2

Future Work

- Comparison of the electrochemical behaviour of SIMFUELs with that of real irradiated fuel
- Experiments using the next batch of SIMFUELs where the grain size and porosity is closer to the values expected in real SNF
- Studies using U_4O_9

Acknowledgements

Lancaster University

A fundamental approach to investigating the radiolytic dissolution of UO_2

Sophie Rennie
Interface Analysis Centre, University of Bristol, Bristol, BS8 1TL, UK.
Email: sophie.rennie@bristol.ac.uk

Distinctive Theme Meeting
Rheged Centre
17th October 2017

Research Councils UK Energy For a Low Carbon Future

EPSRC Pioneering research and skills

AWE

DISTINCTIVE

Corrosion of UO_2

Problem: Dissolution of spent UO_2 fuel on exposure to water, resulting in the release of radionuclides [2].

The primary mechanism of UO_2 corrosion is **oxidative dissolution** [4]:

$$UO_2 \rightarrow UO_{2+x} \rightarrow UO_2^{2+}$$

1. Radiolytic production of oxidants.
2. Cathodic reduction of oxidants.
3. Anodic oxidation and dissolution of the fuel.

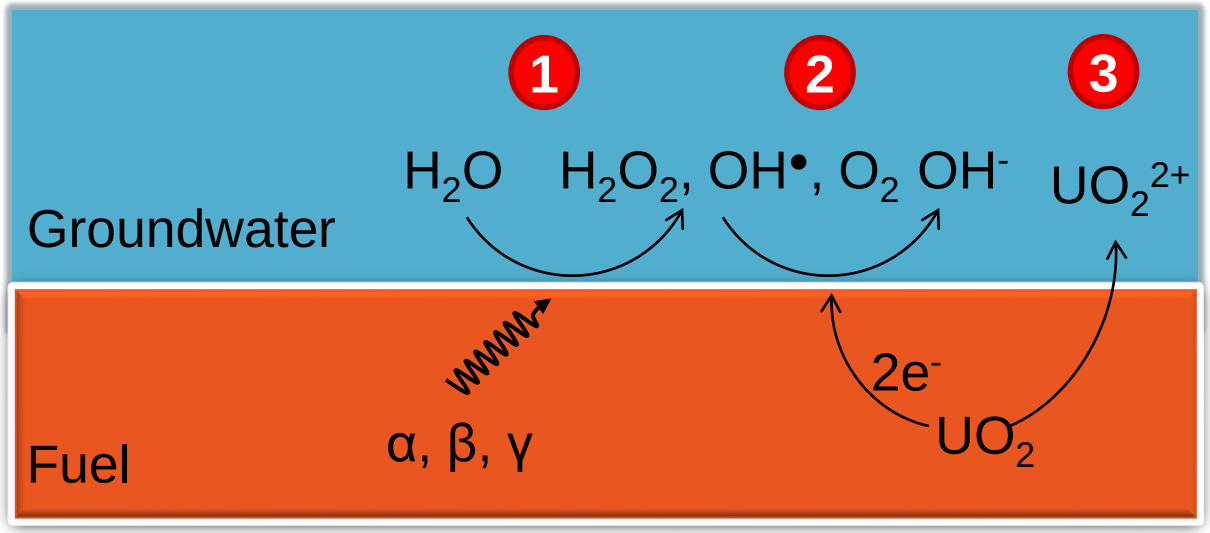

[4] D. W. Shoesmith, J. Nucl. Mater. **282**, (2000).

Research Councils UK Energy For a Low Carbon Future
EPSRC Pioneering research and skills
AWE
DISTINCTIVE

A Thin Film Approach

Bridging the gap between experimental investigations on complex spent fuel materials and idealised modelling studies.

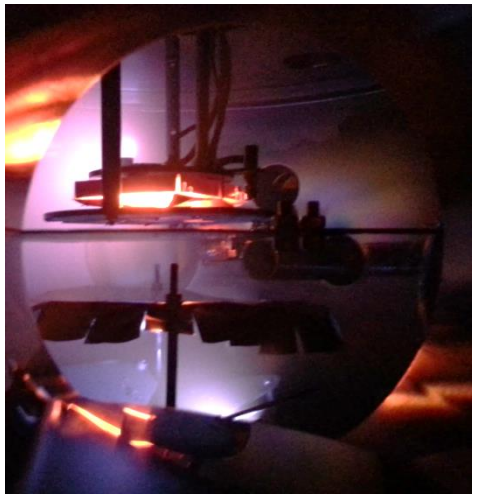

Engineered for purpose

- Single crystal or polycrystalline
- Thickness range 0.1 - 500 nm
- Stoichiometry control

Idealised surfaces

- Roughness < 10 Å (rms)
- Enhanced surface sensitivity

Low activity

- Classification: exempt or accepted

UO_2 (001) / YSZ (001)

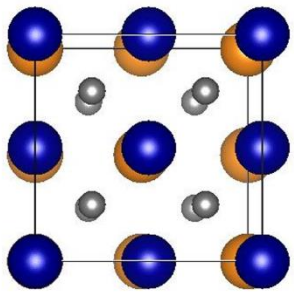

UO_2 (110) / YSZ (110)

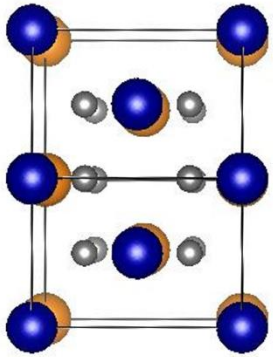

UO_2 (111) / YSZ (111)

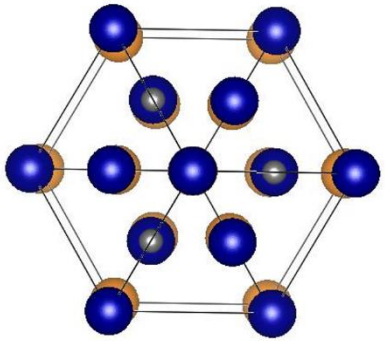

Research Councils UK Energy For a Low Carbon Future

EPSRC Pioneering research and skills

AWE

DISTINCTIVE

X-ray Reflectivity

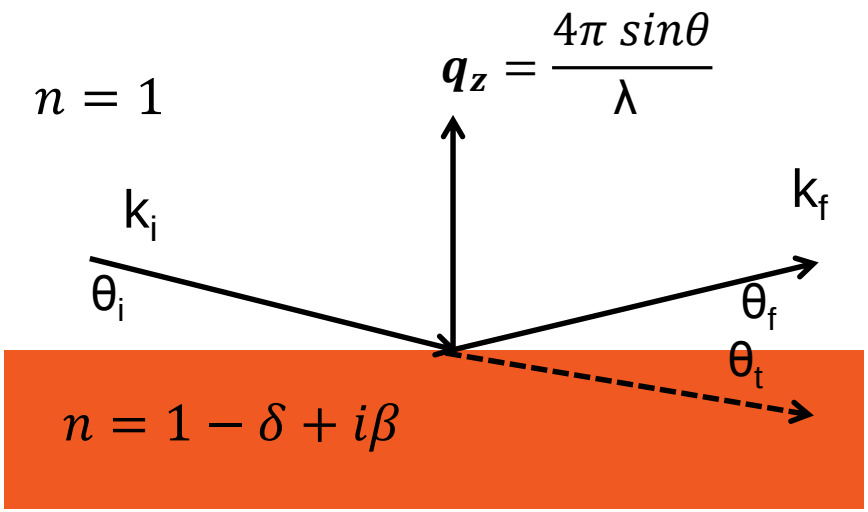

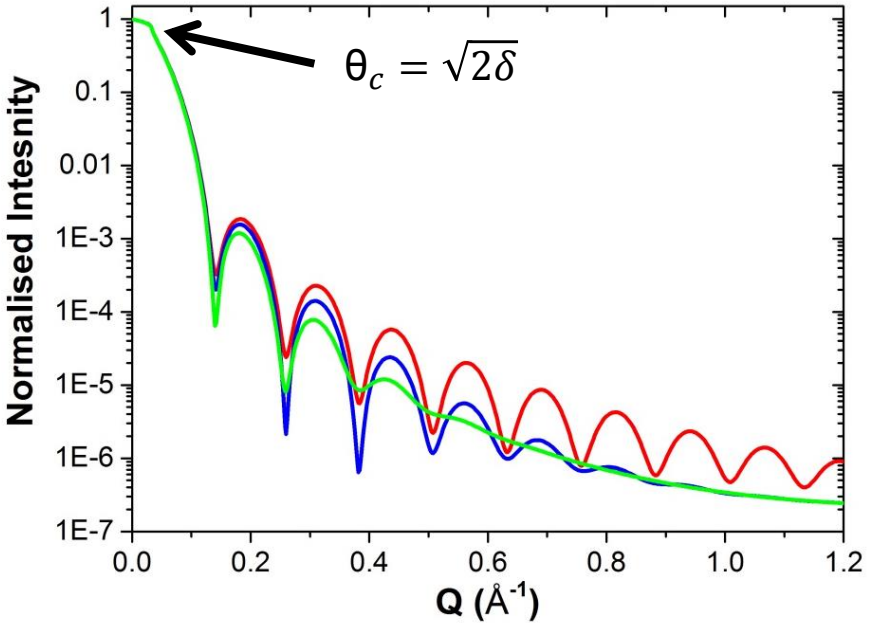

1) Electron density as a function of depth.
2) Layer thickness
3) Interfacial roughnesses

Research Councils UK Energy For a Low Carbon Future

EPSRC Pioneering research and skills

AWE

DISTINCTIVE

Synchrotron Induced Dissolution

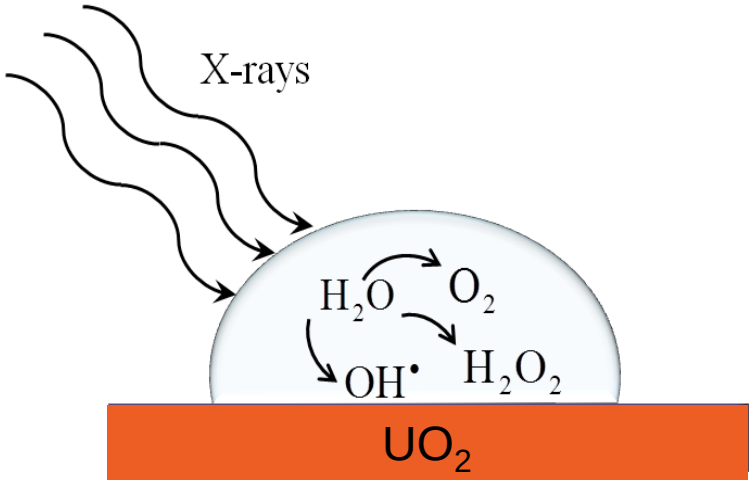

Ingredients required for UO_2 dissolution:

- H_2O / UO_2 interface
- Radiation source: α, β, γ, **x-rays**

The x ray beam was used as:
A source – to radiolyse the water,
A probe – to investigate changes in surface morphology using XRR.

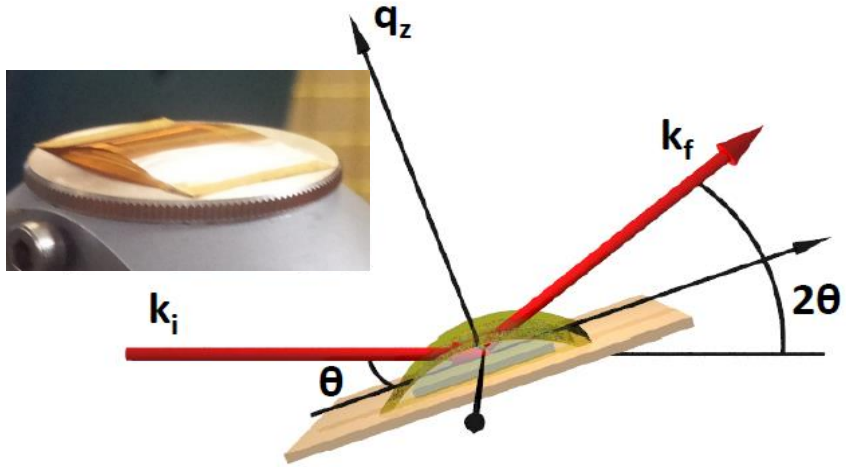

Research Councils UK Energy For a Low Carbon Future

EPSRC Pioneering research and skills

AWE

DISTINCTIVE

Dissolution of (111) – oriented UO_2

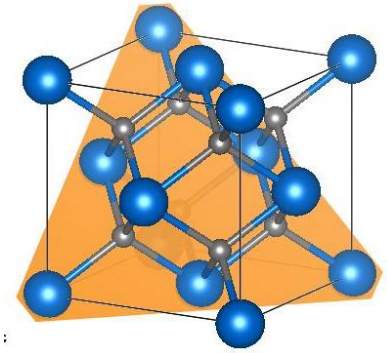

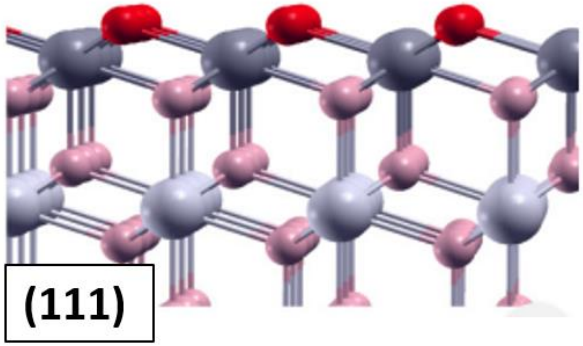

- Most stable surface
- O terminated bulk
- Non - polar

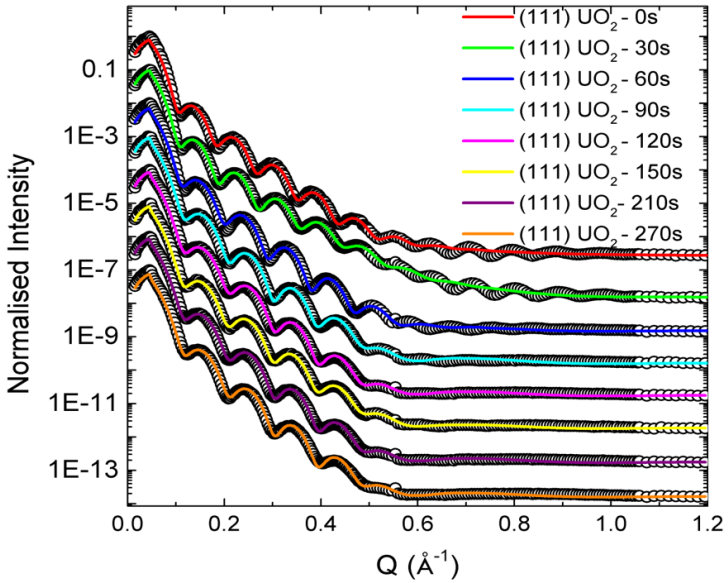

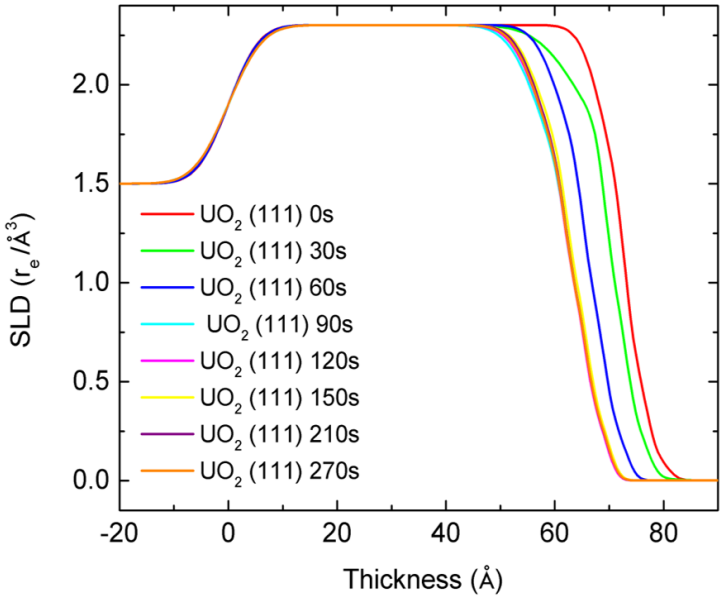

Research Councils UK Energy For a Low Carbon Future

DISTINCTIVE

Dissolution of (110) – oriented UO_2

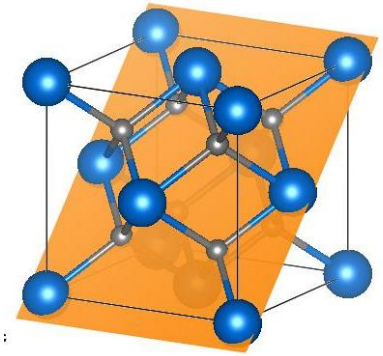

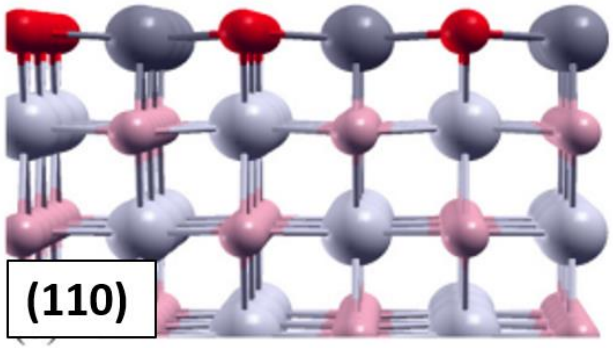

- Stable surface
- Stoichiometric termination
- Bulk like, with outward relaxation of the oxygens
- Neutral

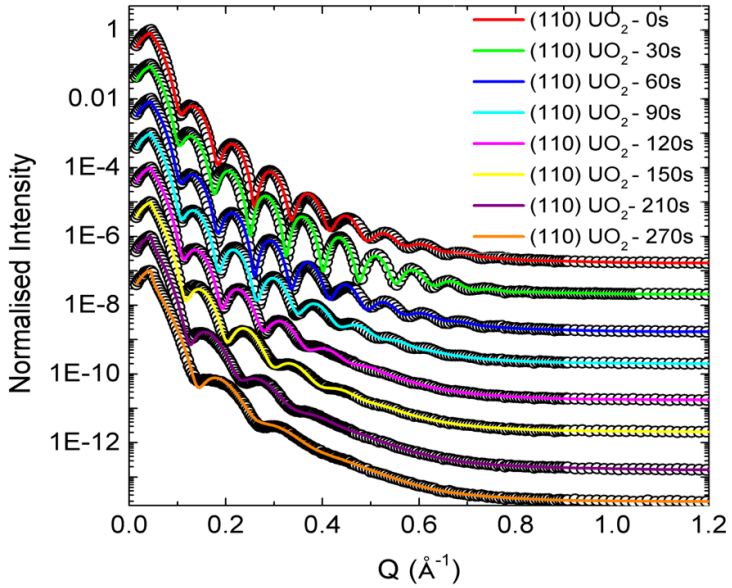

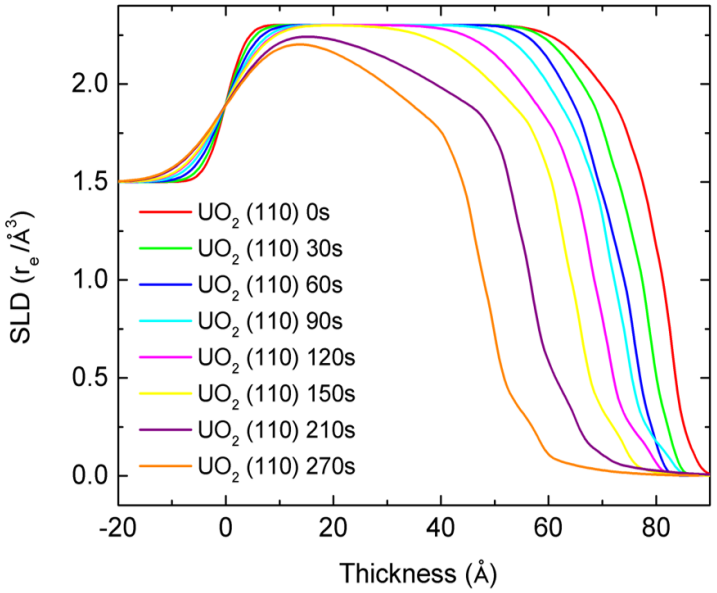

Research Councils UK Energy For a Low Carbon Future

DISTINCTIVE

Dissolution of (001) – oriented UO_2

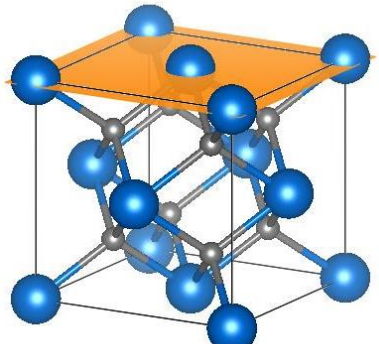

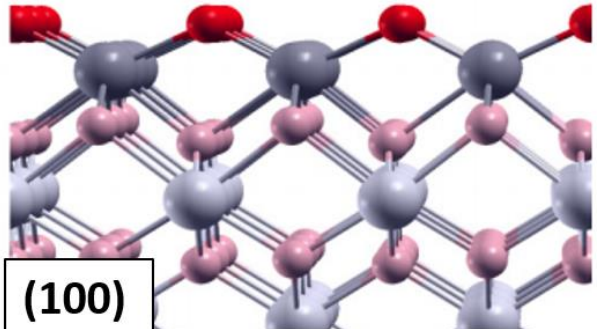

- Least stable surface
- Polar
- Formation of O overlayers

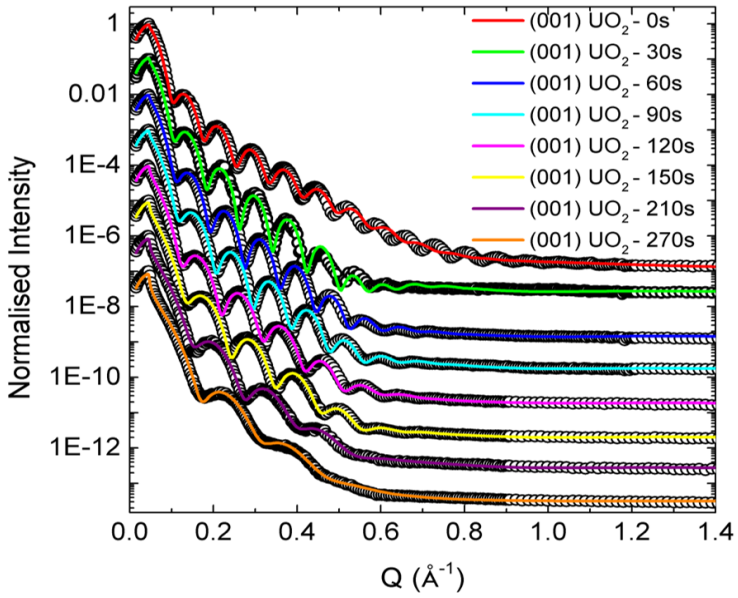

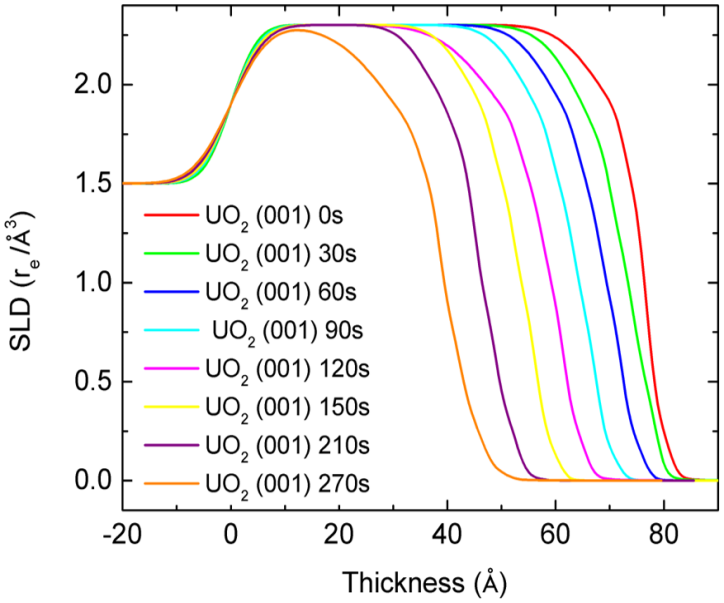

Energy
For a Low Carbon Future

DISTINCTIVE

Orientation Dependence

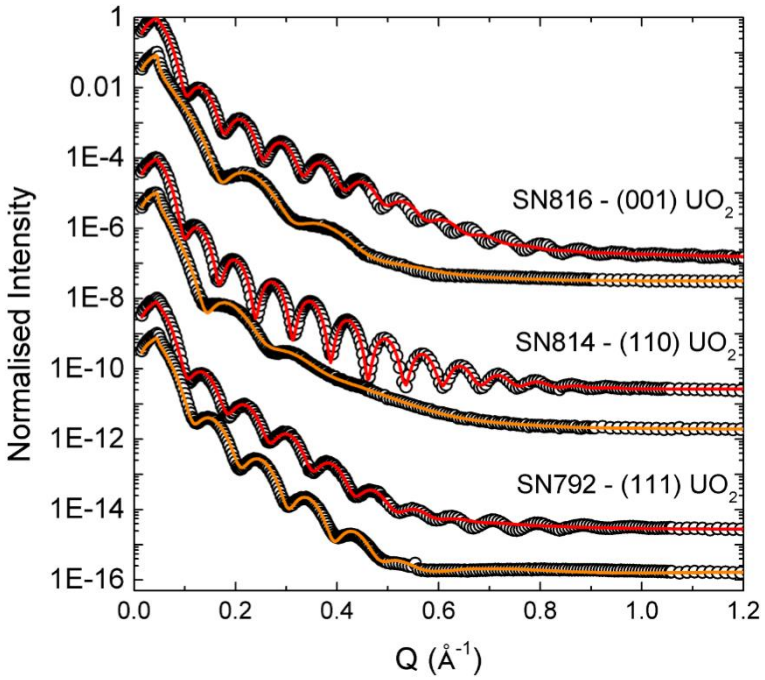

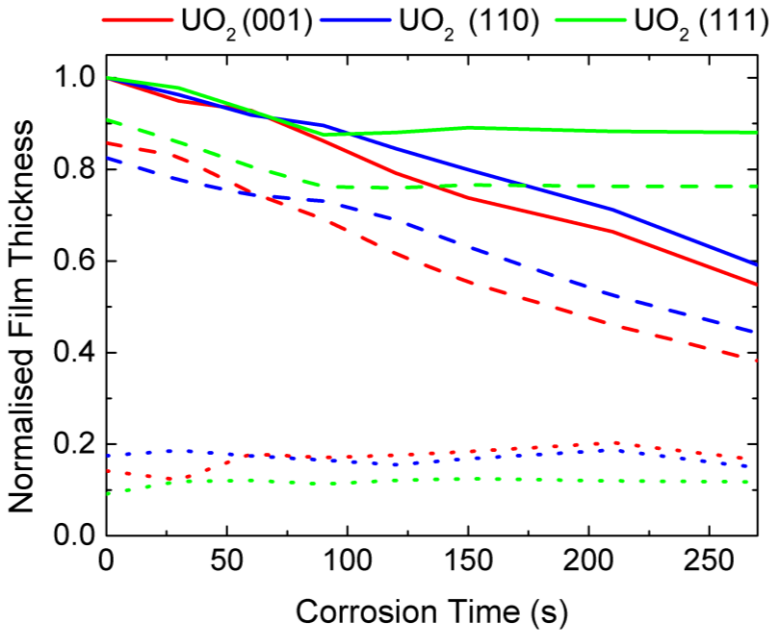

	(001)	(110)	(111)
Δt_{uo2} (Å)	-38.1 ± 0.8	-32.9 ± 0.3	-11 ± 0.9
Δt_{uox} (Å)	1.6 ± 2.8	-2.2 ± 0.6	-1.9 ± 1.1
Δt_{total} (Å)	-36.5 ± 3.6	-35.1 ± 0.9	-12.9 ± 2

Research Councils UK Energy For a Low Carbon Future

DISTINCTIVE

Remaining Question

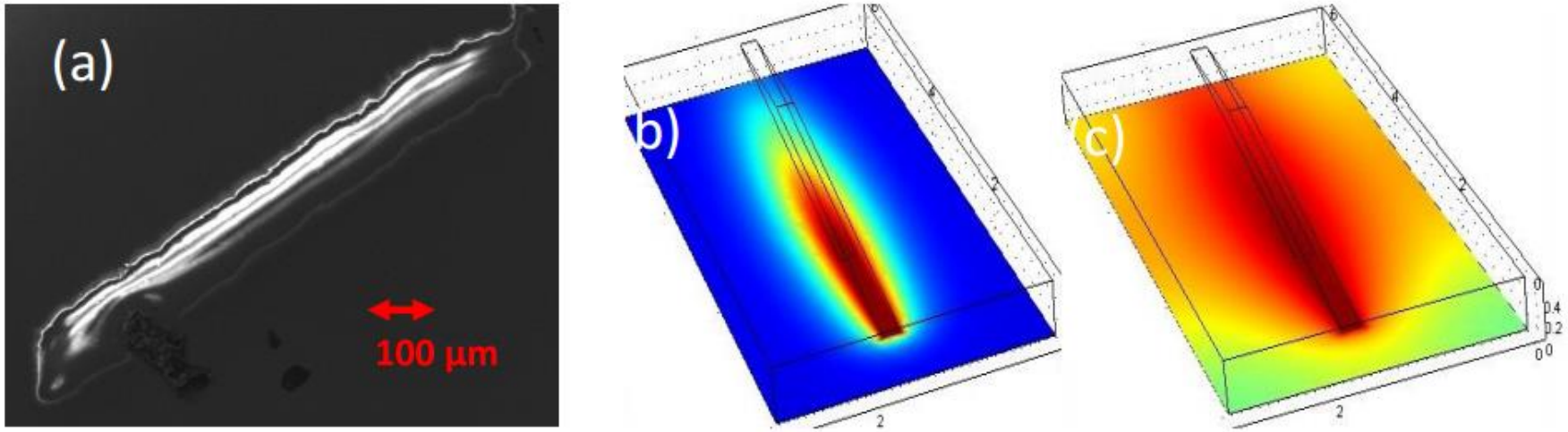

(a) SEM image of a corroded UO2 single crystal thin film,(b) and (c) are images of the corrosion footprint after 500 s, as calculated using finite element modelling, including H_2O_2 surface diffusion and bulk diffusion constants, respectively [5].

Why surface diffusion?

1) Beam enhanced surface effect – photocatalysis?
2) A more reactive short lived oxidising species

[5] R. S. Springell S. Rennie et al., Faraday Discussions (2015) DOI: 10.1039/C4FD00254G.

Research Councils UK Energy For a Low Carbon Future

EPSRC Pioneering research and skills

AWE

DISTINCTIVE

Future Work

- Comparative polycrystalline studies

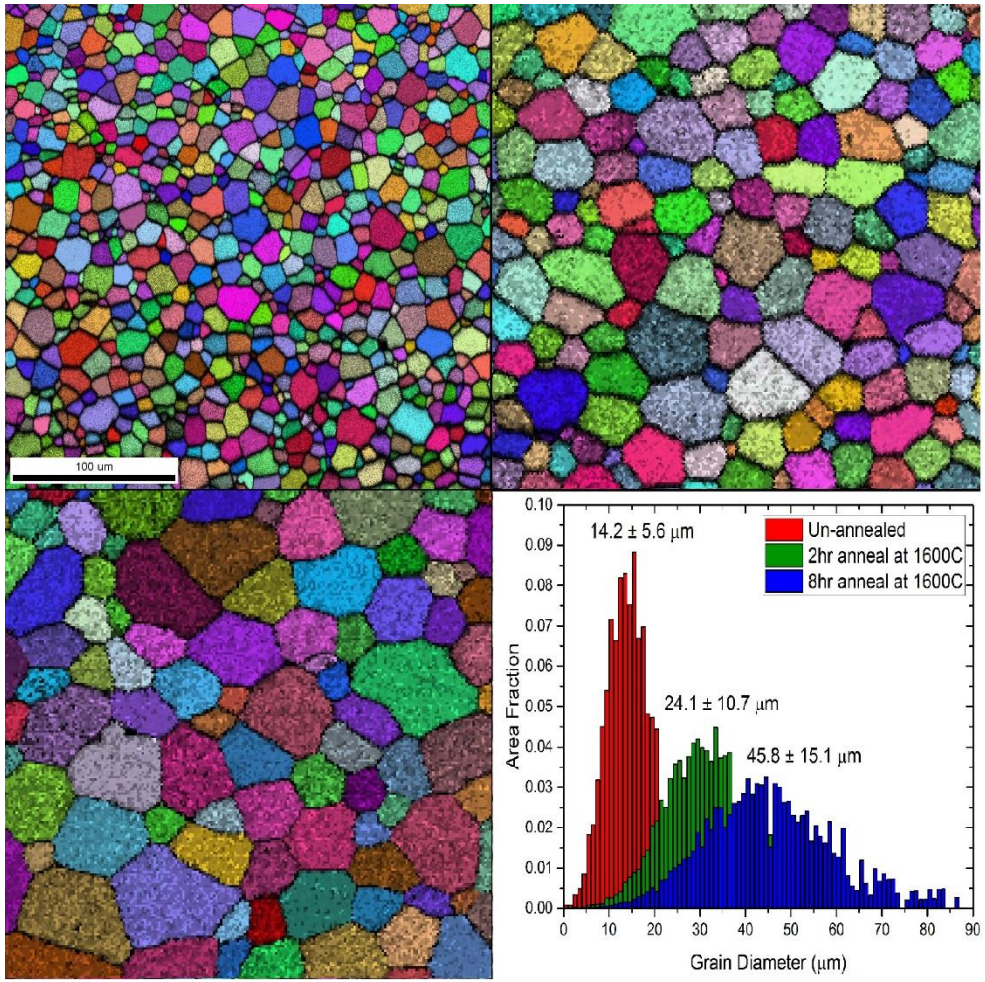

Research Councils UK Energy For a Low Carbon Future

DISTINCTIVE

Future Work

- Comparative α radiation study, to elucidate the role of individual oxidant species

Radiation	$G(H_2O)$	$G(H_2)$	$G(H_2O_2)$	$G(e^-_{aq})$	$G(H^\bullet)$	$G(OH^\bullet)$	$G(HO_2^\bullet)$
γ, fast β	-0.43	0.047	0.073	0.28	0.062	0.28	0.0027
12MeV α	-0.294	0.115	0.112	0.0044	0.028	0.056	0.007

- Comparative technique for investigating the corrosion properties of potential ATFs

Acknowldegments

R. Springell, J. E. Darnbrough, E. Lawrence Bright, J. Sutcliffe, I. Griffiths, L. Costelle C. A. Stitt & T. B. Scott

R. Burrows & H. Sims

P. Thompson & D. Wermeille

J. Rawle & C. Nicklin

C. A. Lucas & E. Cocklin

W. J. Nuttall

G. H. Lander

G. Allen, D. Geeson, J, Glasscott

Transitioning of Spent AGR Fuel from Wet to Dry Storage

James Goode
University of Leeds

Theme 1 Distinctive Meeting 2017
17th October 2017
Rheged Centre, Cumbria

Research Councils UK Energy For a Low Carbon Future

DISTINCTIVE

Introduction

- After decades of use large quantities of nuclear fuel has accumulated in storage ponds;
- Fuel can not be stored in ponds indefinitely;
- In many countries dry storage of spent nuclear fuel (SNF) is used as an interim measure;
- Key requirements for dry storage are criticality prevention, integrity maintenance and retrievability;
- All of these are affected by corrosion and hence the interaction with water.

J. Kyffin, Technological Development to Support a Change in the United Kingdom's Strategy for Management of Spent AGR Oxide Fuel, in: Proceedings of the International Conference on Management of Spent Fuel from Nuclear Power Reactors, IAEA, Vienna, 2015.

"Ongoing Receipt of AGR Fuel | Sellafield Ltd." Accessed July 29, 2014. http://www.sellafieldsites.com/solution/spent-fuel-management/ongoing-receipt-of-agr-fuel/.

Research Councils UK Energy For a Low Carbon Future

DISTINCTIVE

Thesis Outline

- Part 1-Sample Preparation
  - What does the fuel look like when removed from the pond and can I reproduce this.
- Part 2-Vacuum and Flowed Gas Drying
  - A comparison of vacuum and flowed gas drying techniques.
- Part 3-End Point Analysis
  - What indicators are there that drying has completed.

Bound water

- Numerous samples prepared.
  - IGC (HNO_3 + Cr(VII))
  - Pitted ($FeCl_3$)
  - As received.
  - Carbon deposits.
- Dried by TGA with MS.
- Aluminium samples show oxide dehydration.

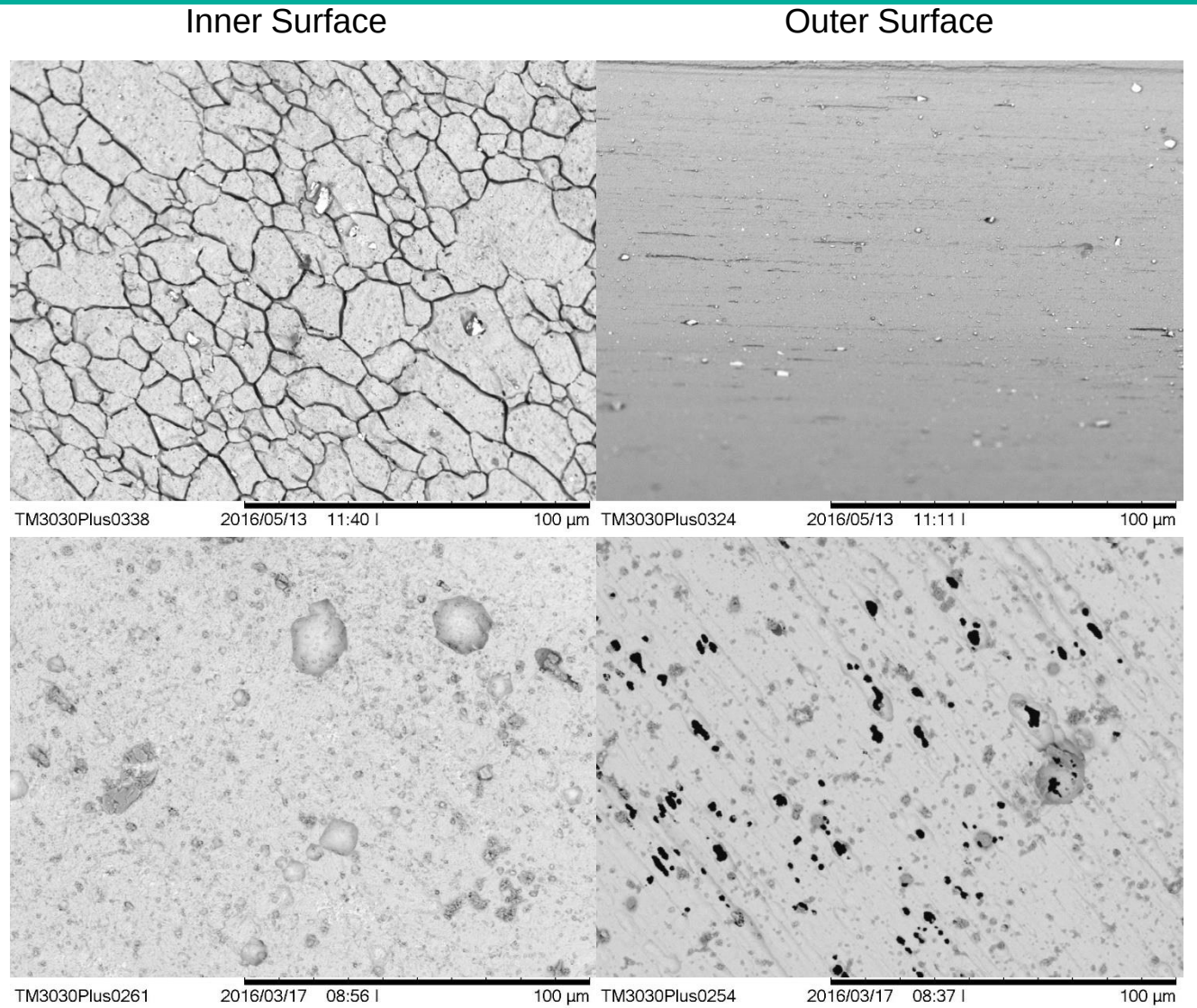

Research Councils UK Energy For a Low Carbon Future

DISTINCTIVE

Surface Differences

- Hardness

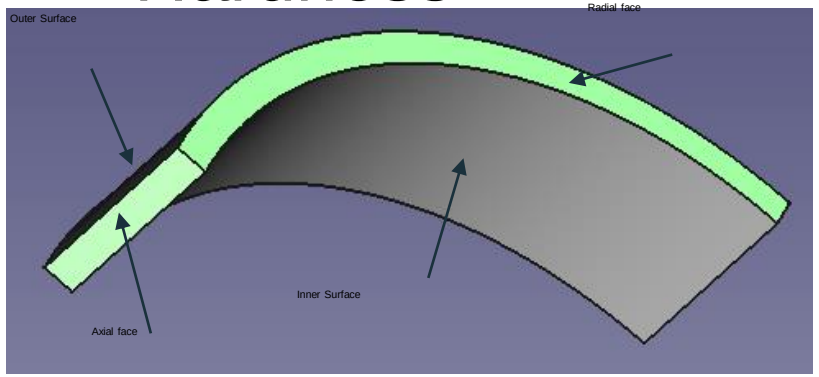

Outer Surface		
Position	Radial	Axial
	[Hv 0.05]	[Hv 0.05]
1	284.3	284.9
2	269.6	288.3
3	271.6	300.9
4	259	286.3
5	279.9	270.5
Average	272.88	286.18
	8.007788	8.83825
RSD	3%	3%
Average	279.53	

Inner Surface		
Position	Radial	Axial
	[Hv 0.05]	[Hv 0.05]
1	278.2	222
2	180.9	268.4
3	233.9	253.6
4	239.2	239.9
5	249.2	190.5
Average	236.28	234.88
	28.88295	24.61269
RSD	12%	10%
Average	235.58	

- TEM/EDX

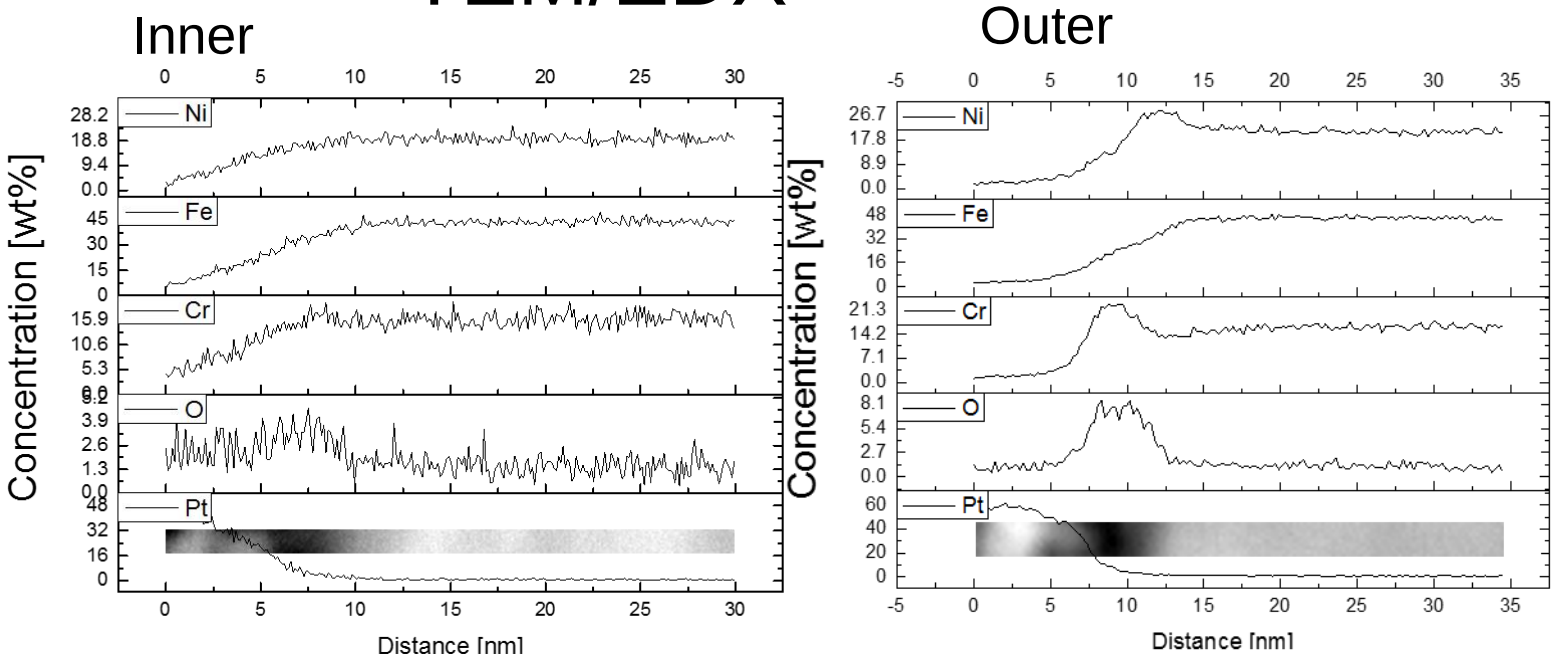

Outer surface is harder and has clearer oxide layer which appears thicker than inner. Outer shows evidence of multiple layers including Si rich band.

Research Councils UK Energy For a Low Carbon Future

DISTINCTIVE

Adsorbed Water

IGC

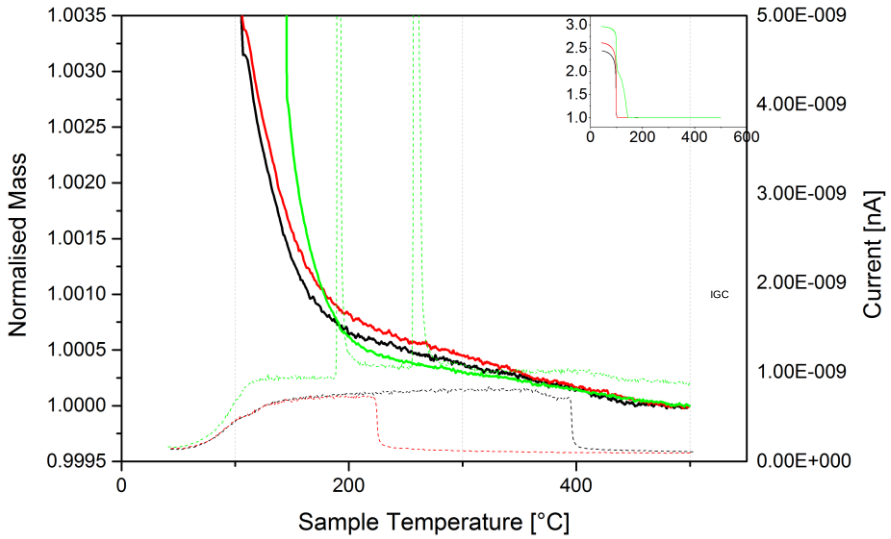

Carbon deposits

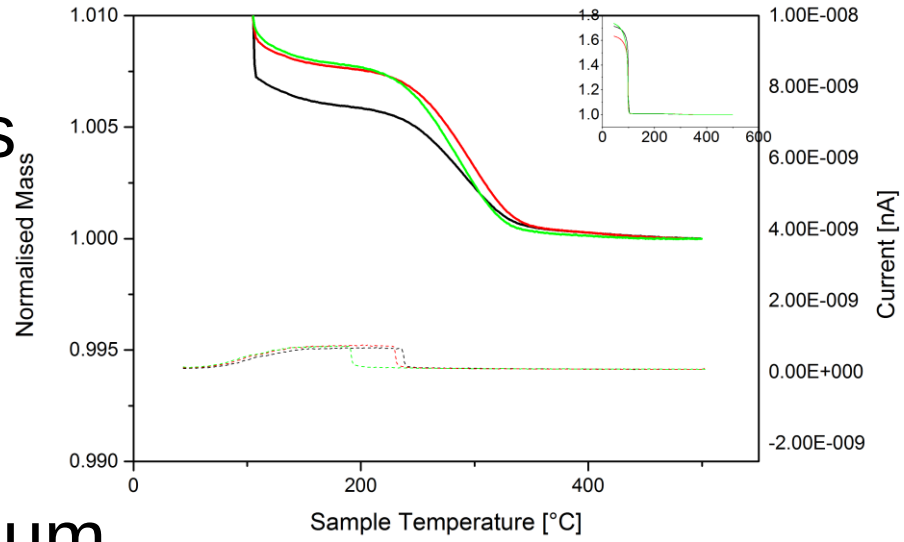

Pitted

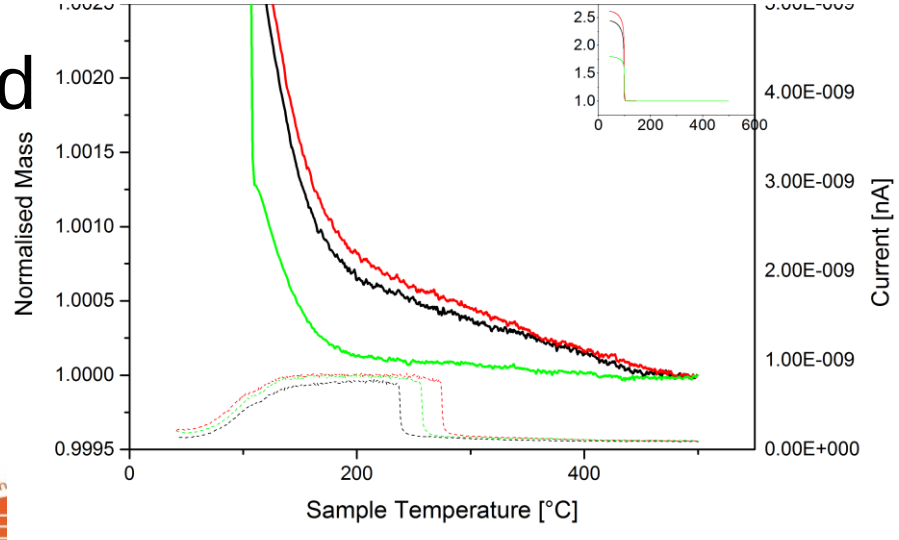

Aluminium

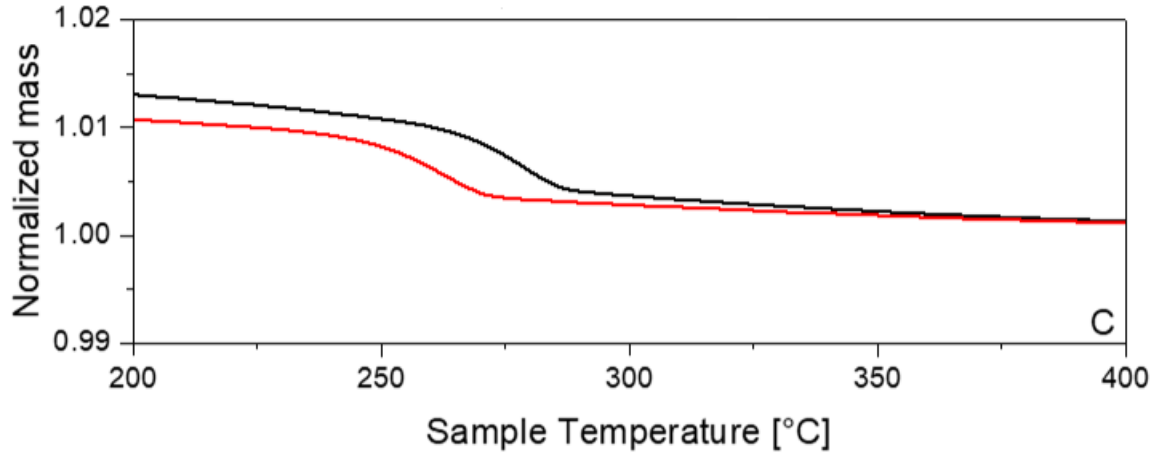

DISTINCTIVE

Stress Corrosion Cracking

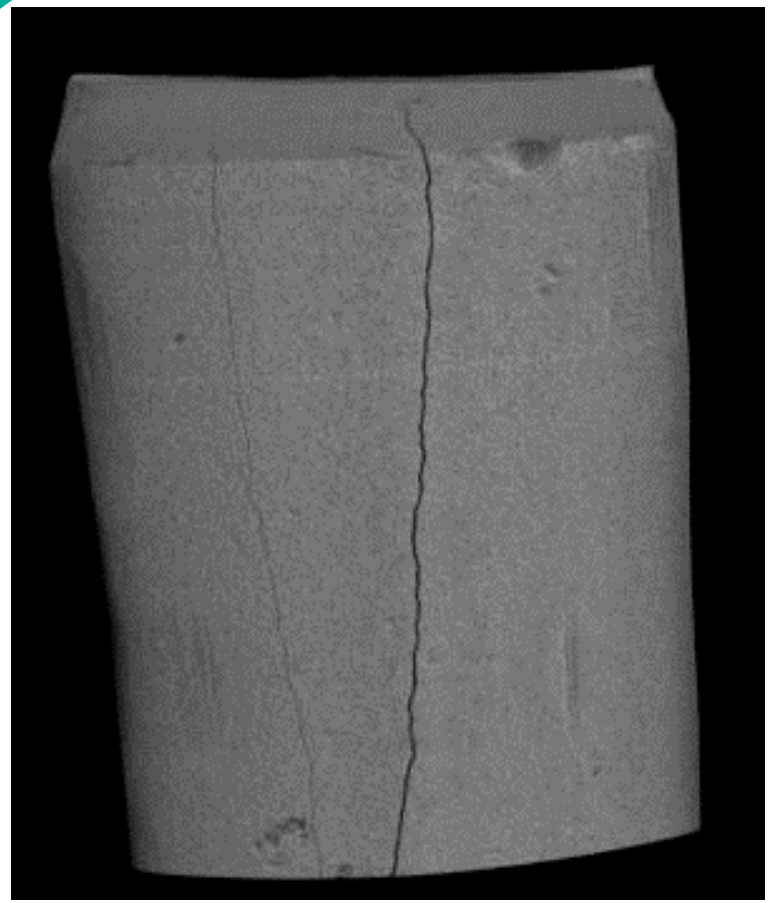

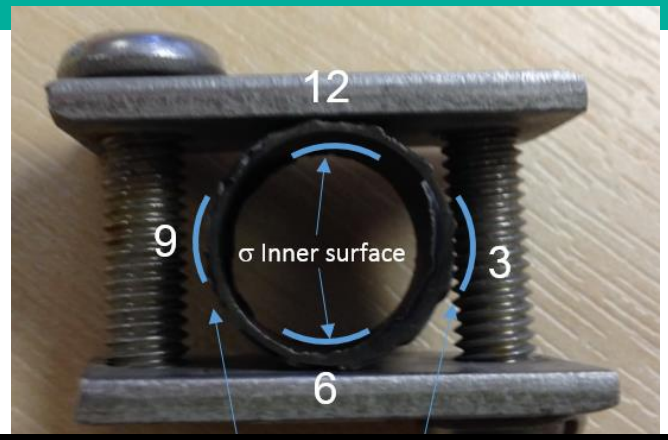

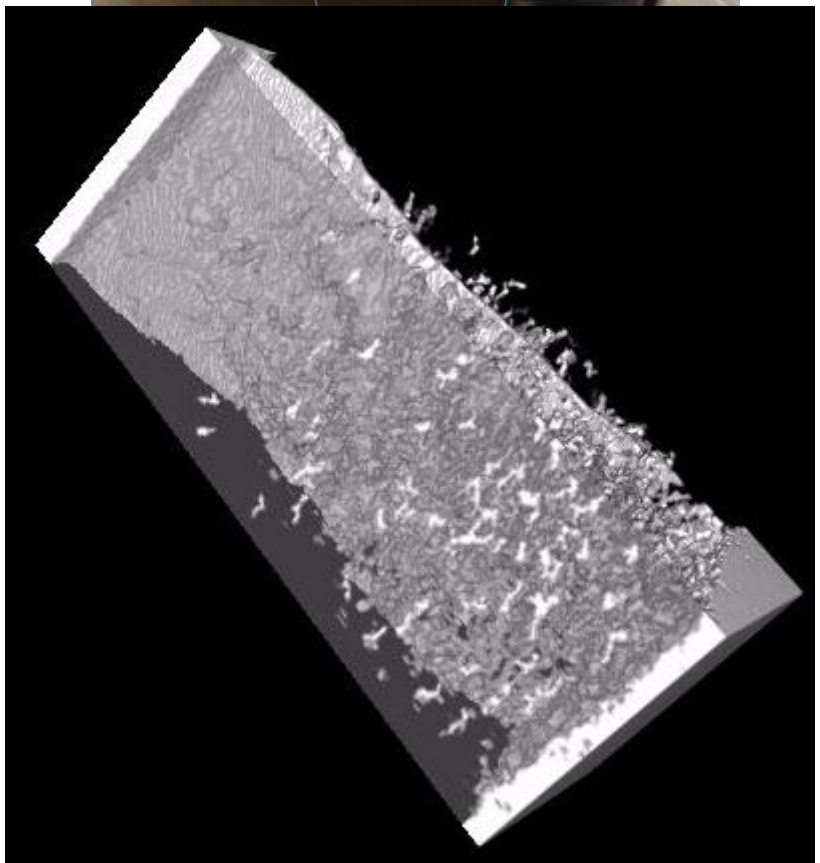

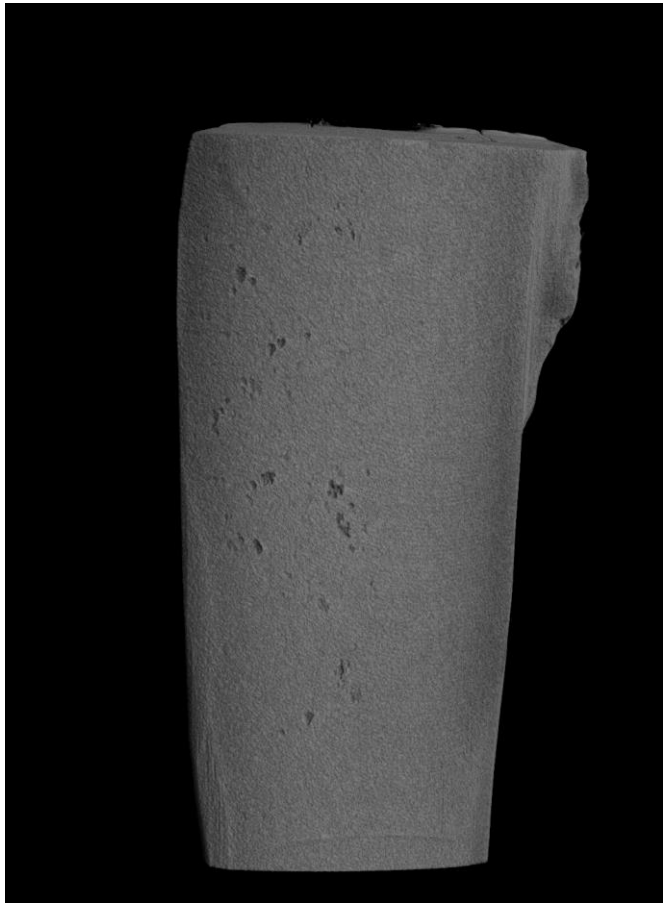

Research Councils UK Energy For a Low Carbon Future

DISTINCTIVE

Drying Rig

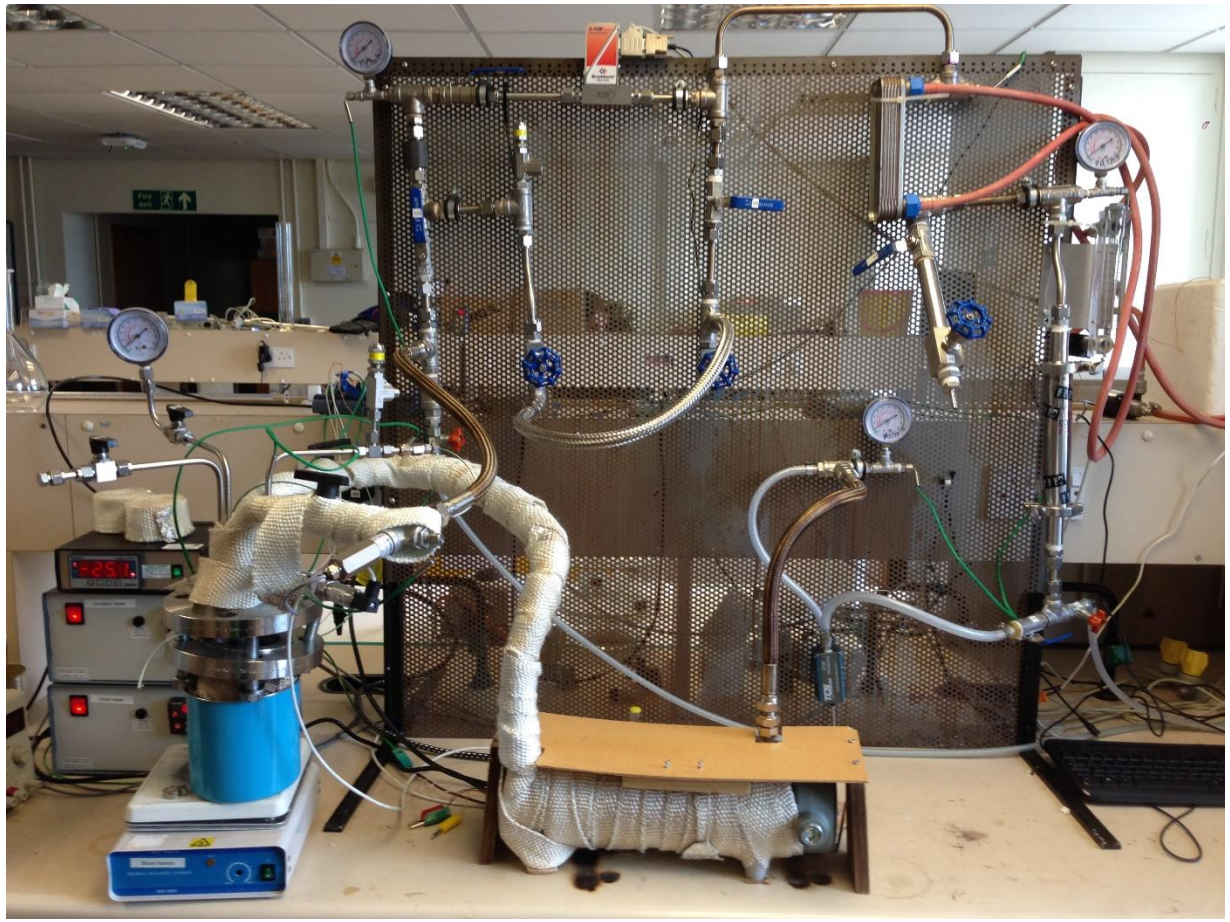

Research Councils UK Energy For a Low Carbon Future

DISTINCTIVE

Vacuum Drying

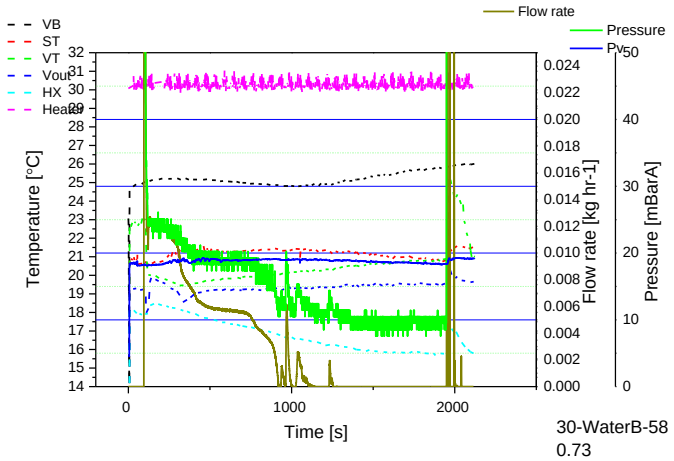

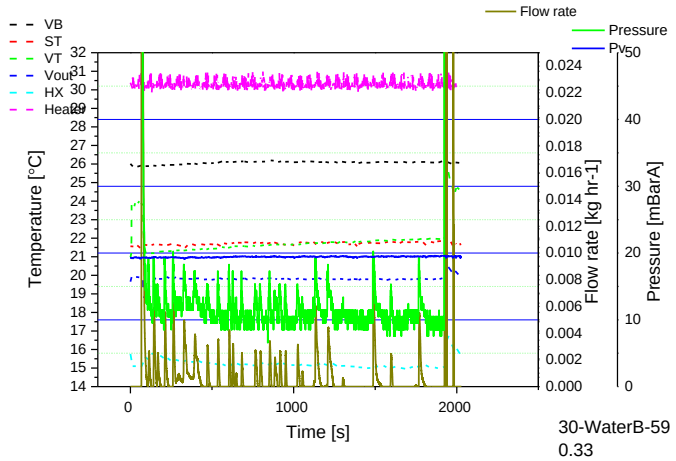

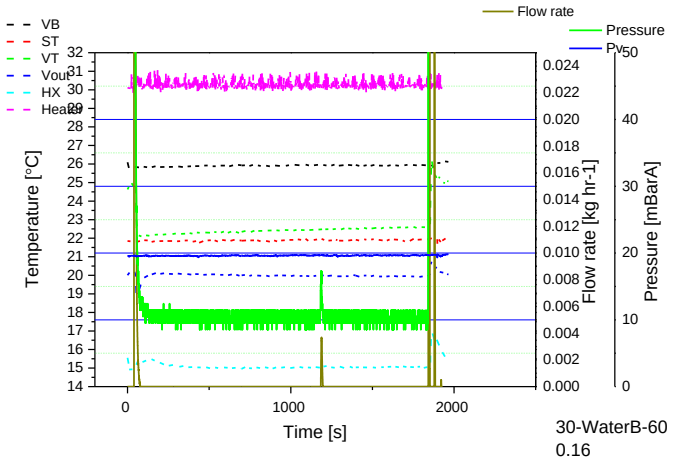

- Three drying regimes- reducing drying rate.
- Generally show similar drying rates for different TP's.

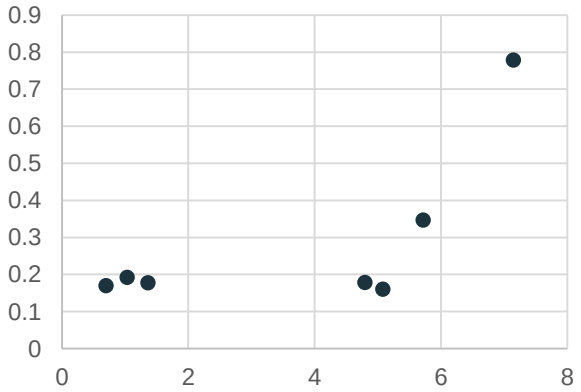

- All three regimes seen in long test.

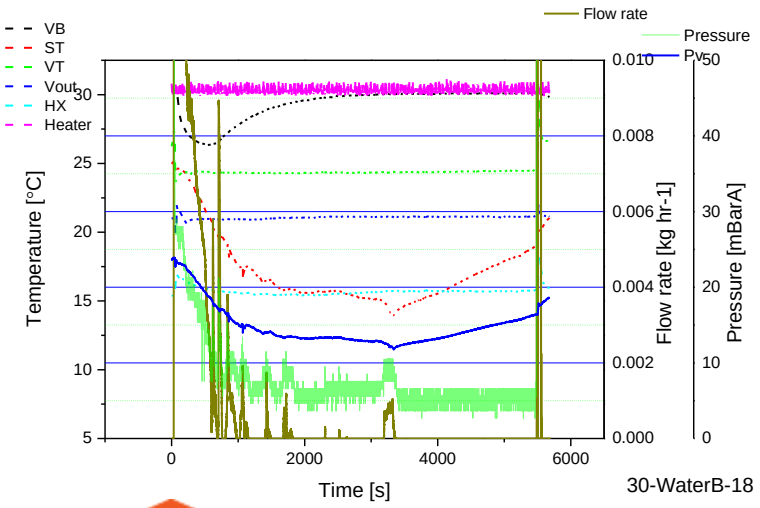

Research Councils UK Energy For a Low Carbon Future

DISTINCTIVE

Cracked Sample Drying

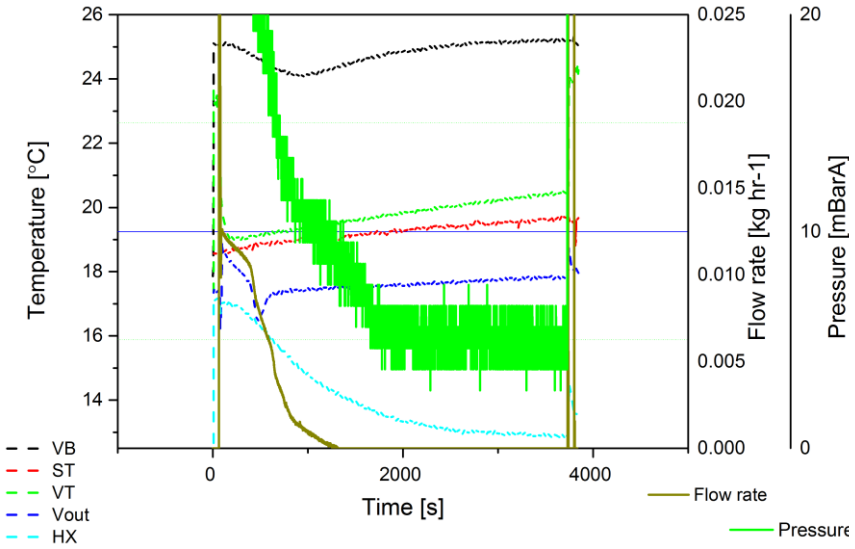

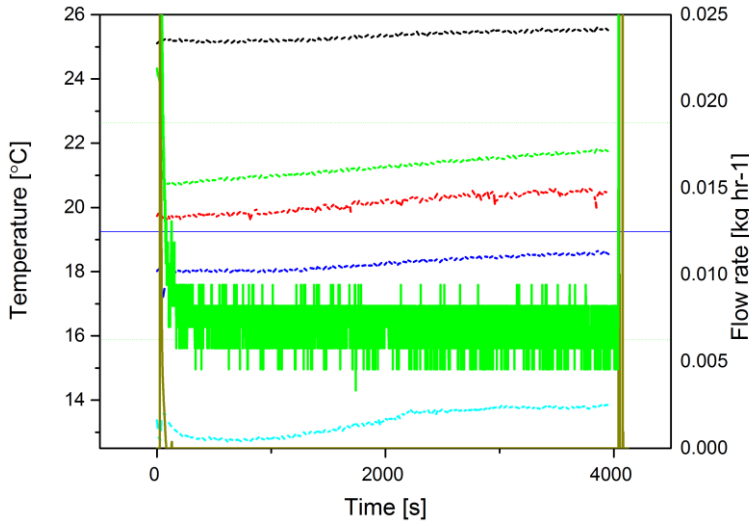

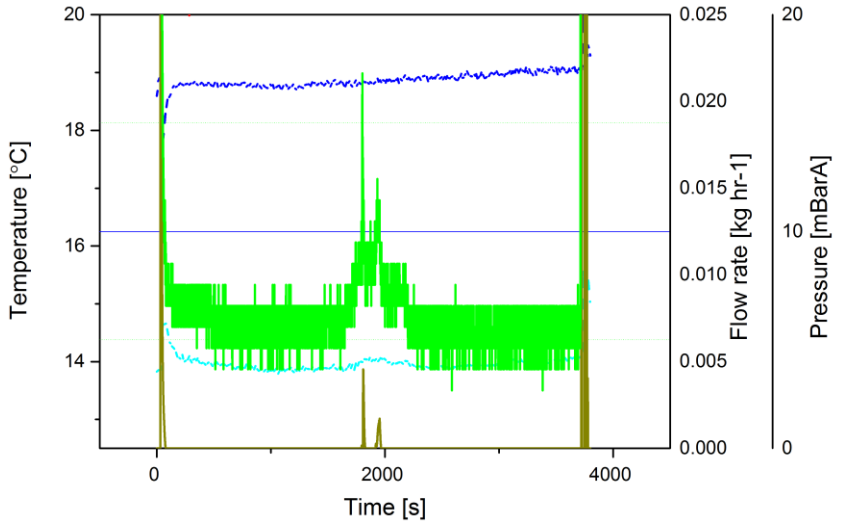

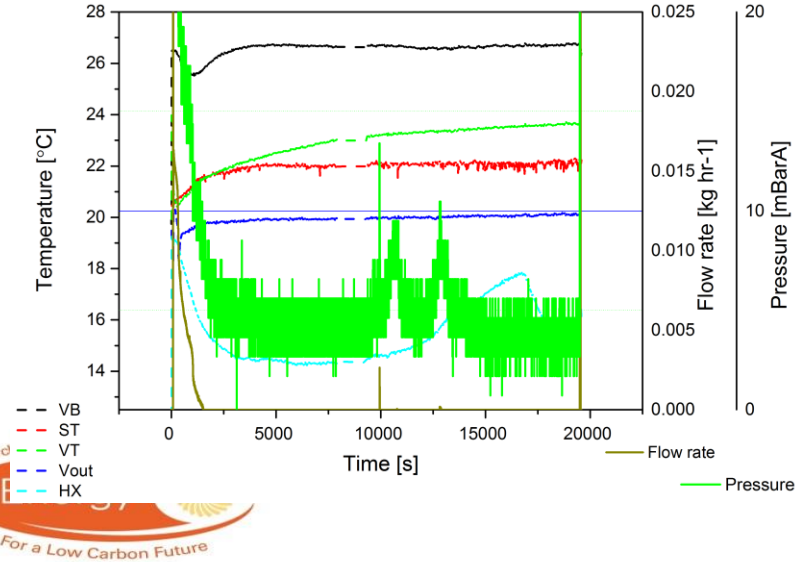

- Generally see three different drying regimes.
- Regime 1 and 2 is broadly similar for both cracked and pinholed samples.
- Regime 3 is significantly slower for cracked sample.

DISTINCTIVE

Flowed Gas Drying

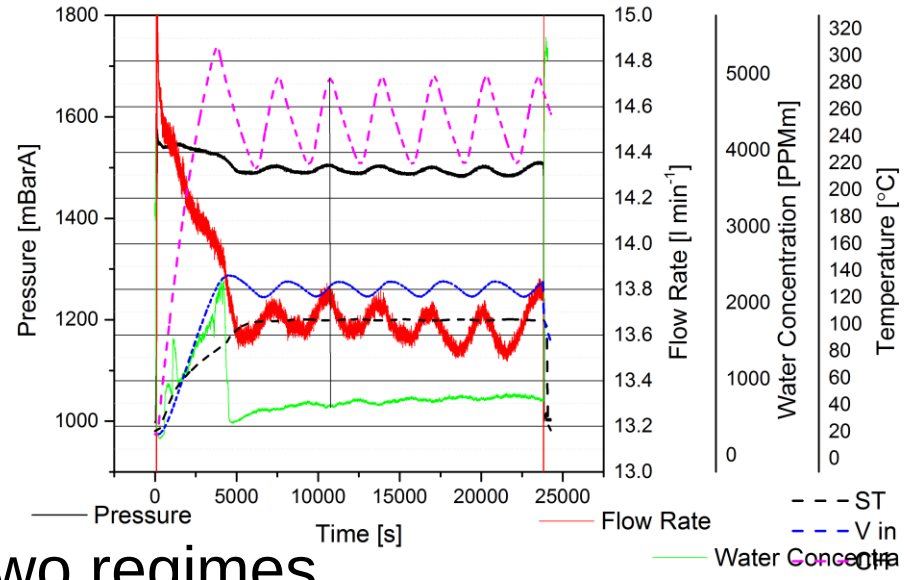

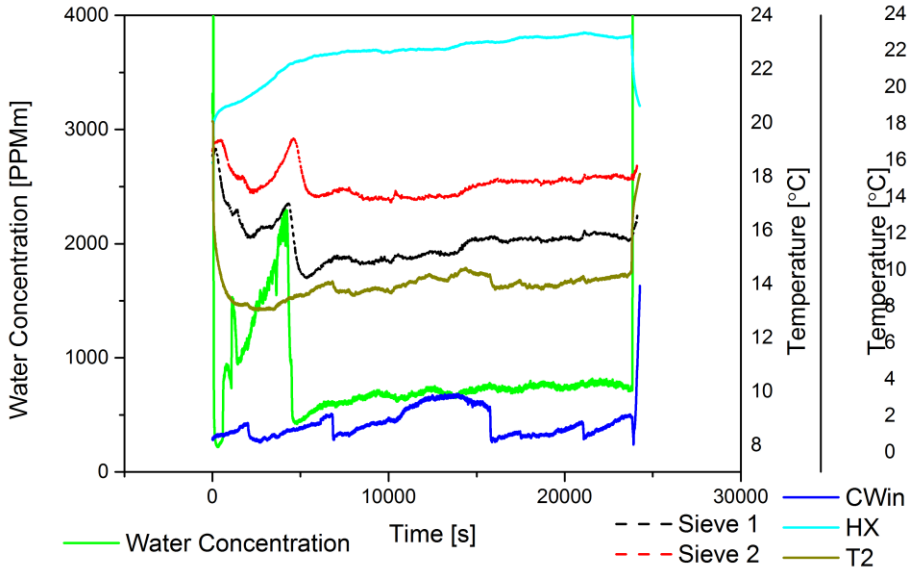

- FGD two regimes
  - initial regime as liquid water forced out and boiled off
  - Evaporation
- Boiling point often not reached despite possibility of pressure drop across defect.

- Drying rates of CSS and SSP again comparable at regime 1 but not at 2.

Research Councils UK Energy For a Low Carbon Future

DISTINCTIVE

Drying Summary

- When TP full there is little difference in rates between two methods or indeed between the two TP's.
- When the TP is empty (evaporation only) VD of pinholed TP is 50% faster for pinholed and 4-10 faster for cracked.
- If the cost of drying is counted then VD remains most efficient.
- Efficiencies likely to be higher for hotter fuel in which case VD may not require any external heating.
- FGD primarily used to prevent overheating.

End Point Determination

- Currently end point determination requires a vacuum rebound test.
- Is it possible to use other data to confirm that an end point has been reached.
- Early indications suggest that from pressure and dew point readings it is possible.

Further Questions

- How does scaling up impact heat transfer?
- How does presence of pellets inside cladding impact drying rate?
- How much slower are much smaller defects (~2μm)?
- How dry does fuel need to be?
- Details on manufacturing of fuel?

Oxidation of UC: an *in situ* high temperature environmental scanning electron microscopy study

Claudia Gasparrini [a], Renaud Podor [b], Denis Horlait [a,c], Michael J Rushton [a], Olivier Fiquet [d], Duncan Coppersthwaite[e], and William Edward Lee [a]

[a] Centre for Nuclear Engineering, Dpt. Materials, Imperial College London, London, UK

[b] Institut de Chimie Séparative de Marcoule, BP17171, 30207 Bagnols-sur-Cèze, France

[c] CNRS, Centre d'Etudes Nucléaires de Bordeaux-Gradignan, 33175 Gradignan, France

[d] Commissariat a l'Energie Atomique (CEA), Cadarache, France

[e] National Nuclear Laboratory, Preston, Lancashire, UK

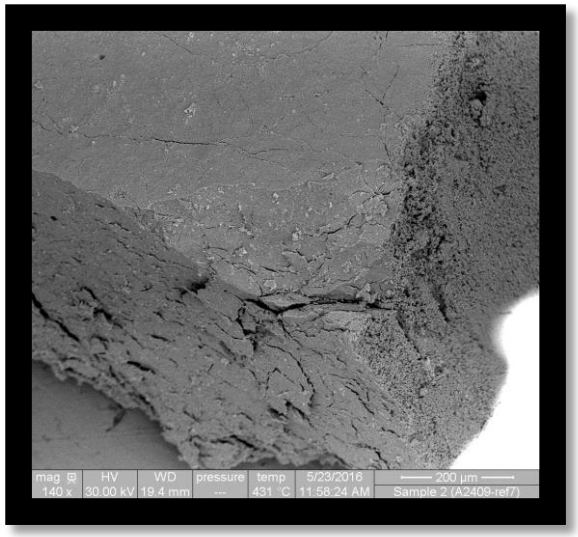

EPSRC
Engineering and Physical Sciences Research Council

Imperial College London

Exotic Fuels: fuel legacy from Prototype Fast Reactor (PFR)

Dounreay PFR

4.5 tonne of Depleted UC are stored at NNL waiting for treatment

Uranium carbide (UC) was used in the '50s in the UK (Dounreay Prototype Fast Reactor) and now has been reconsidered as an advanced nuclear fuel thanks to its :

✓ High thermal conductivity (25 W/(m K) from 1150 – 2250 °C)

✓ Higher fissile material density (1.34 times UO_2)

However it presents further challenges compared to most common UO_2 and $(U,Pu)O_2$:

✗ **UC is reactive with moisture and gases** → Direct disposal is not an option

✗ **UC tends to ignite** (pyrophoricity) → **Hazard**

A solution for disposal? Oxidation!

A **suitable oxide form** needs to be achieved: **C content, specific surface area (SSA)** and **humidity** kept under control

Research problems

Problems encountered at NNL (National Nuclear Laboratory) during past oxidation experiments :

1) Complete conversion to an oxide can not be achieved

No matter the high temperatures (900 -1050^{o}C) and many hours of exposure in the furnace

2) Carbon is found in the oxide

Could either be C of UC left

3) What is the mechanism of oxidation of UC?

4) UC ignition mechanism

Not clear what are the controlling factors (at least 12 factors have been listed in literature!), temperature control in furnace oxidation becomes difficult

Imperial College London

Oxidation of UC: a key step prior immobilisation

Understanding uranium carbide (UC) oxidation is important as it is used for reprocessing or as conditioning treatment before disposal :

DISPOSAL/REPROCESSING

UC
(U,Pu)C

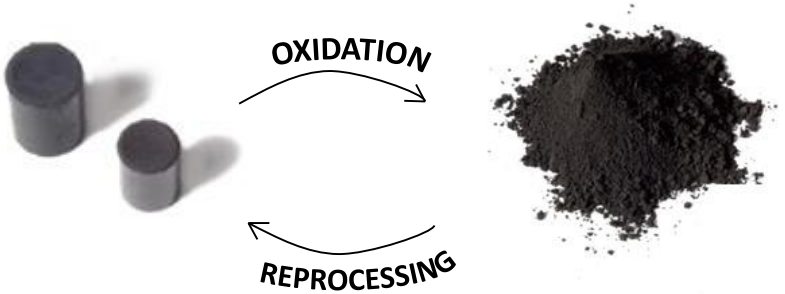

UO_2/U_3O_8
$(U,Pu)O_2$

Proposed mechanism of UC oxidation in oxygen environment:

$$UC \xrightarrow{O_2/\ AIR} U_3O_8$$

Oxidation

$$(1)\ UC + O2 \rightarrow UO_2 + C$$

$$(2)\ C + O_2 \rightarrow CO_2$$

$$(3)\ 3UO_2 + O_2 \rightarrow U_3O_8$$

Ignition

$$UC + \frac{7}{3}O_2 \rightarrow \frac{1}{3}U_3O_8 + CO_2$$

* Iyer, V. S. et al. "Oxidation behavior of carbide fuels". *Nucl. Technol.* 91, 388–393 (1990).

Imperial College London

NATIONAL NUCLEAR LABORATORY

Conversion and C% vs Temperature

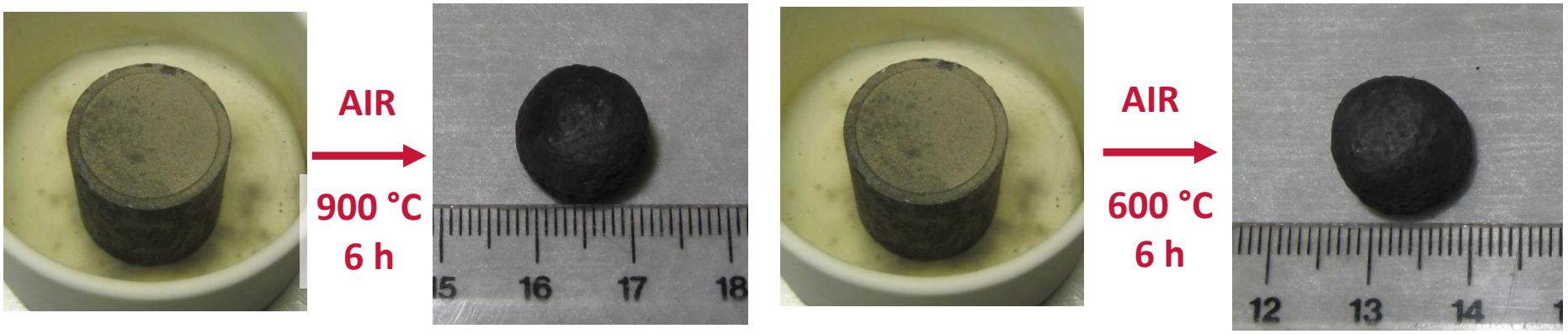

	Mass (g)	T (°C)	Heating rate (°C/min)	Dwell Time (h)	Time in furnace (h)	Ø (mm) UC core	H (mm) UC core	Carbide core mass (g)	Conversion %	C (ppm)
UC	81.54	900	10	6	22	13.39	15.63	21.78	73%	2010
UC	81.85	600	10	6	17	12.86	14.46	19.68	76%	4690

Imperial College London

NATIONAL NUCLEAR LABORATORY

Results:

1) Complete conversion to an oxide can not be achieved

Small scale oxidation experiments on UC pellets and fragments in furnaces

T=600 °C - 4h

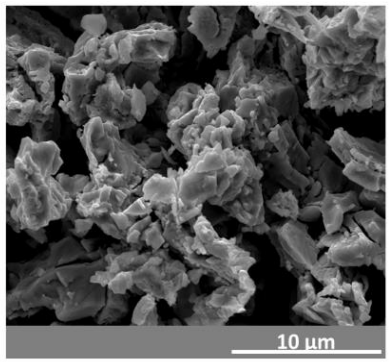

T=900 °C - 4h

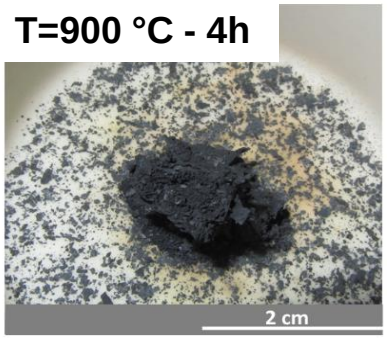

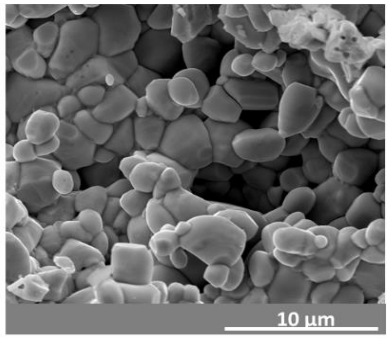

T=900 °C – 17 h

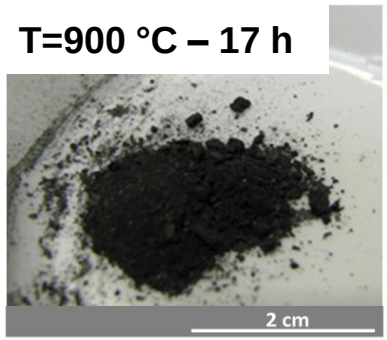

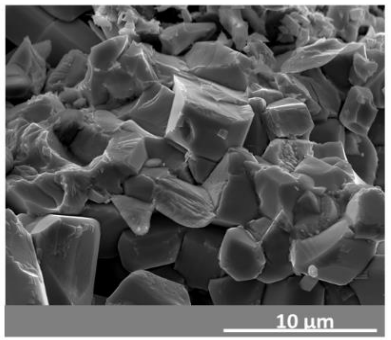

$UC \xrightarrow{\text{OXIDATION}} U_3O_8$

T

900 °C ↘ 600 °C

↑ SSA ↓ TIME ↑ CONVERSION

- ✓ At 900 °C the oxide sinters and acts as a barrier to oxidation.
- ✓ Reducing the temperature to 600 °C helps oxide conversion, fine powder is formed.

Imperial College London

Temperature influence (T≥ 600°C) on oxidation: oxide sintering

10 Pa O_2 T = 600°C → oxidation completed in 20 minutes

Oxidation occurs all over the surface as soon as sample is in contact with oxygen

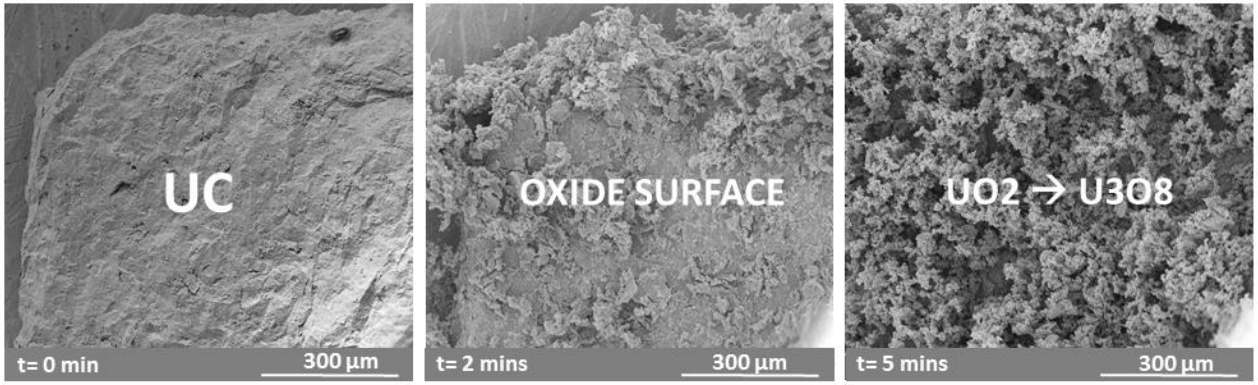

10 Pa O_2 T = 800°C → oxidation not yet completed in 3 hours

Oxidation occurs at the edges first whilst the top surface appeared compact due to partial sintering of the oxide. Stress build-up promotes cracks which generate the next surfaces to oxidise.

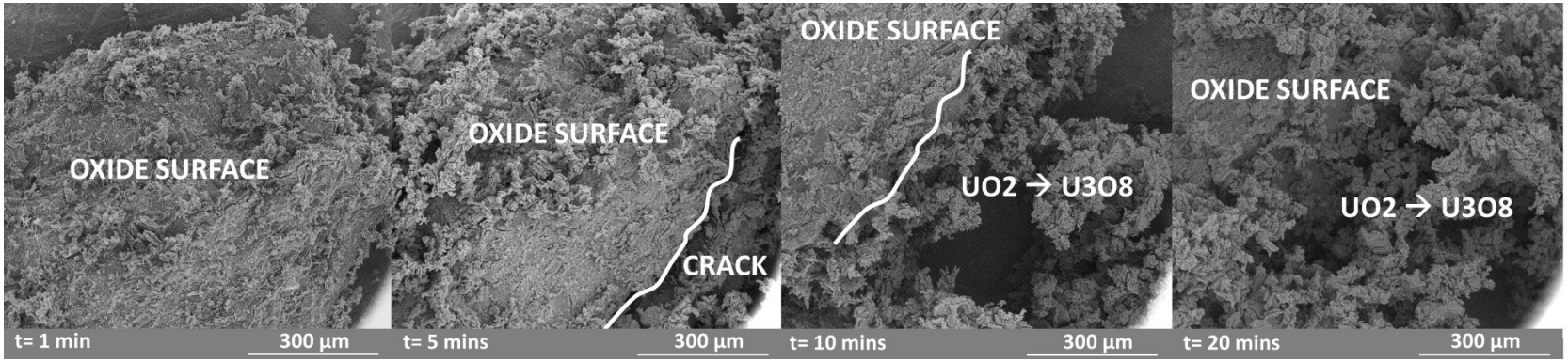

Imperial College London

Imperial College London

Results:

4) UC oxidation and ignition mechanism

UC samples manufactured from CEA, Cadarache, France were transported to ICSM, Marcoule, France for HT-ESEM experiments.

Transformation from UC to UO_2 and UO_2 to U_3O_8 was investigated in atmosphere of 10-100 Pa O_2 from 450-575°C

- **UC → UO_2**

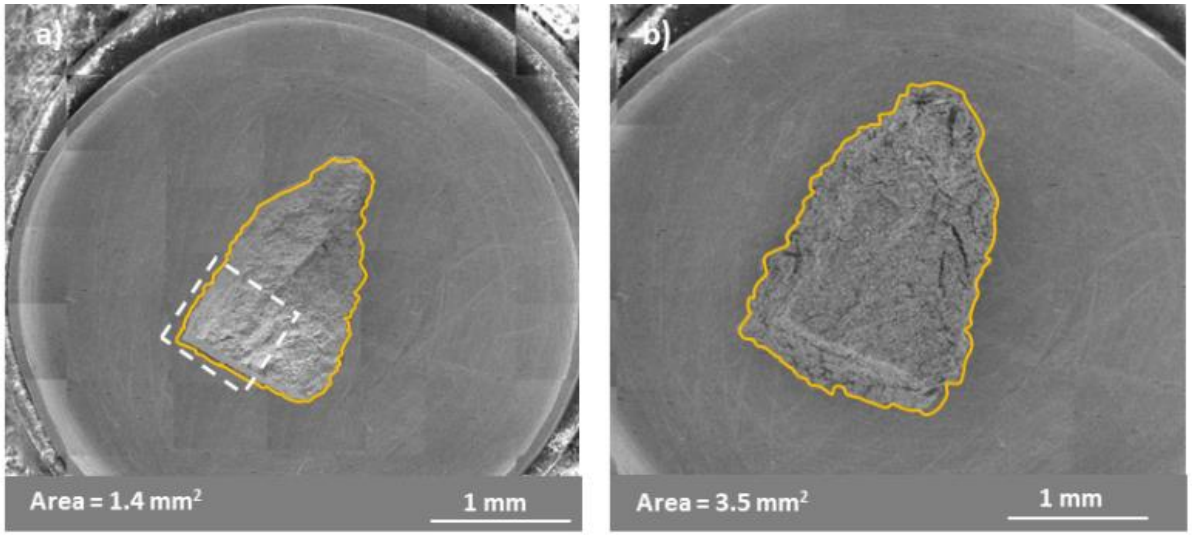

10 Pa O_2 450 °C

Imperial College London

Image analysis techniques: sample area expansion and crack propagation

Image processing via Fiji ImageJ is used to get information on sample expansion, crack propagation, crack length and network during oxidation.

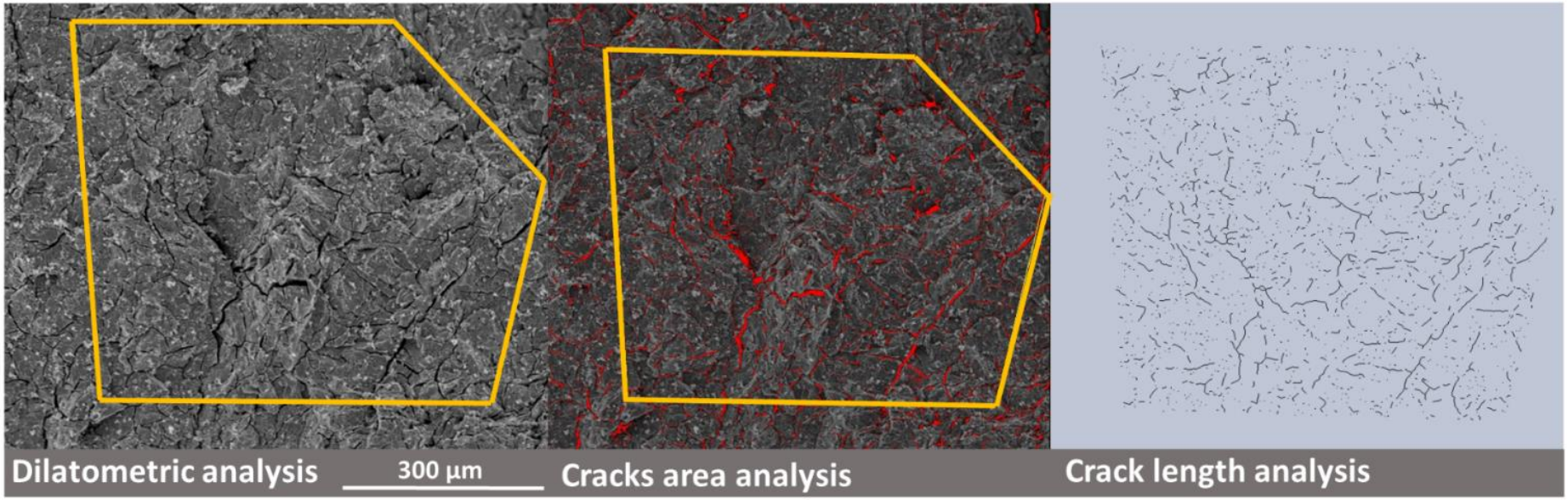

* Gasparrini, C et al. "Oxidation of UC: an *in situ* high temperature environmental scanning electron microscopy study". *J Nucl Mat*, 494, 127-137, (2017)

In situ UC oxidation in a HT-ESEM

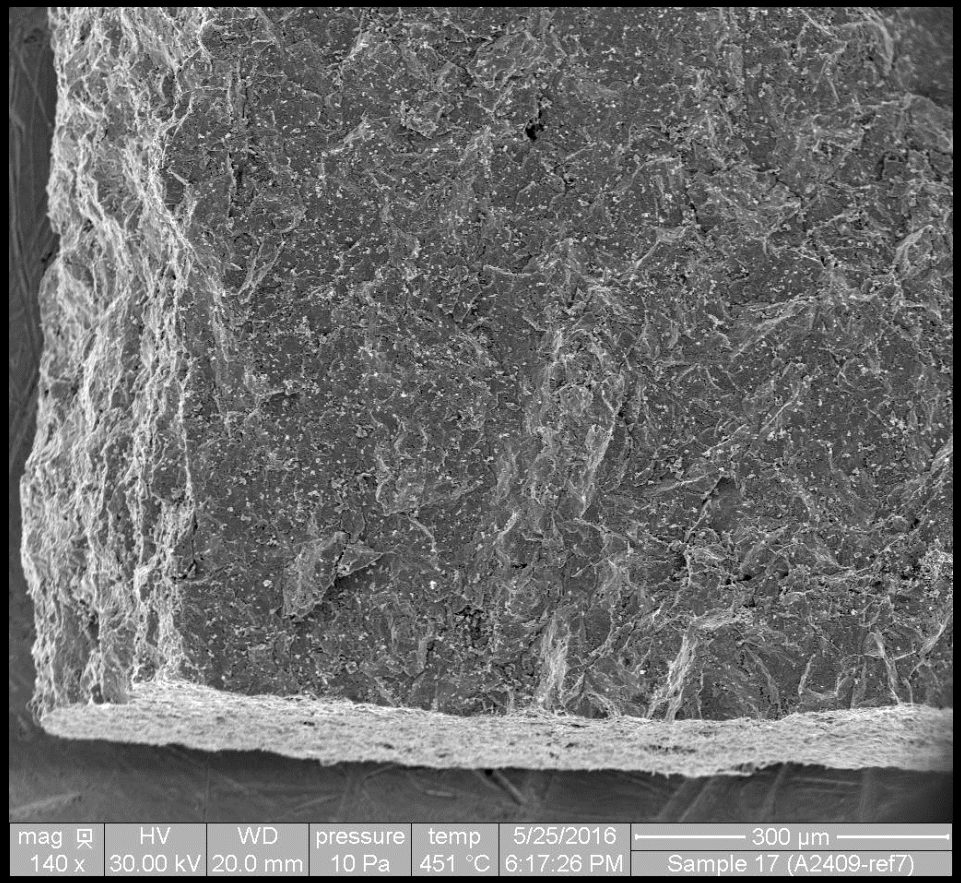

T = 450˚C

PO_2 = 10 Pa

Time = 6 h (shown in 35 seconds)

UC transformation to UO_2 (450 ^oC 10 Pa O_2)

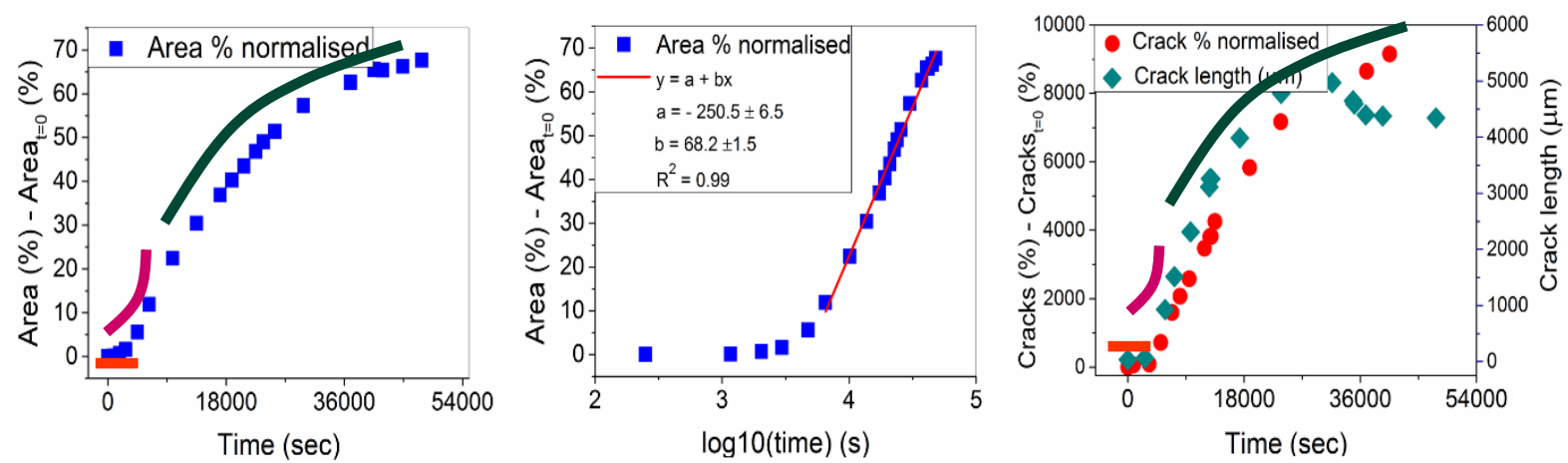

Sample area expansion and crack propagation follow a similar trend comprised of: induction period, exponential area expansion and crack propagation followed by and logarithmic trend.

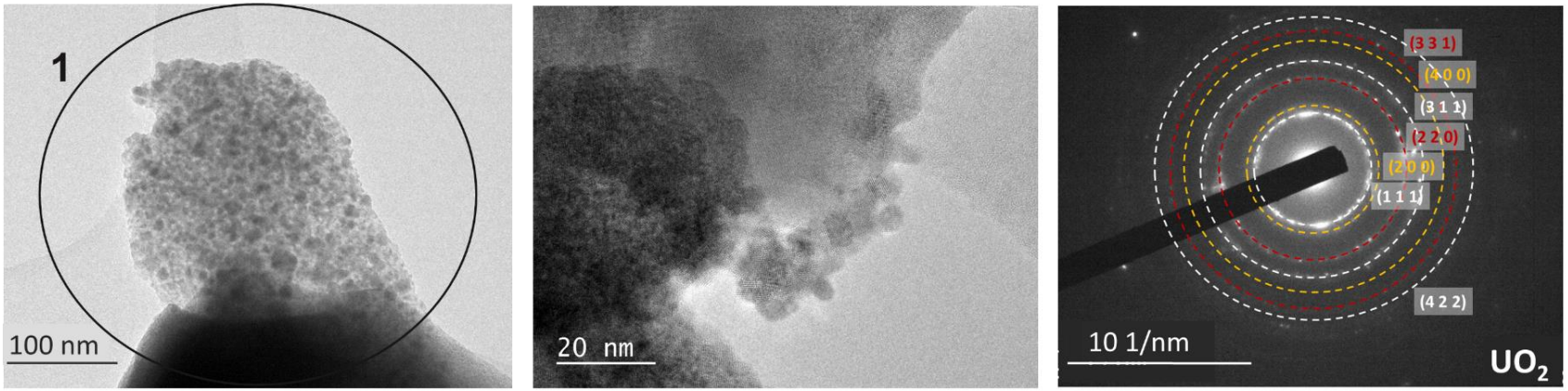

HRTEM analysis shows the oxide to be polycrystalline UO_2

Imperial College London

Results:

4) UC oxidation and ignition mechanism

- UC → U_3O_8

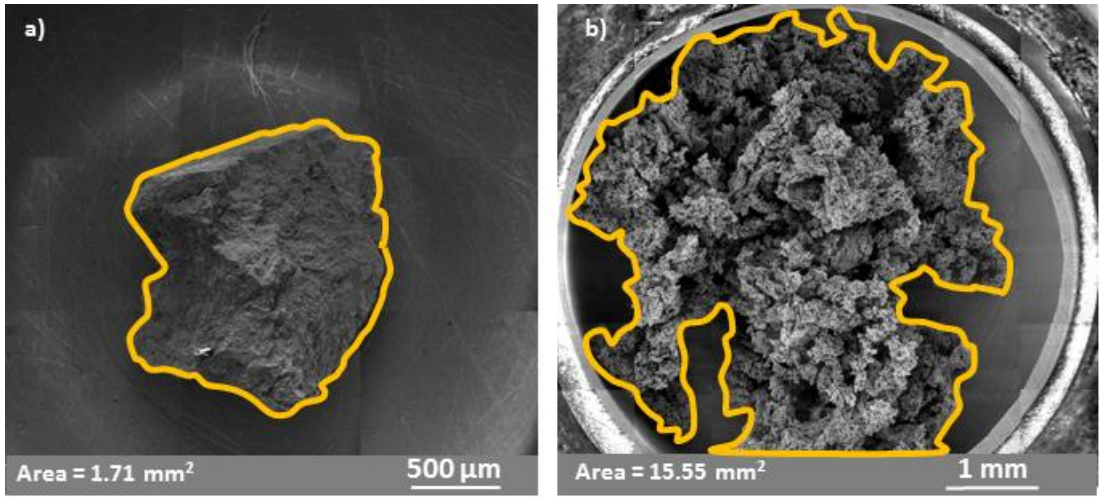

50 Pa O_2 450 °C

UC oxidation in a HT-ESEM

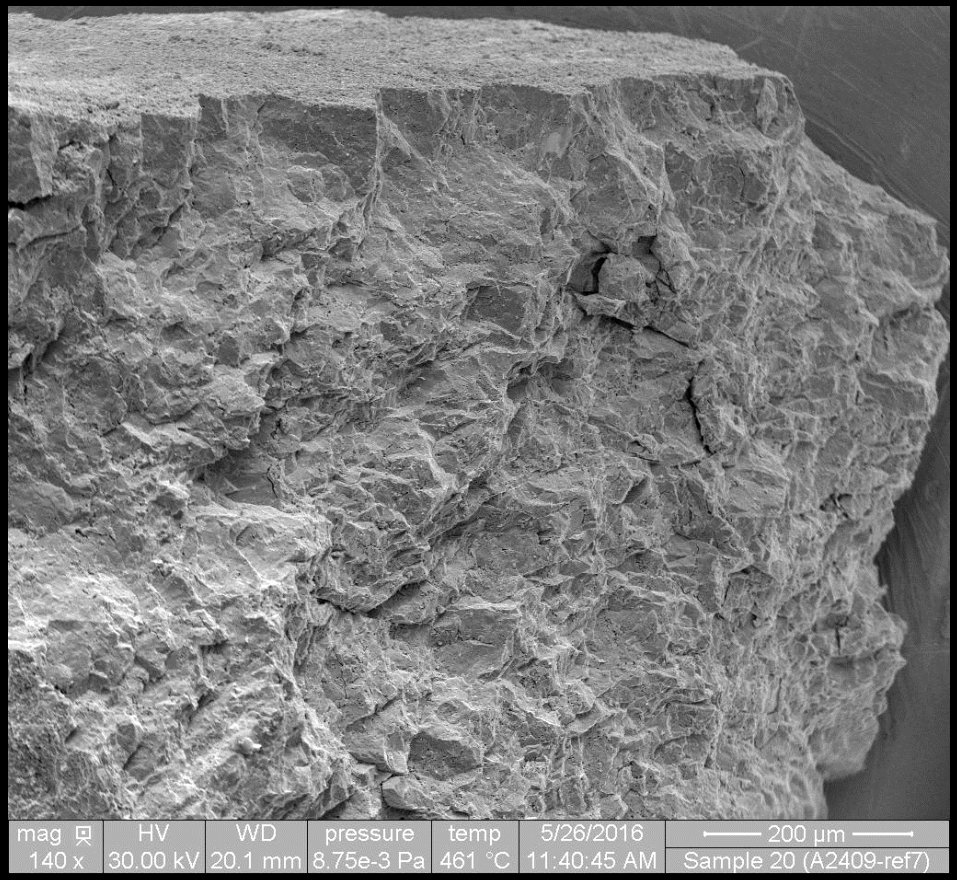

T = 450˚C

PO_2 = 50 Pa

Time = 3 h (shown in 23 seconds)

Imperial College London

UC transformation to U_3O_8 (450 ^oC 50 Pa O_2)

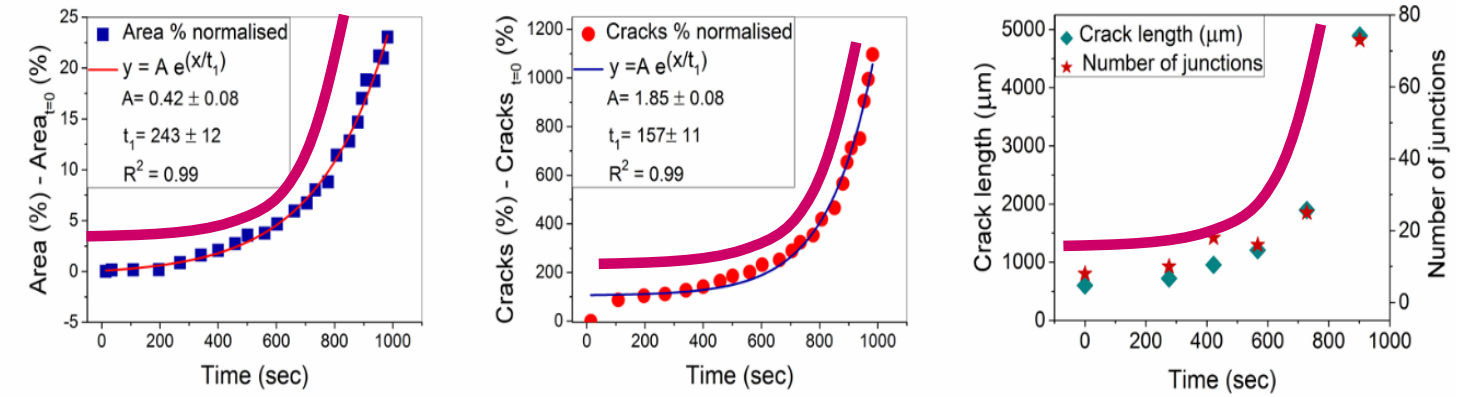

Sample area expansion, crack propagation crack length and number of junctions all follow an exponential trend. UC ignition is triggered by the fragmentation of the sample.

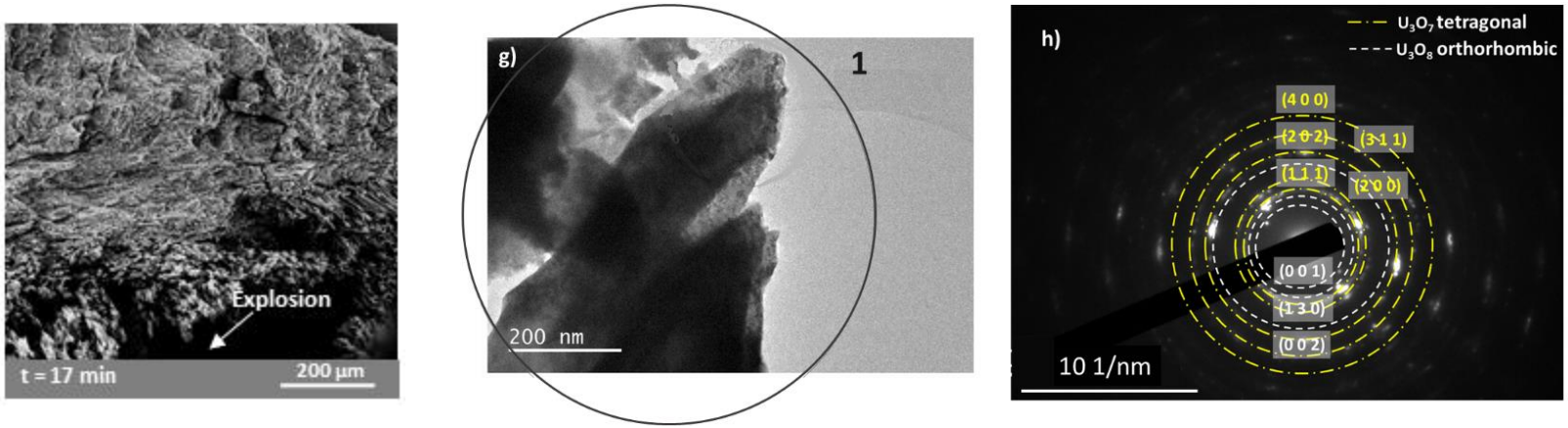

HRTEM analysis shows the oxide to be orthorhombic U_3O_8 and tetragonal U_3O_7. U_3O_8 transformation is triggered by ignition of UC which propagates as a SHS reaction.

Imperial College London

Self-propagating high-temperature synthesis (SHS)

The slow motion popcorn-like explosion recorded on a sample oxidised at 575 °C in 10 Pa O_2 shows the propagation front of the SHS reaction.

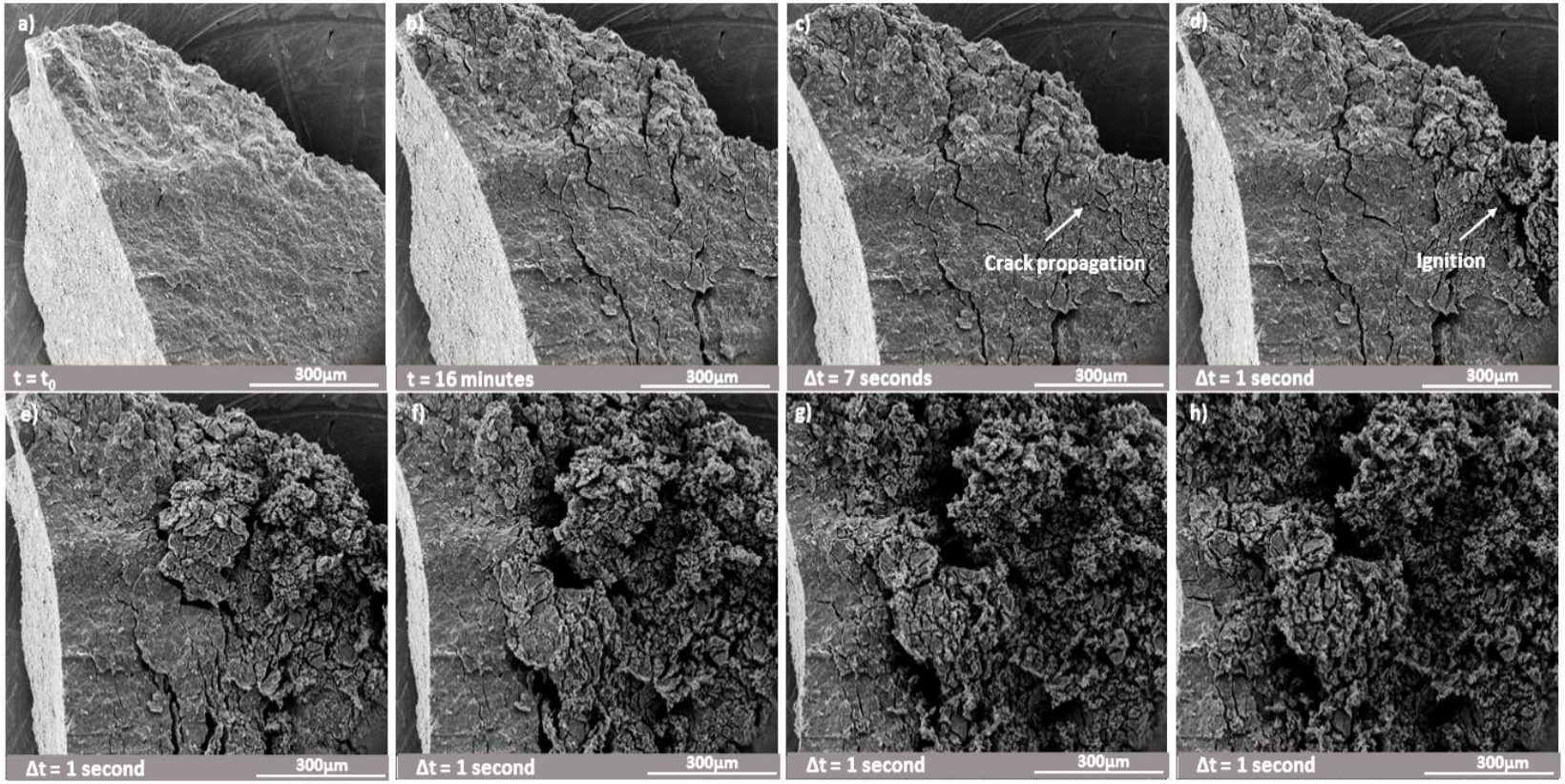

The SHS reaction in this sample propagates with a speed between 150 – 500 ± 50 µm/s across the sample.

Imperial College London

UC oxidation pathways

The morphological changes during transition from UC to UO_2 and from UC to U_3O_8 have been monitored *in situ*. These are characterised by two pathways: a non explosive (pathway 1) and an explosive one (pathway 2).

Pathway 1: UC → UO_2

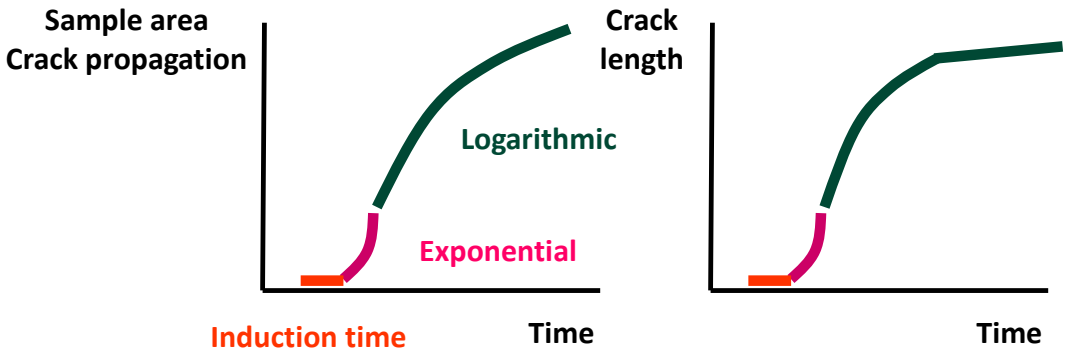

Pathway 2: UC → U_3O_8

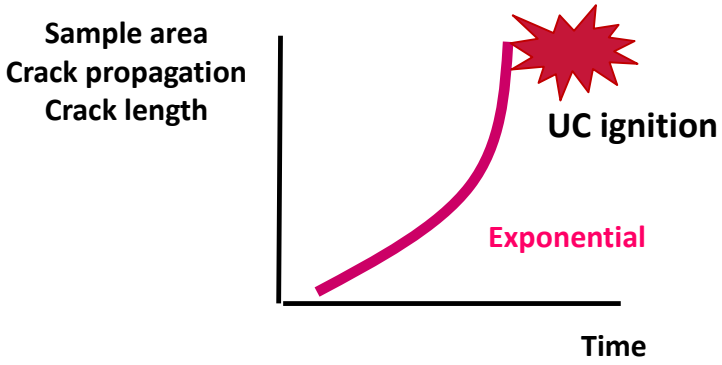

t_1 > 740 ± 49 s

Exponential law : $y = A\, e^{(x/t_1)}$

t_1 < 470 ± 14 s

* Gasparrini, C et al. "Oxidation of UC: an *in situ* high temperature environmental scanning electron microscopy study". *J Nucl Mat*, 494, 127-137, (2017)

Imperial College London

Conclusions

$UC \rightarrow UO_2$

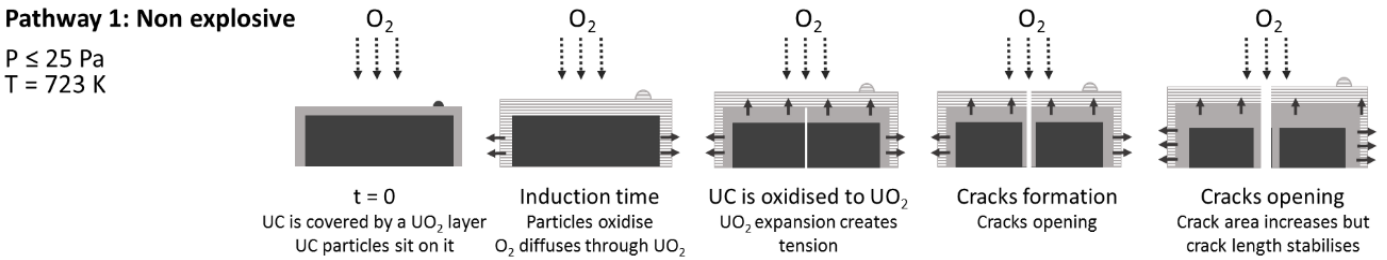

$UC \rightarrow U_3O_8$

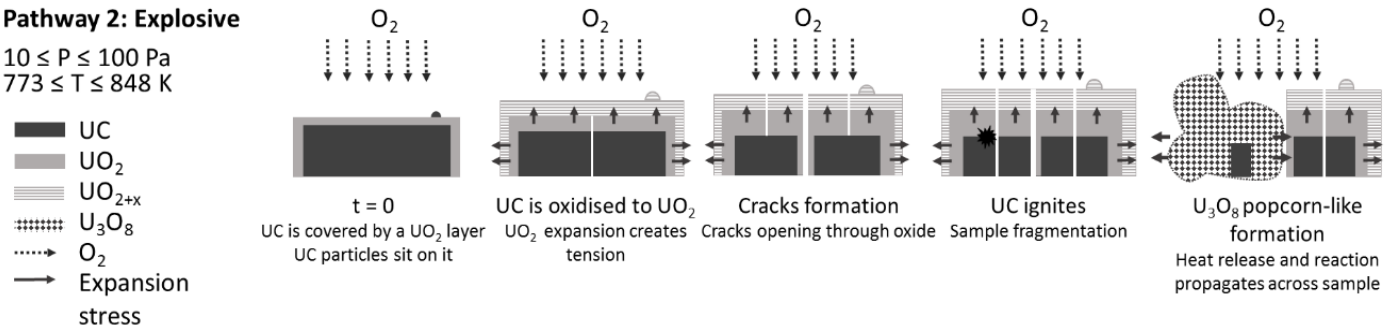

- *In situ* HT-ESEM study on UC oxidation reveals the influence of T and PO_2 on the transformation between UC to UO_2 and U_3O_8 below 600 °C.
- Above 600 °C the oxide sinters and limits the oxidation acting as a barrier
- A method for the correlation of crack propagation and sample expansion has been developed via Fiji ImageJ. Crack network is responsible for UC ignition. UC oxidises to UO_2 when growth factor $t_1 \geq 740 \pm 49$ s, or to U_3O_8 when $t_1 \leq 470 \pm 14$ s.
- UC ignition to U_3O_8 triggers a SHS reaction which propagates throughout the sample.

Thanks for your attention!

And special thanks to all the people at NNL, ICSM, CEA and Imperial that made this project possible !

NATIONAL NUCLEAR LABORATORY

icsm

DE LA RECHERCHE À L'INDUSTRIE cea

EPSRC
Engineering and Physical Sciences Research Council

Particle Technology & Fluidization
Life Cycle Assessment
Research
Group

UCL

A life cycle approach to Used Nuclear Fuels management

Mr. Andrea Paulillo & Prof. Paola Lettieri
Department of Chemical Engineering, University College London

Prof. Roland Clift
Centre for Environmental Strategy, The University of Surrey

Dr. Jonathan M. Dodds & Dr. Stephen J. Palethorpe
National Nuclear Laboratory

Mr. Andrew Milliken
Sellafield Ltd.

Presentation outline

- Introduction: Life Cycle Assessment – What? Why? How?
- Objectives
- A novel methodology for assessing radionuclides impact in LCA
- LCA case studies
  - Assessing the impact of the current approach in the UK
  - Looking at future options
- Conclusions and future work

Life Cycle Assessment

What is it?

LCA is a technique for assessing potential impacts of industrial systems.

Life Cycle Assessment

Why?

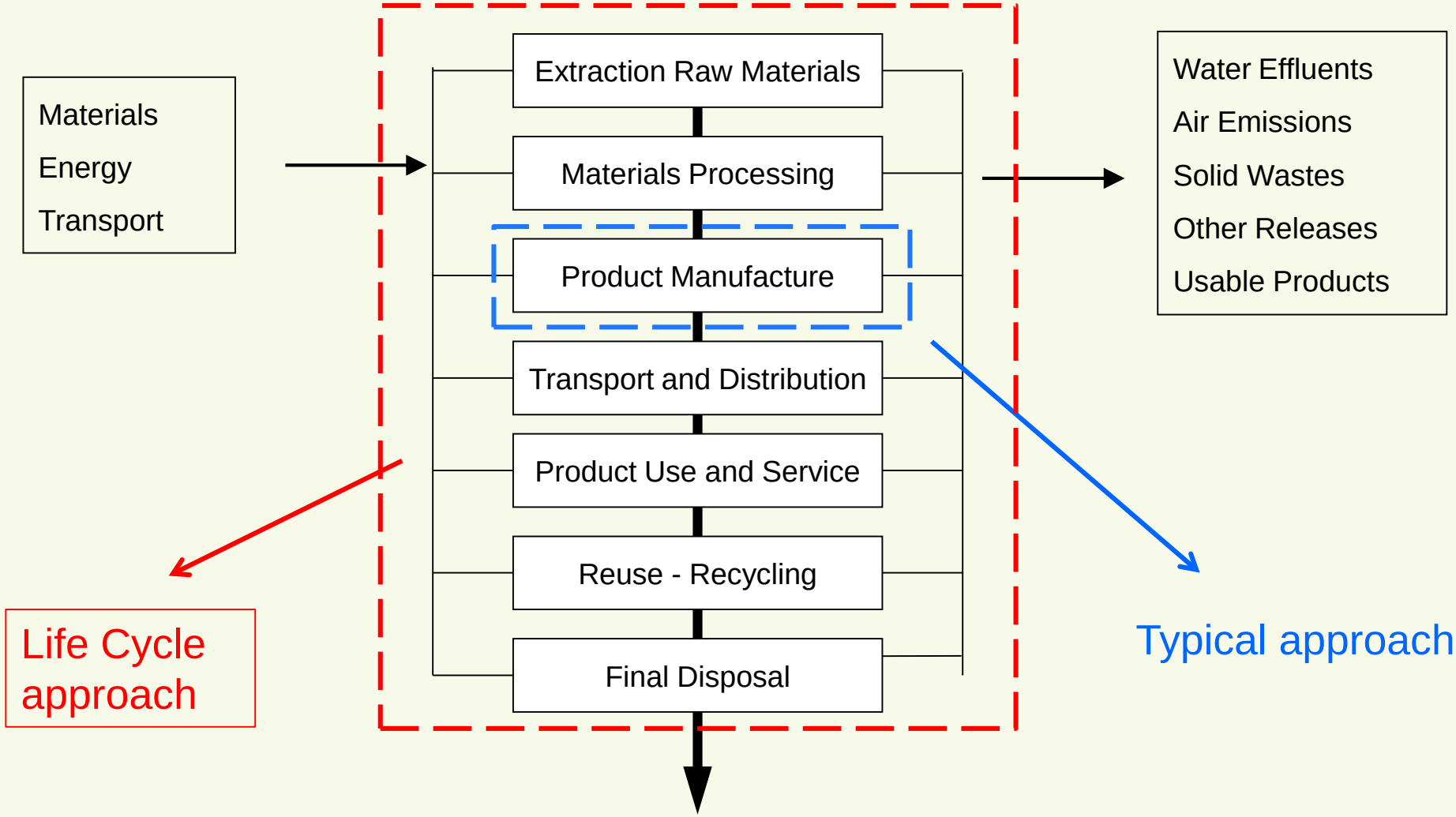

Life Cycle Assessment
How?

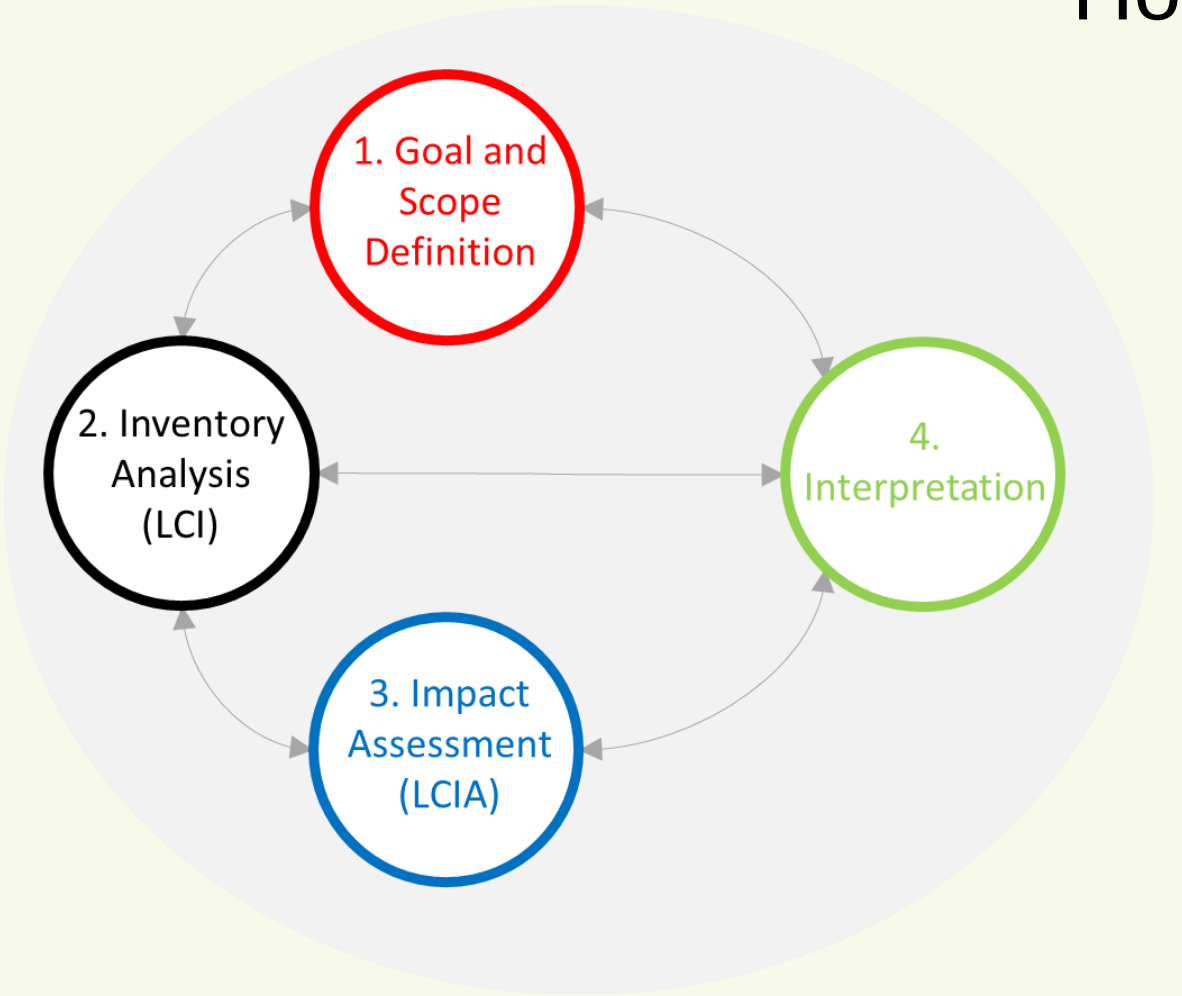

Life Cycle Assessment framework

Impact categories	Units
Acidification	Mol H^{+-}eq.
Climate Change	kg CO2-eq.
Eutrophication	Kg/mol N-eq.
Ozone Depletion	kg CFC-11-eq.
Human Toxicity	CTUh
Ecotoxicity	CTUe
Etc…	

Pollutant (kg emitted)	CC Impact factor (kg CO_2 equiv.)
CO_2	1
CH_4	24
CFC	400

The issue of applying LCA to the nuclear industry

- Very few and not comprehensive LCA studies.
- **Reason:** lack of a standard, comprehensive methodology for assessing the impacts of radioactive emissions and solid nuclear waste.

Objectives

1. Develop a LCA methodology for assessing the human impacts of radioactive emissions and solid nuclear waste disposed in a final repository.

2. Assess the impacts of current and future approaches for managing Used Nuclear Fuels (UNFs) and nuclear wastes in the UK.

Use:

- ❑ Support **decision-making process** within the nuclear industry;
- ❑ Improve **public knowledge** of the nuclear energy.

USErad: a multimedia environmental model

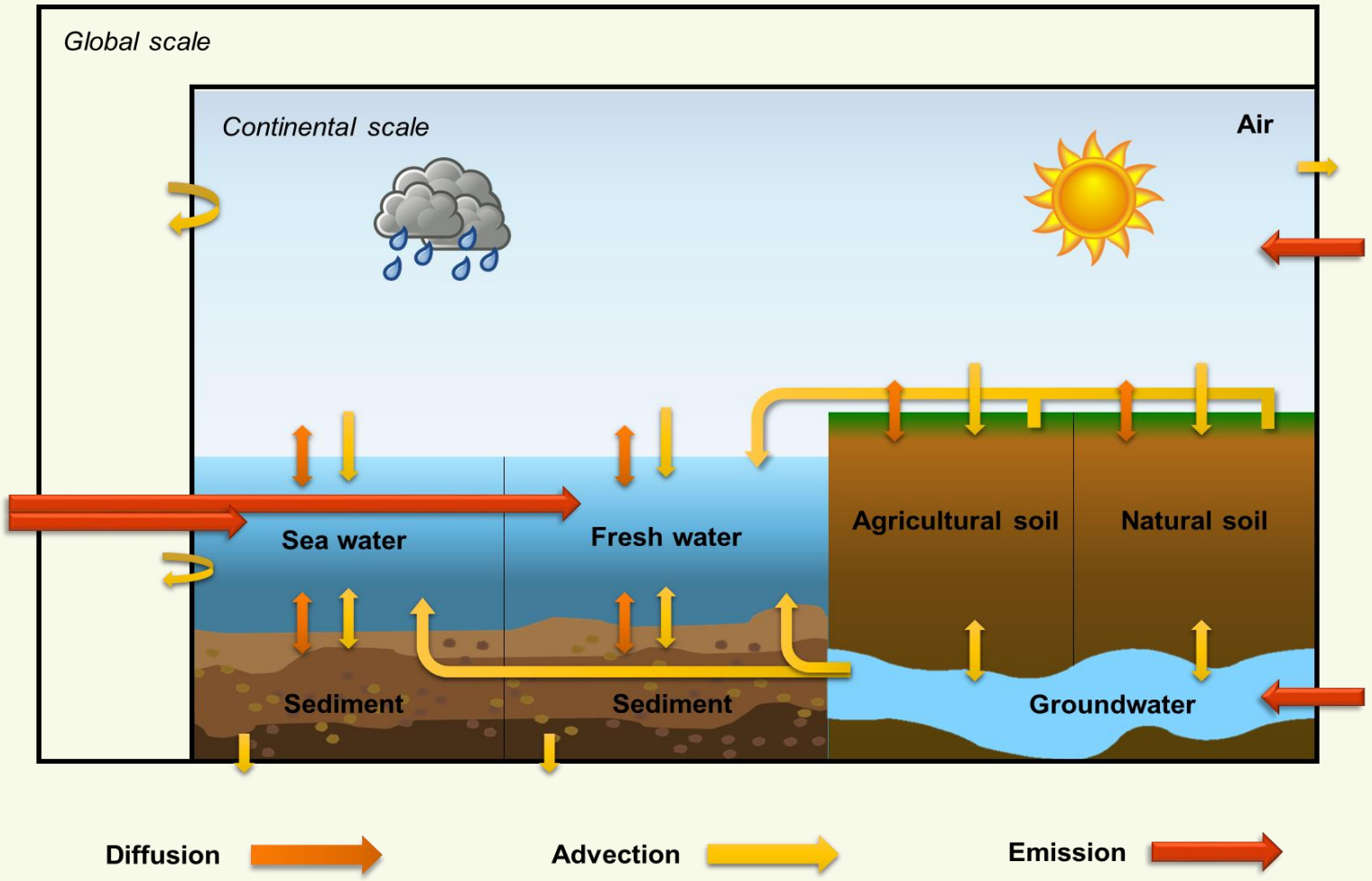

Compartment setup of USErad model

Impact categories:

- Ionising Radiations - IR:
  Impacts of direct gaseous and liquid discharges of radionuclides.

- Ionising Radiations (waste) - IRw:
  Impacts arising from solid waste disposed in a final repository.

LCA case studies

1. Retrospective attributional LCA :

   Assessing the impacts of the current approach for managing Used Nuclear Fuels in the UK

2. (Short-term) Prospective LCA:

   Reprocessing vs Direct Disposal of Used Nuclear Fuels: Assessing the impacts of future scenarios for the back-end of the UK nuclear fuel cycle

Impact categories

Selected impact categories	Metrics
Climate Change	[kg CO2-eq.]
Ecotoxicity (freshwater)	[CTUe]
Eutrophication (freshwater)	[kg P eq.]
Human Toxicity (cancer)	[CTUh]
Human Toxicity (non- cancer)	[CTUh]
Ionising Radiations	[Bq U235 air-eq.]
Ionising Radiations (waste)	[Bq U238 I/LLW-eq.]
Resource depletion	[kg Sb-eq.]

1. The current approach

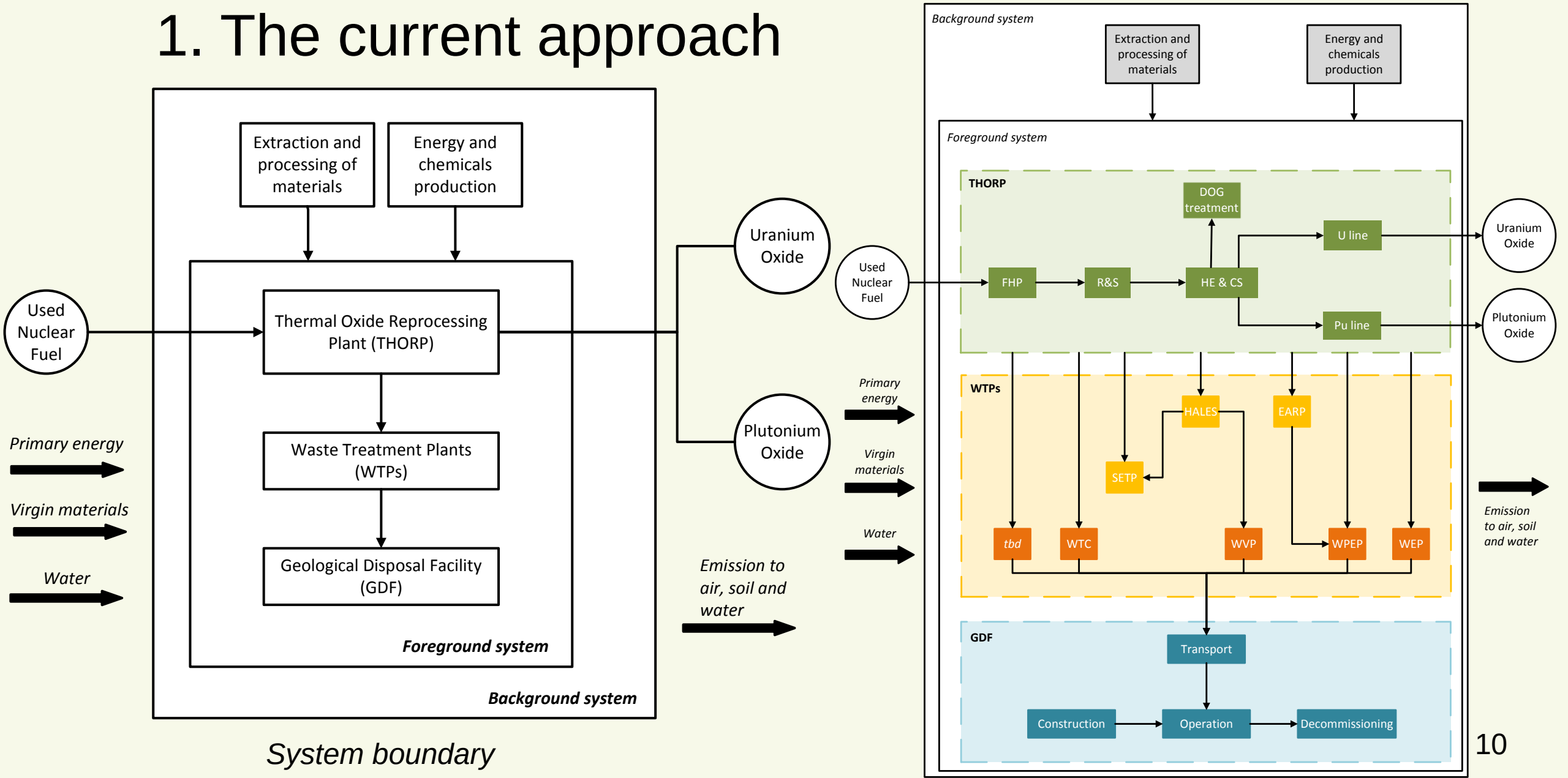

System boundary

The Geological Disposal Facility (GDF)

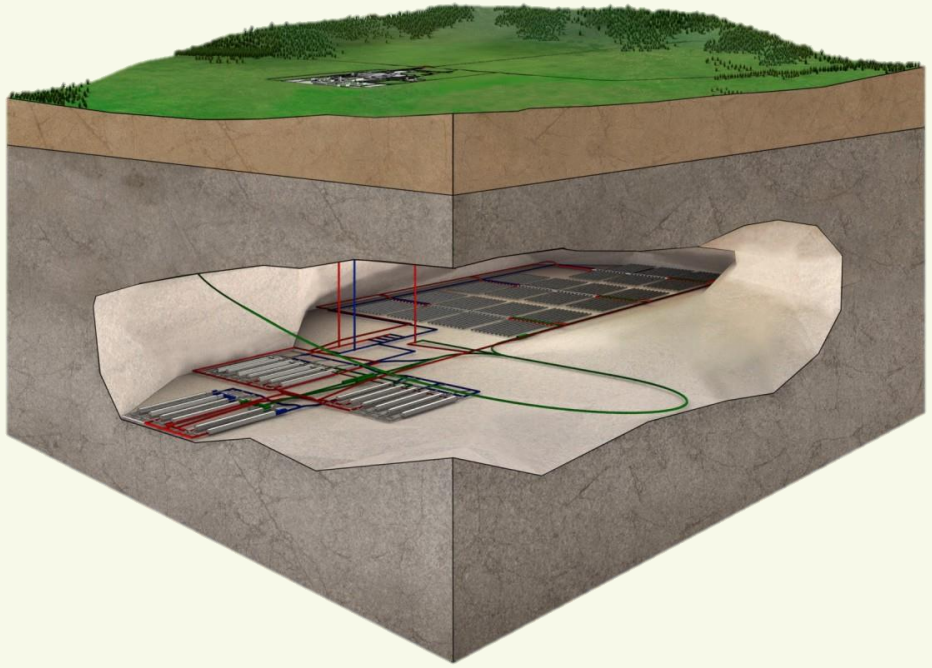

Illustration of the Geological Disposal Facility concept

(Ref: RWM (2010) Generic Post-closure Safety Assessment)

The multi barrier system concept for waste disposal

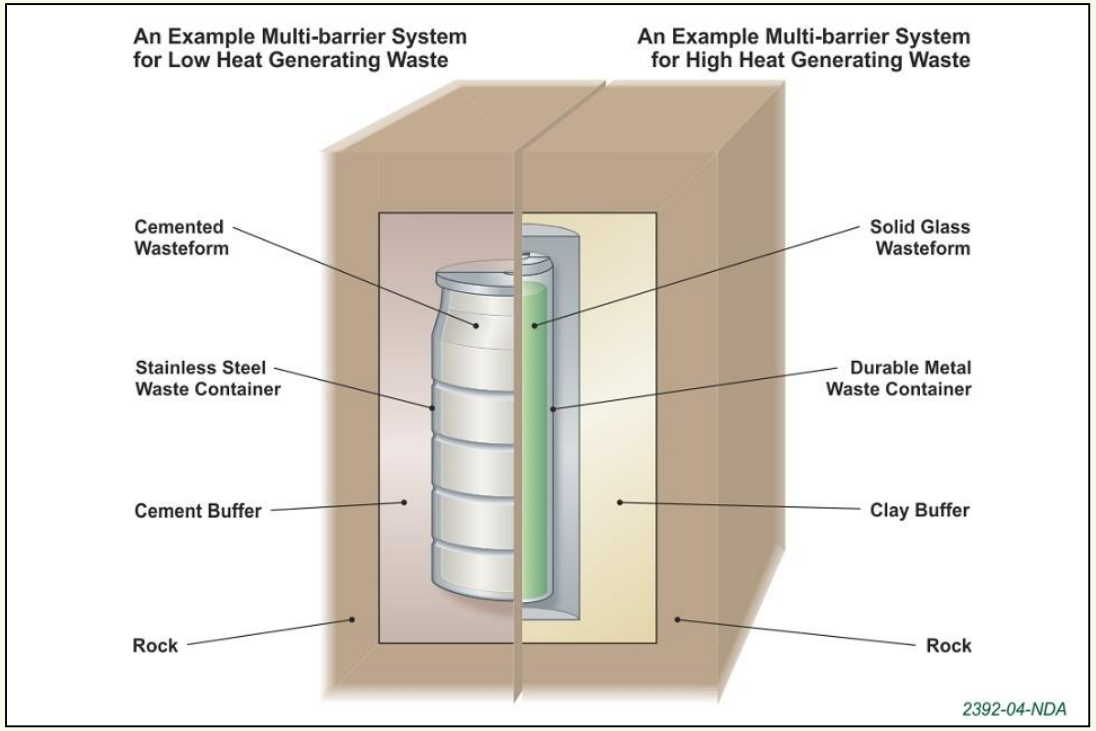

(Ref: RWM (2010) Generic Post-closure Safety Assessment)

LCIA results: high level hot-spot analysis

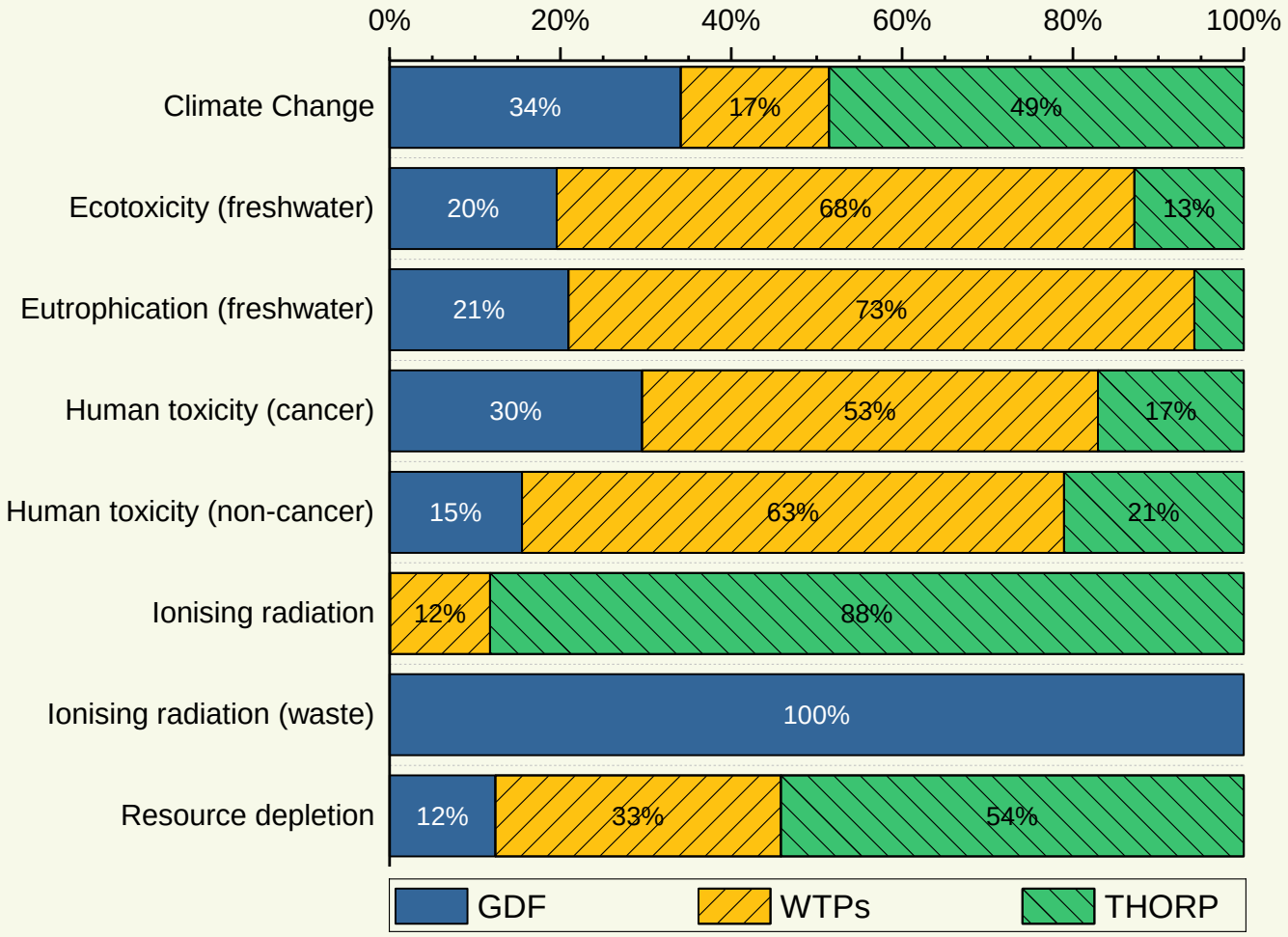

GDF: Geological Disposal Facility

WTPs: Waste Treatment Plants

THORP: Thermal Oxide Reprocessing Plant

- THORP is largest contributor to CC, IR and RDm, while WTP to ECf, Ef, HT-c and nc.
- GDF impacts are appreciable for CC.
- IRw category (by definition) is dominated by GDF

LCIA results: THORP hot-spot analysis

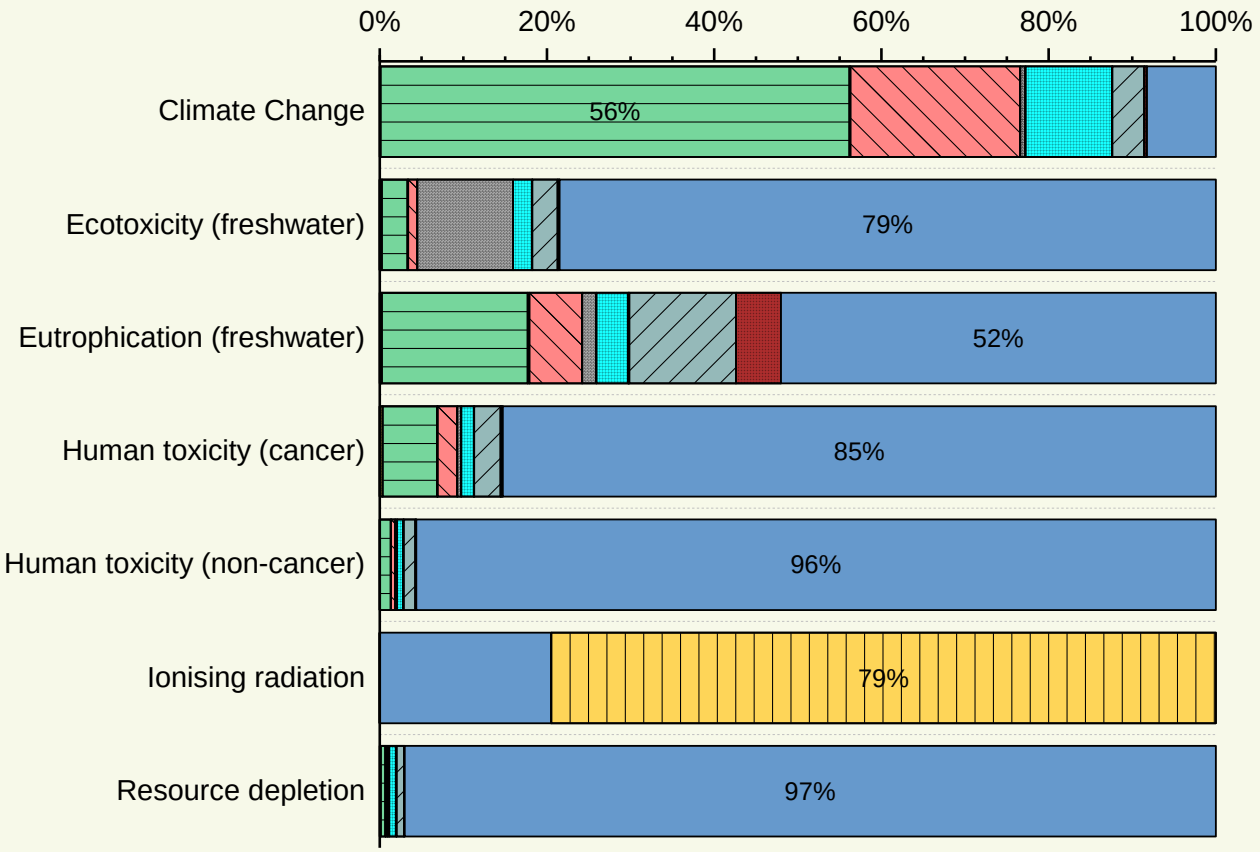

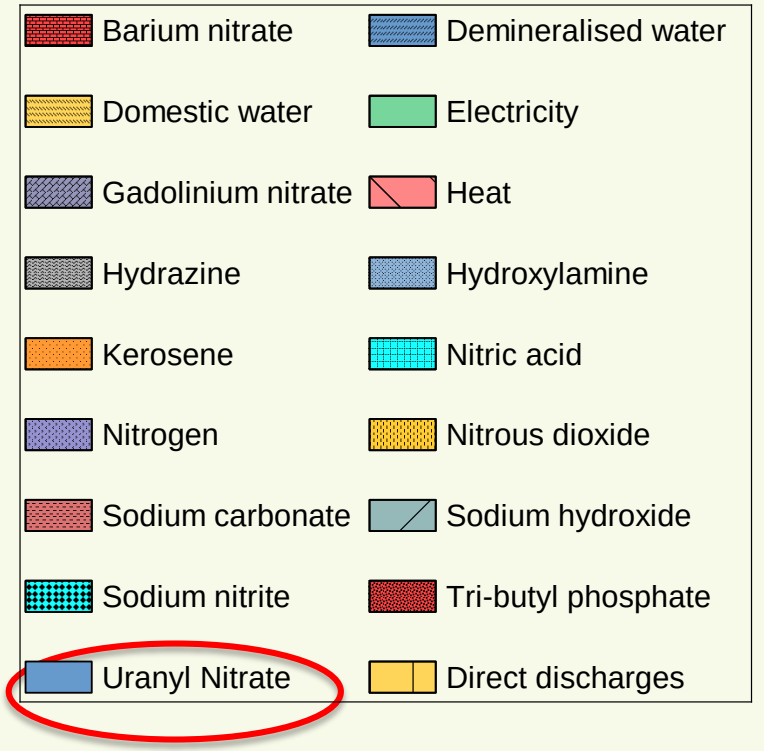

- Indirect emissions from production of uranyl nitrate are the dominant source of impacts in all but CC and IR (climate change) and IR categories.

LCIA results: Waste Vitrification Plant hot-spot analysis

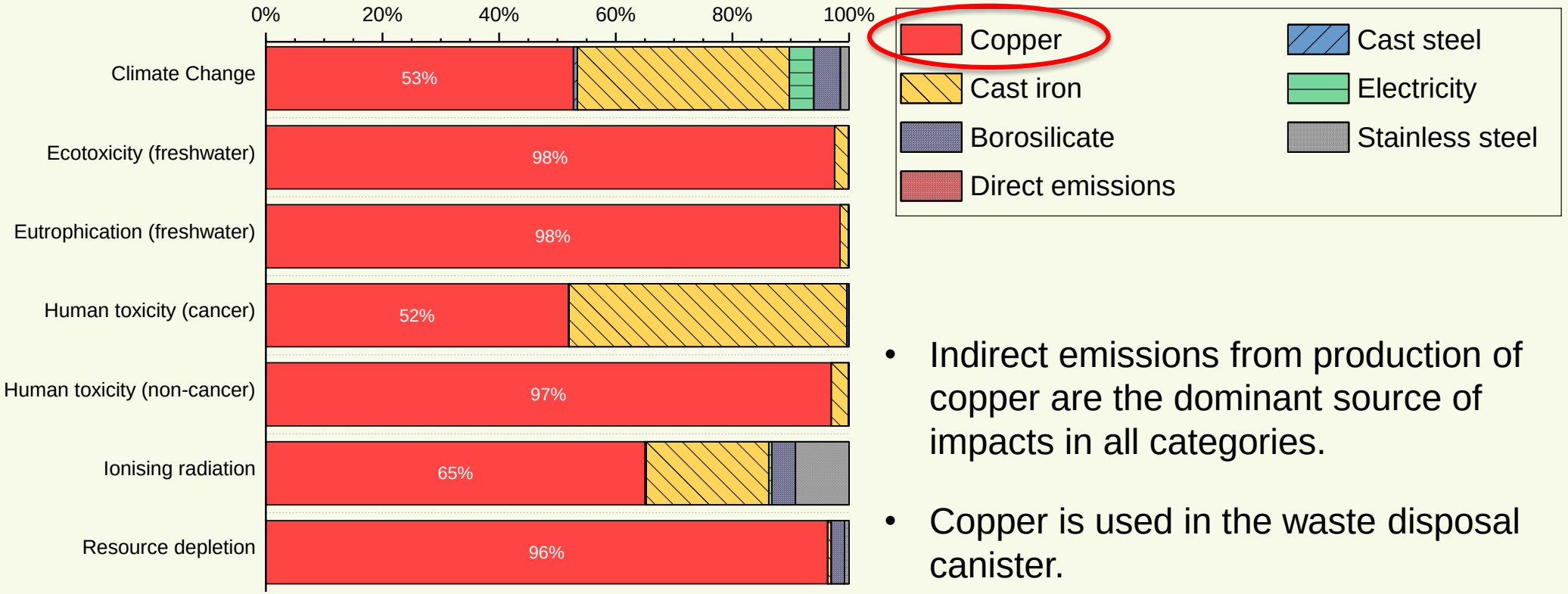

- Indirect emissions from production of copper are the dominant source of impacts in all categories.
- Copper is used in the waste disposal canister.

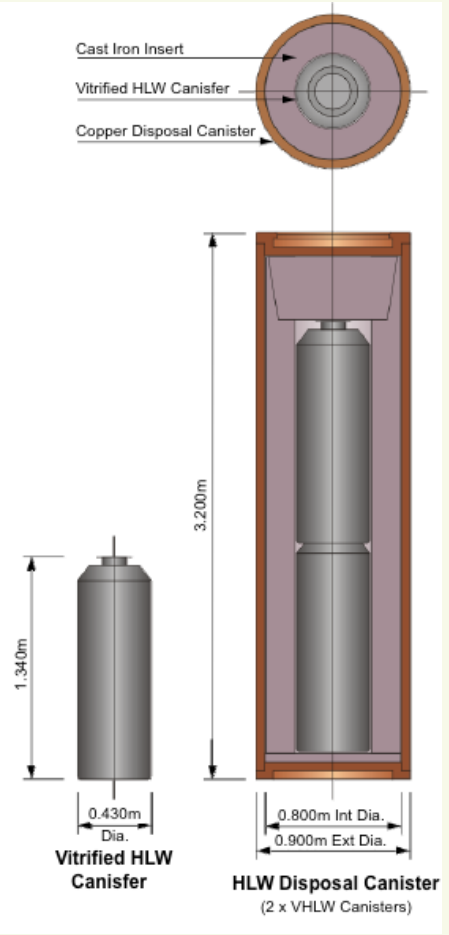

(Pöyry Energy Ltd, 2010. Development of the Derived Inventory of HLW and Spent Fuels Based on the 2007 UK Radioactive Waste Inventory)

LCA case studies

1. Retrospective attributional LCA :

   Assessing the impacts of the current approach for managing Used Nuclear Fuels in the UK

2. (Short-term) Prospective LCA:

   Reprocessing vs Direct Disposal of Used Nuclear Fuels: Assessing the impacts of future scenarios for the back-end of the UK nuclear fuel cycle

2. Future options for the UK: Reprocessing

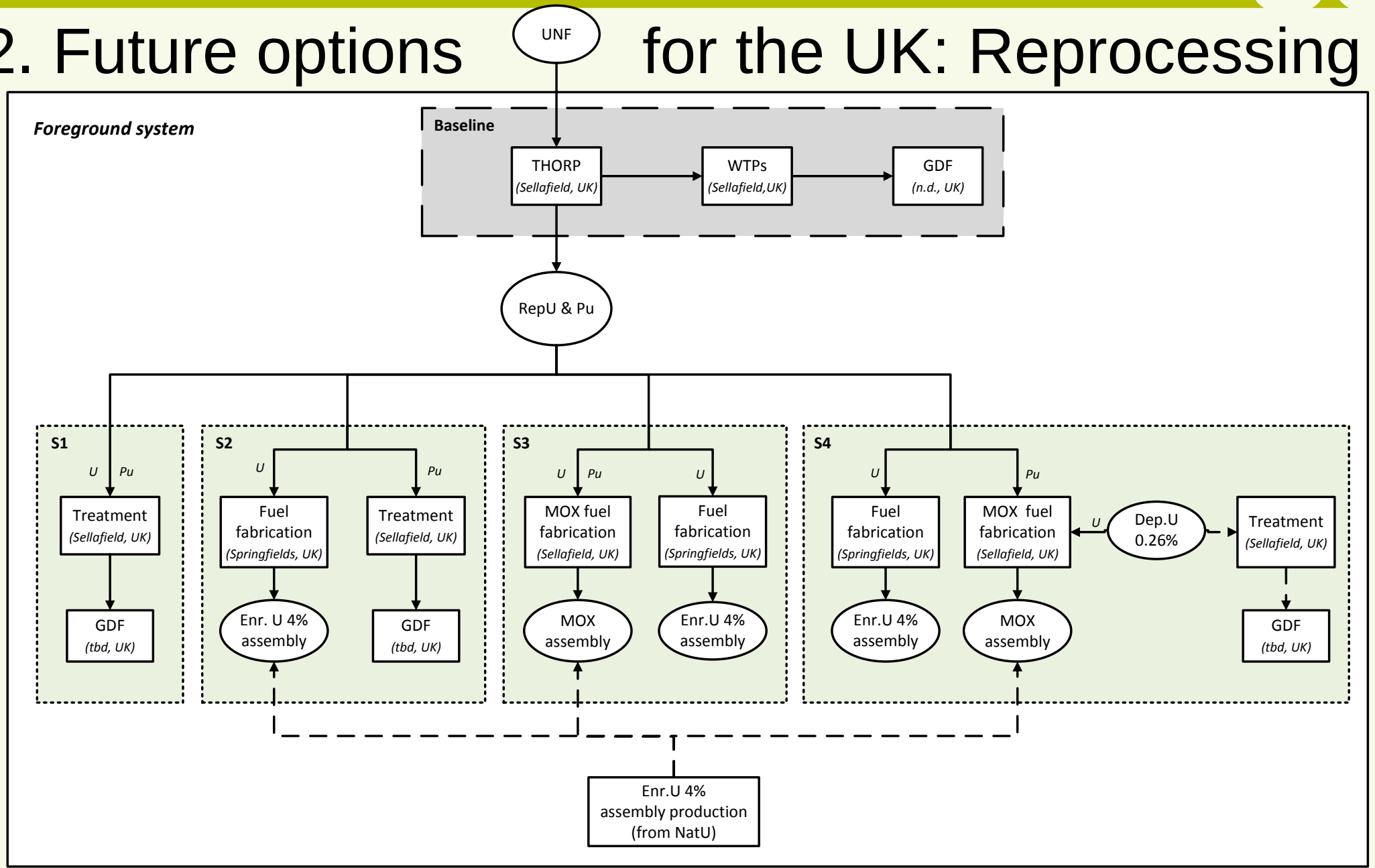

2. Future options for the UK: Reprocessing

- **S1**: RepU & Pu are declared as waste and disposed in a GDF.
- **S2**: Pu is disposed, and U is recycled (to produce enriched uranium).
- **S3:** U & Pu are both recycled (to produced MOX and enriched uranium).
- **S4:** Also DepU is recycled along with U & Pu.

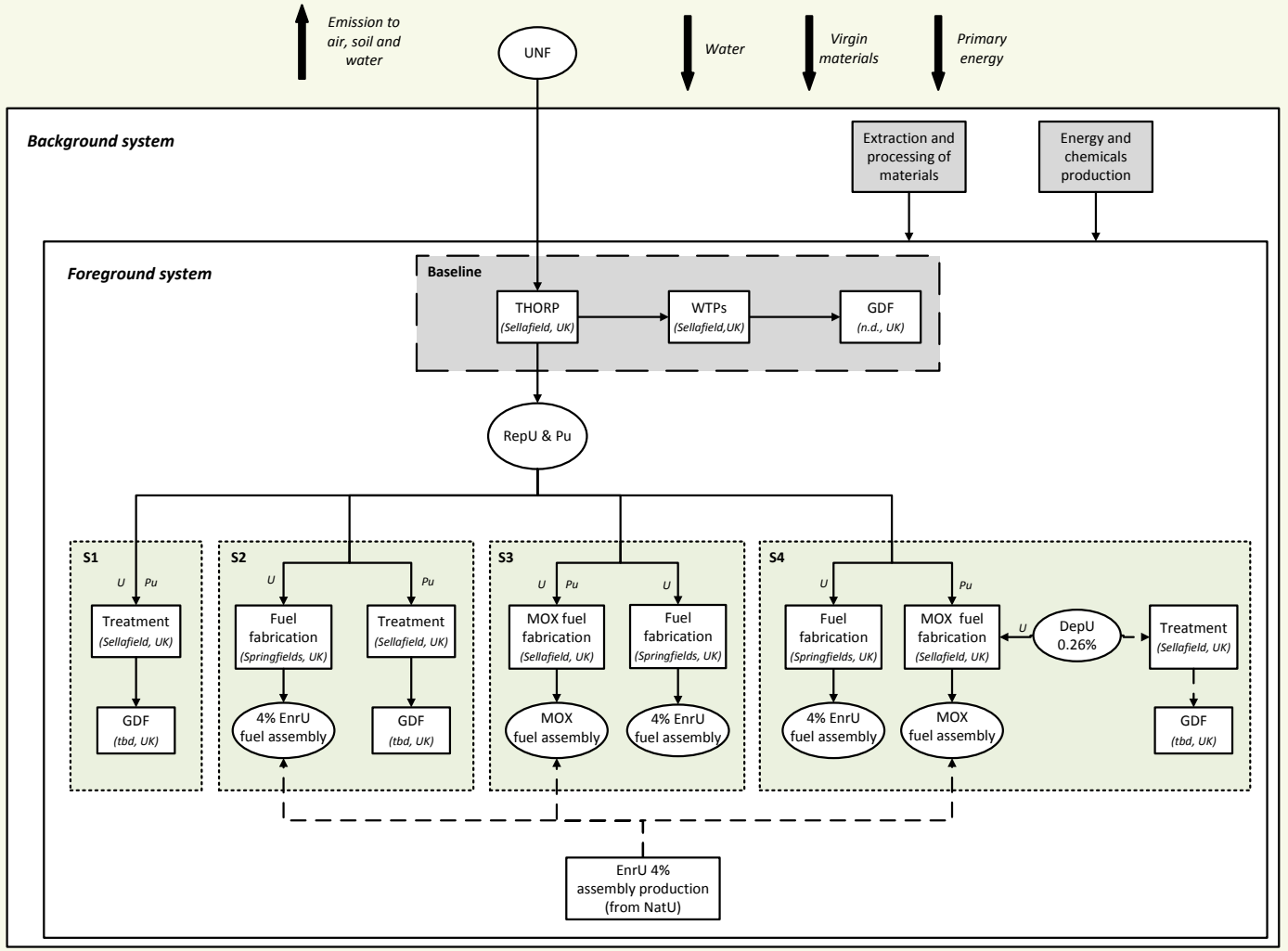

System boundary

2. Future options for the UK: Direct Disposal

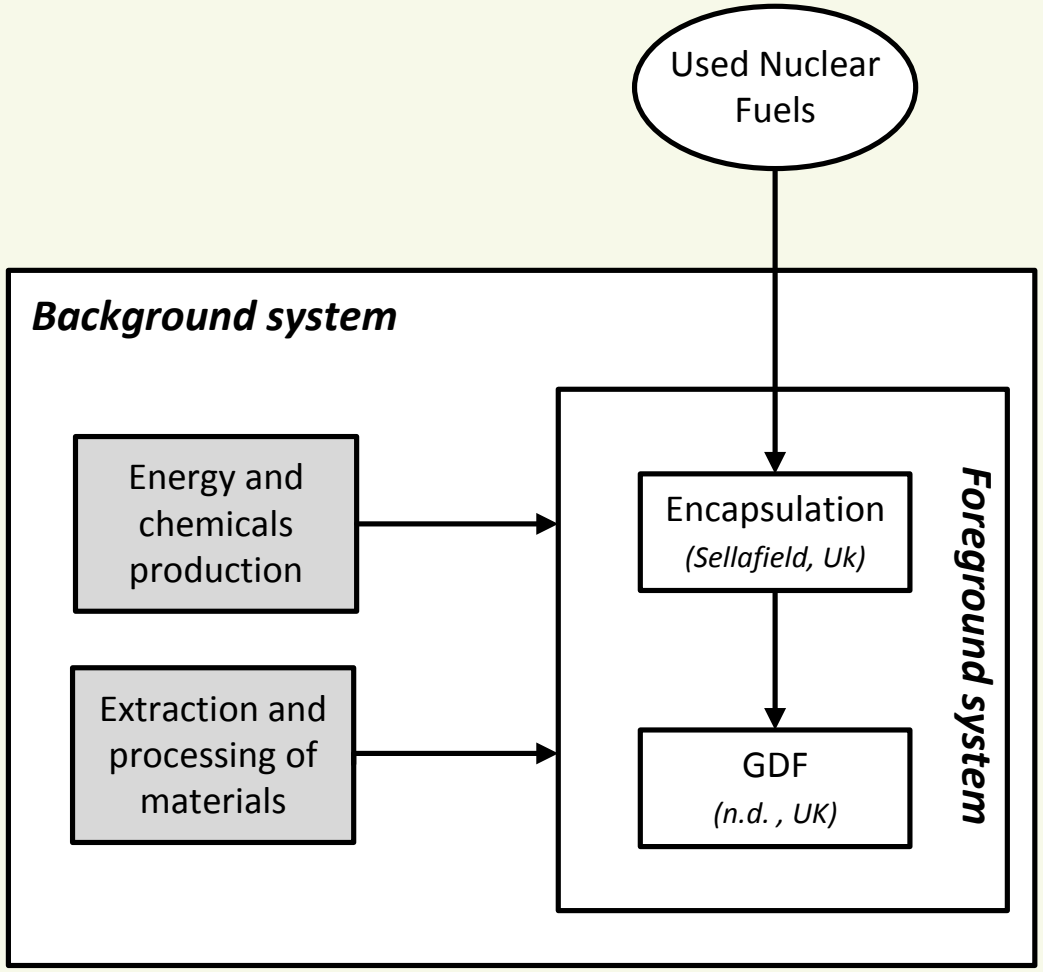

System boundary

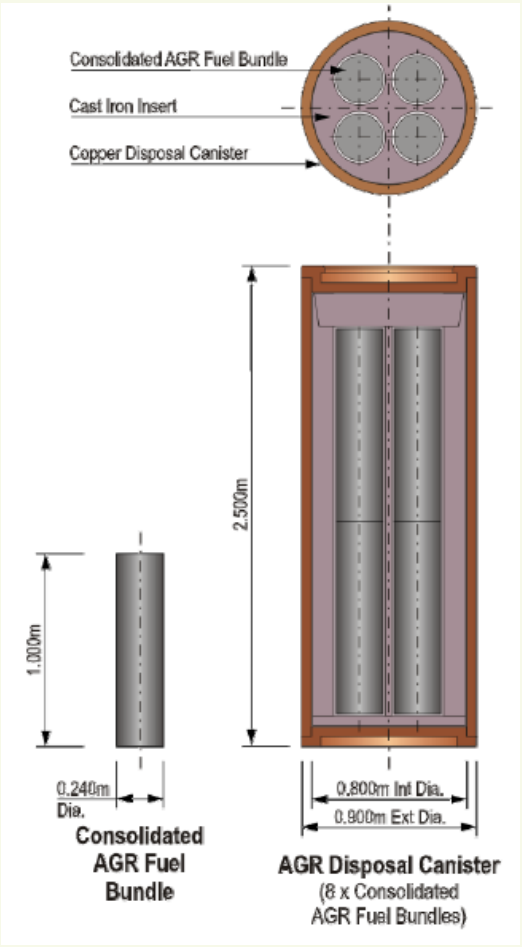

Disposal canister for AGR fuel

LCIA results – Options comparison

Weighted impacts difference between reprocessing and direct disposal

	Reprocessing				Direct disposal
	S1	S2	S3	S4	
Climate Change	116%	-235%	-328%	-262%	0%
Ecotoxicity (freshwater)	-19%	-69%	-96%	-88%	0%
Eutrophication (freshwater)	-18%	-109%	-144%	-129%	0%
Human Toxicity (cancer)	-18%	-77%	-105%	-92%	0%
Human Toxicity (cancer)	-19%	-126%	-163%	-146%	0%
Ionising Radiations	56008%	54624%	54214%	54576%	0%
Ionising Radiations (waste)	-10%	-48%	-56%	-49%	0%
Resource depletion	57%	-2298%	-2714%	-2343%	0%

Colour scale: Red (highest), Green (lowest)

- S1 and direct disposal are the worst performing options.
- Direct disposal has the lowest IR score.
- Recycling of RepU, or RepU and Pu brings significant benefits.
- S3 is the most environmentally sustainable option, followed by S4 and S2.

LCIA results: Reprocessing scenarios hot-spot analysis

Hot-spot analysis of reprocessing scenarios. Impacts are relative to the baseline.

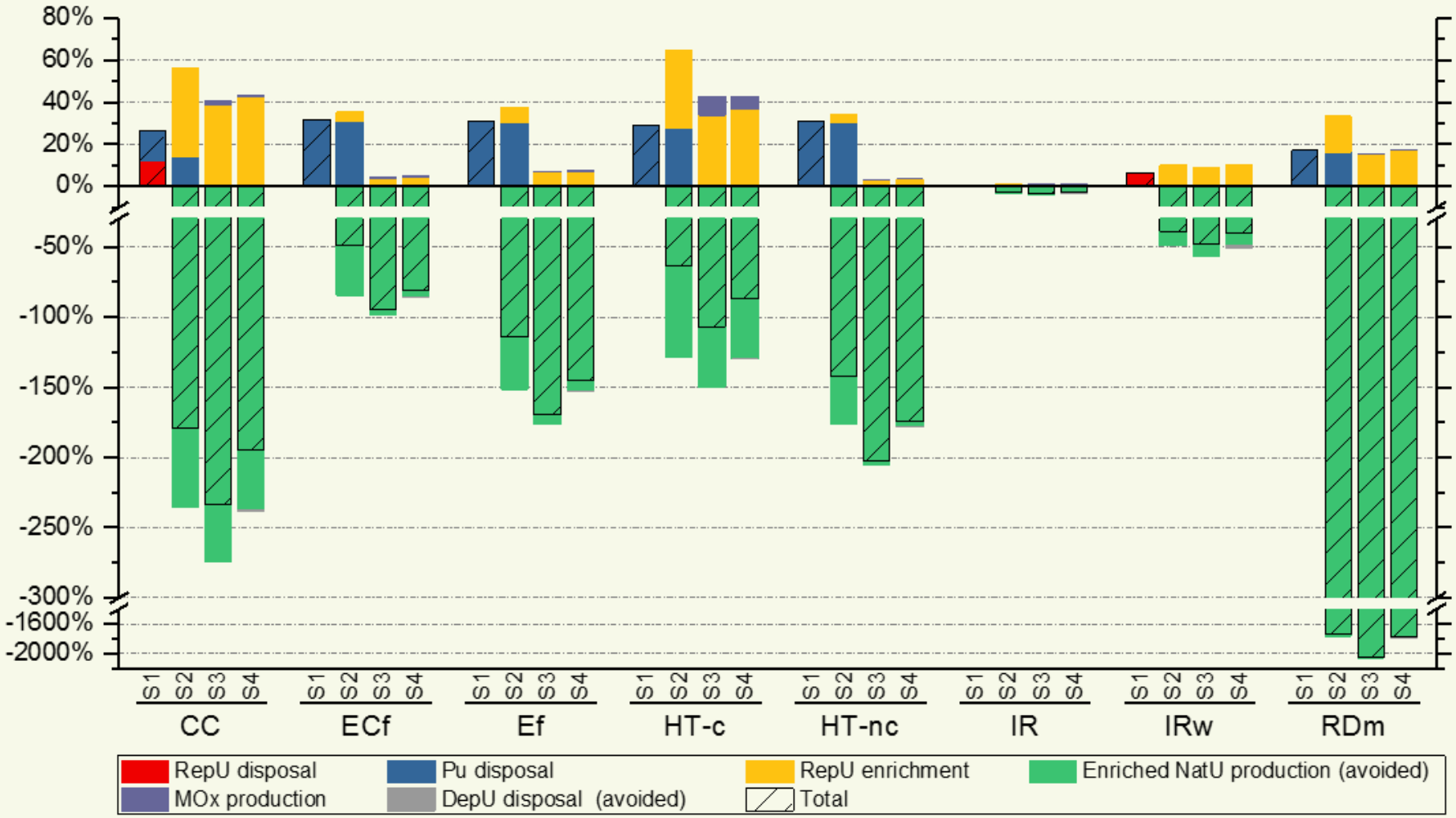

- In S2, S3 and S4 the environmental benefits of avoiding production of enriched NatU offset the additional impacts of RepU enrichment and MOX production.

Conclusions

- A novel methodology for assessing human impacts of radioactive discharges and solid waste has been developed and demonstrated.
- LCA on current practice for management of Used Nuclear Fuels:
  - THORP and WVP are the most impactful units, with GDF having minor impacts.
  - THORP impacts are largely attributable to indirect emissions from production of uranyl nitrate used to separate Pu from U.
  - WVP impacts are related with indirect emissions from production of copper used in disposal canisters.
- LCA on future options for the back-end of the UK nuclear fuel cycle:
  - Reprocessing Scenario 3 is overall the best performing option.
  - Reprocessing with disposal of Pu and RepU is the worst performing option followed by direct disposal.
  - Recycling of RepU, or both RepU and Pu is of paramount importance, as it avoid uranium mining and milling – a very high-impact process!

Future work

- Comparative LCA of electricity generation from nuclear source in:
  1. Uranium-based fuel cycle
  2. Thorium-based fuel cycle

- Thesis submission!

Acknowledgments

Aqueous Speciation & Amorphous Phase Characterisation by TRLFS and Raman Spectroscopy

Victoria L. Frankland, Rachida Bance-Soualhi and David Read

Introduction

- **Aim: Create a spectral database for ‘difficult to characterise’ samples from operational & legacy nuclear sites**

- **Sample phases:**
  - **High quality crystalline mineral phases as reference materials**
  - **Aqueous & non-aqueous solutions**
  - **Amorphous & ultra-thin surface alteration products**

- **Limitations with conventional techniques:**
  XRD - requires good crystallinity
  IR spectroscopy - spectra masked by water features

- **Options:**
  - Time-Resolved Laser Fluorescence Spectroscopy (TRLFS)
  - Raman Spectroscopy
  - NMR etc.

Time-Resolved Laser Fluorescence Spectroscopy (TRLFS)

Fluorescence Spectra (non-time-resolved)

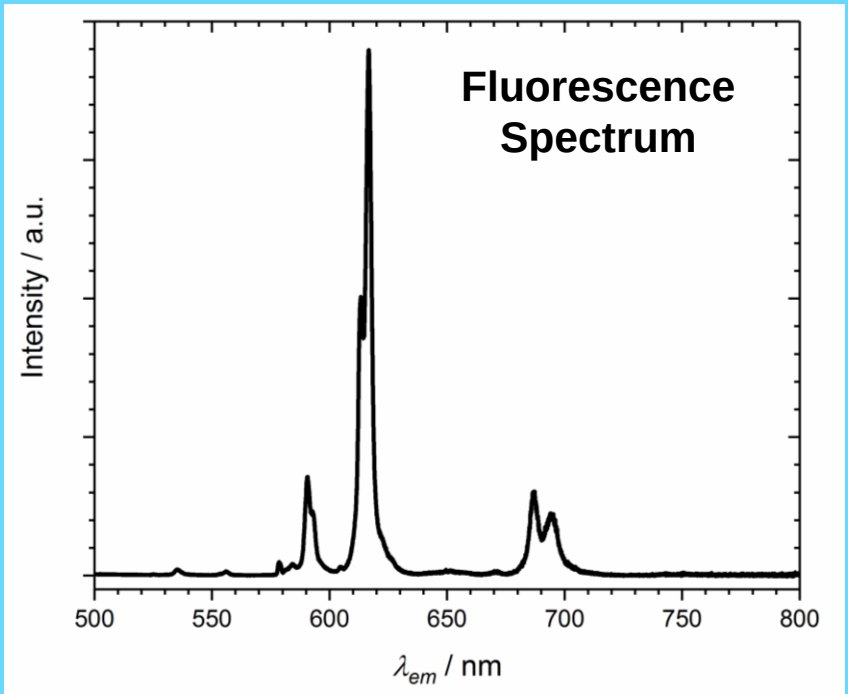

Fluorescence Decay (time-resolved)

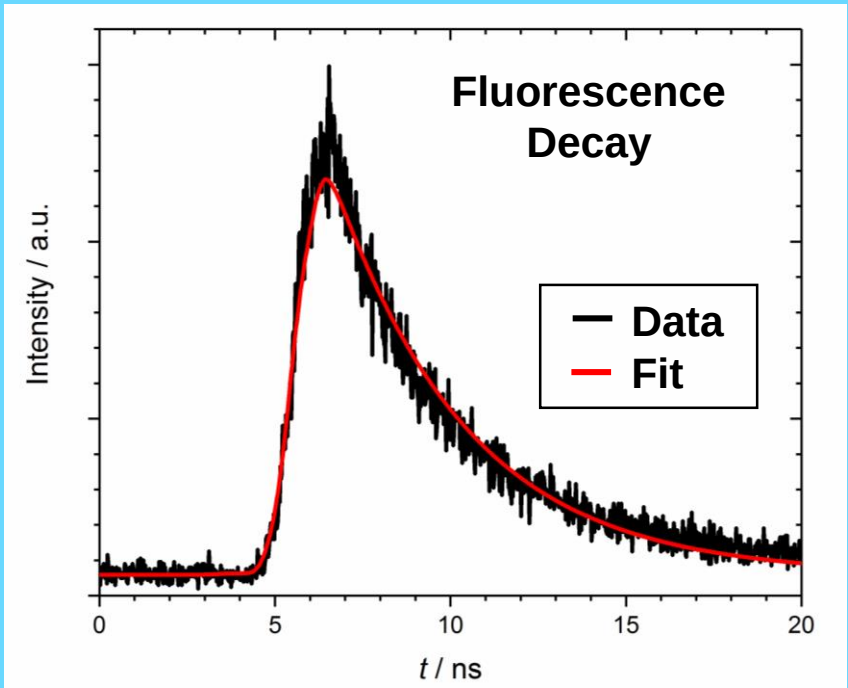

Fluorescence

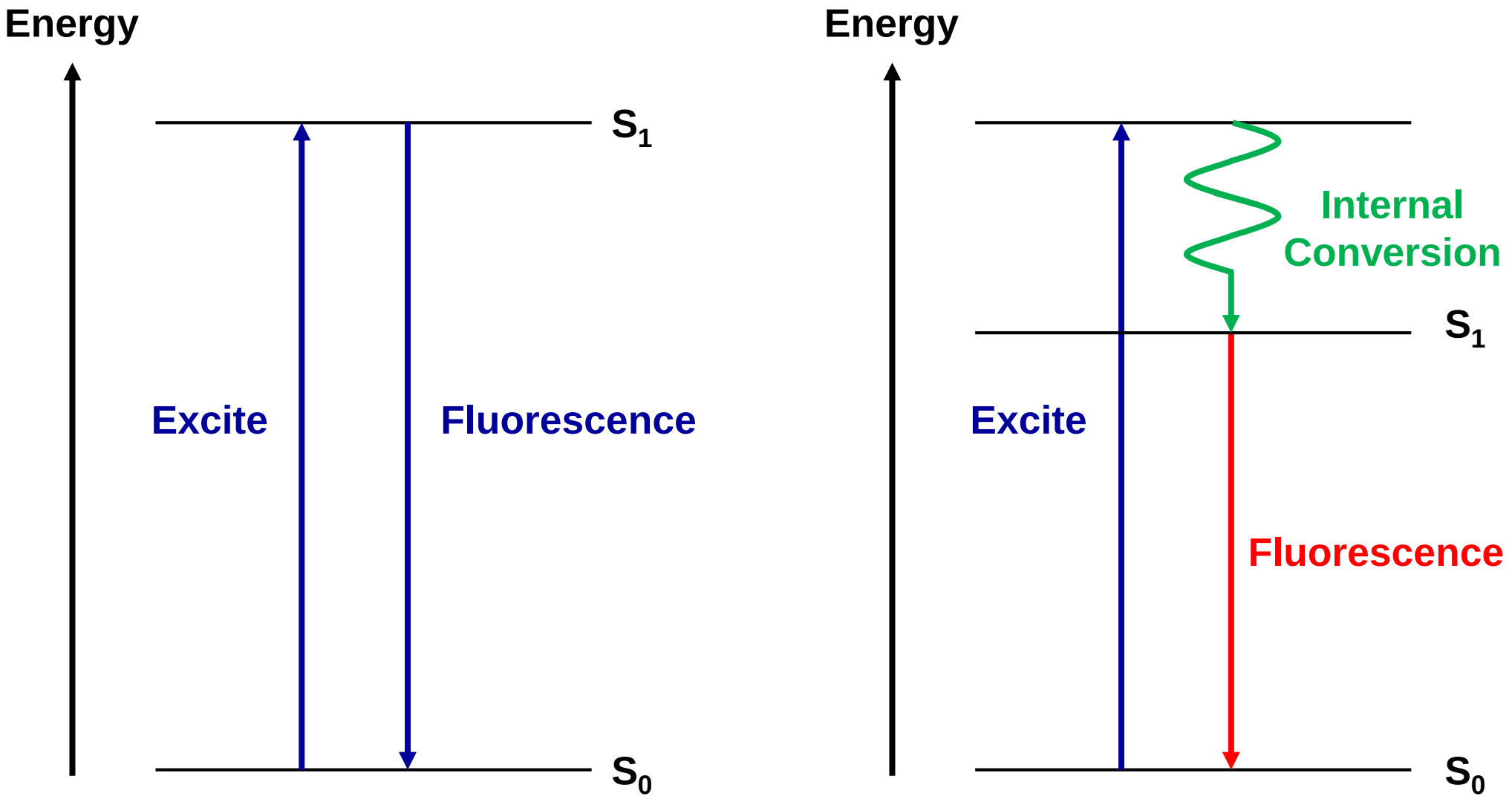

Fluorescence Decay

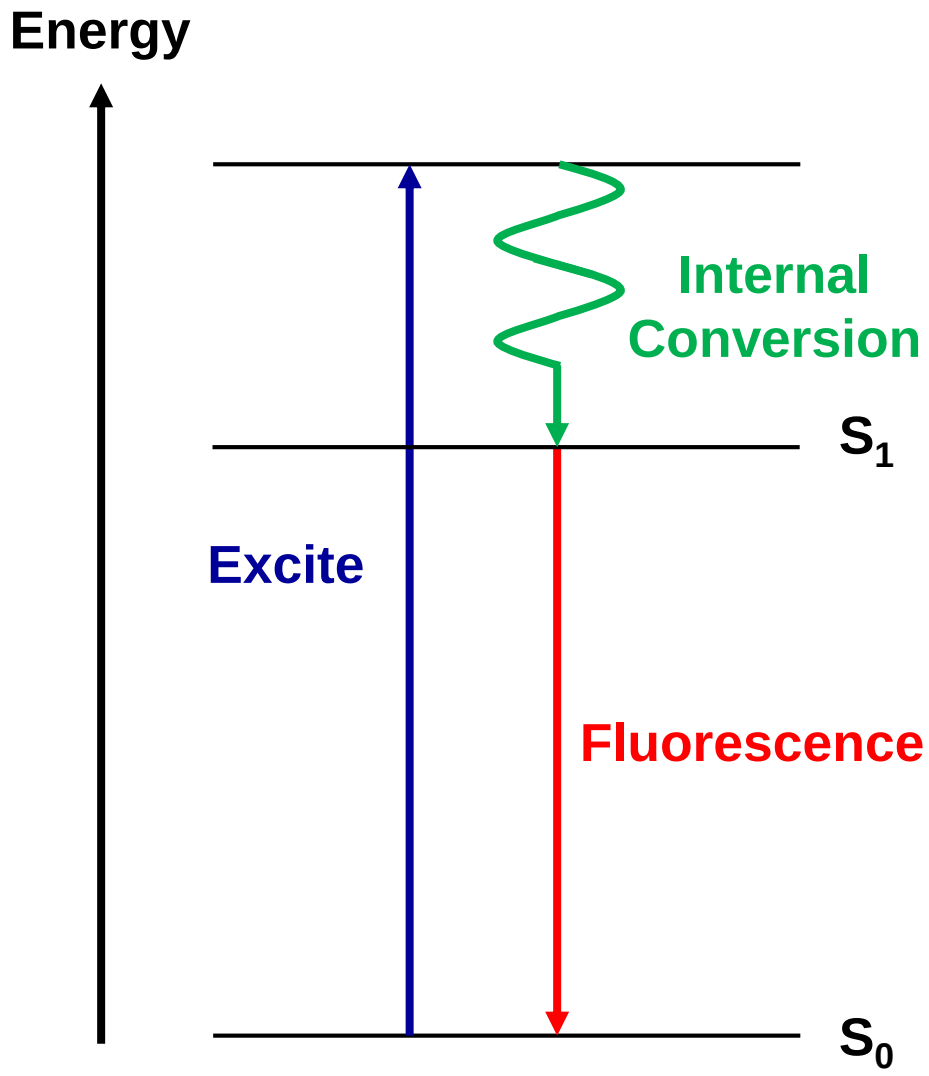

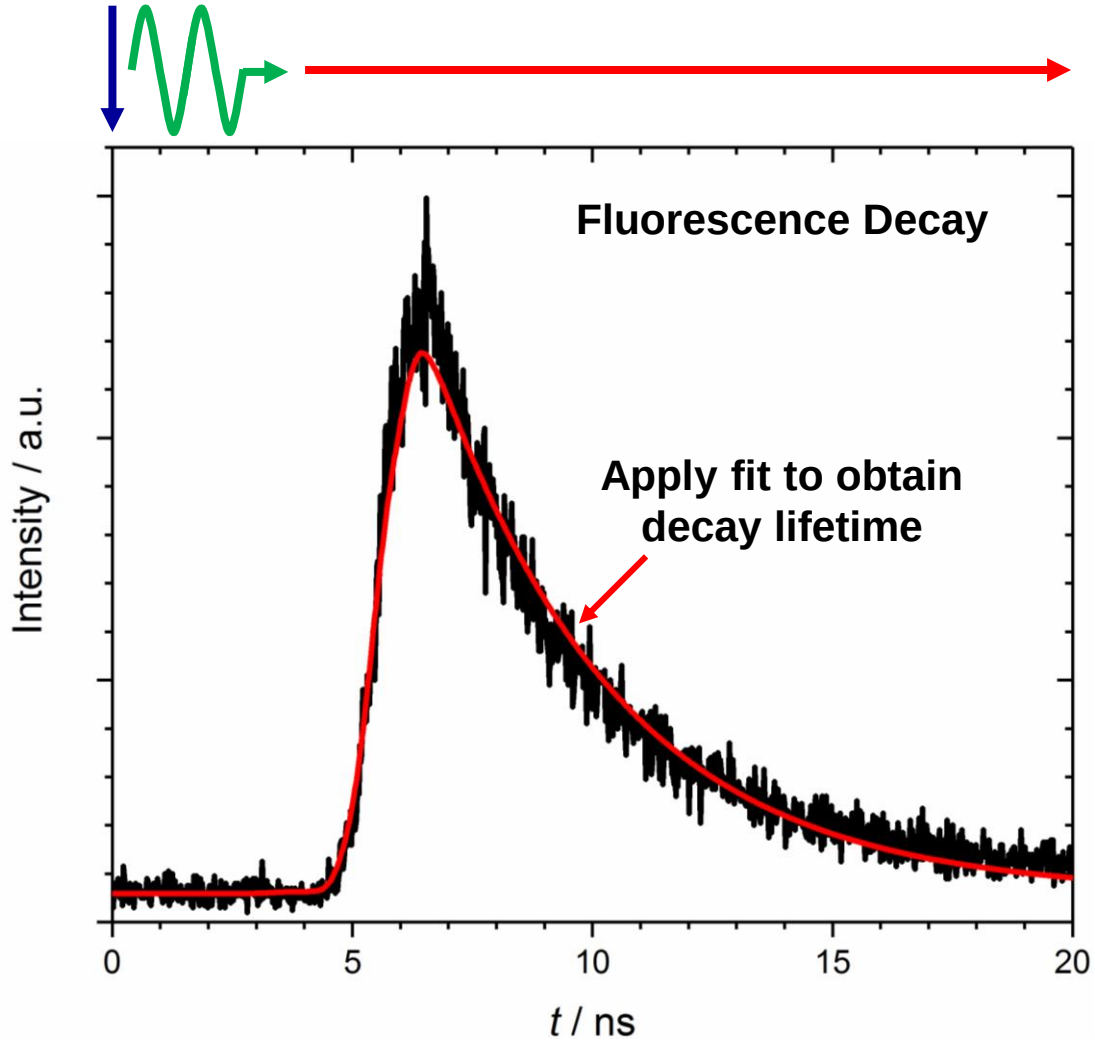

Time Resolved Laser Fluorescence Spectroscopy (TRLFS)

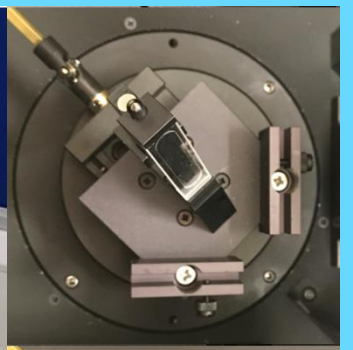

Powders

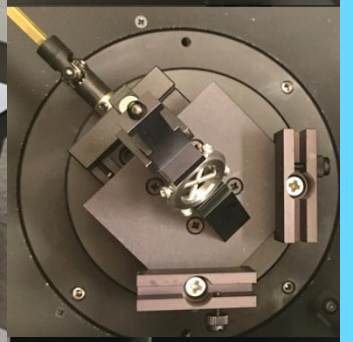

Clusters

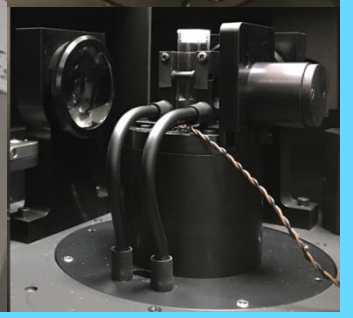

Solutions

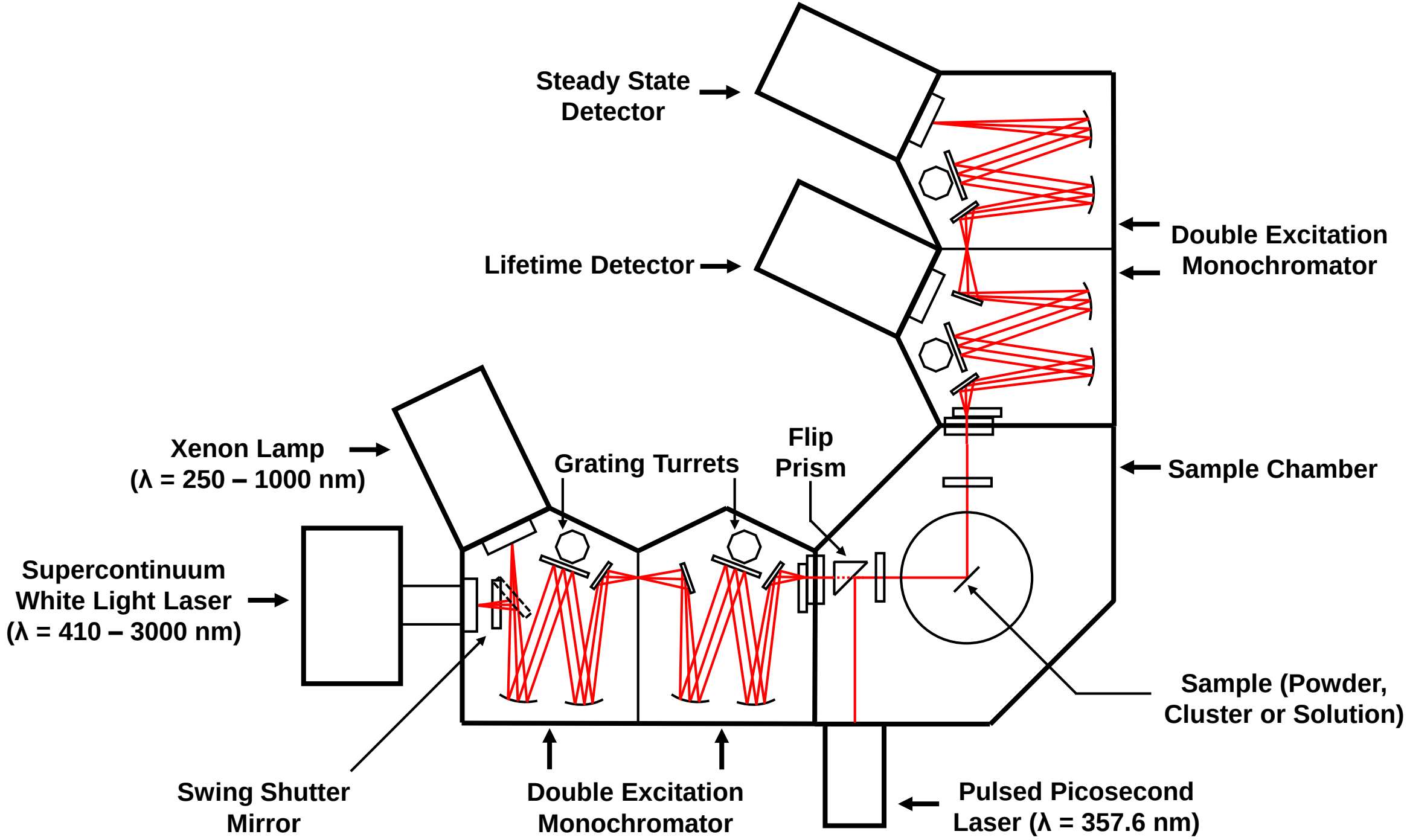
Steady State Detector
Lifetime Detector
Double Excitation Monochromator
Xenon Lamp (λ = 250 – 1000 nm)
Grating Turrets
Flip Prism
Sample Chamber
Supercontinuum White Light Laser (λ = 410 – 3000 nm)
Sample (Powder, Cluster or Solution)
Swing Shutter Mirror
Double Excitation Monochromator
Pulsed Picosecond Laser (λ = 357.6 nm)

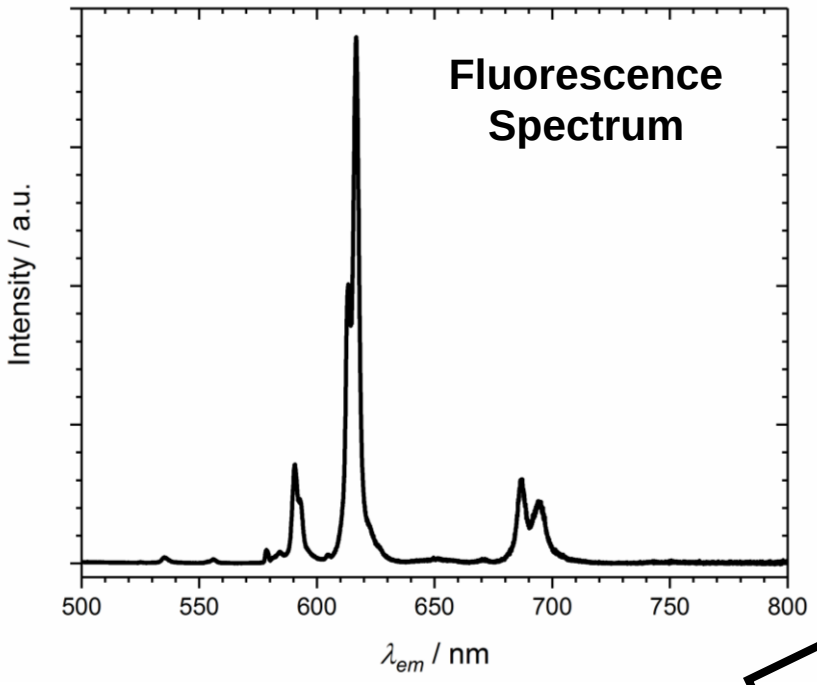

Steady State Detector

Double Excitation Monochromator

Xenon Lamp (λ = 250 – 1000 nm)

Sample Chamber

Sample (Powder, Cluster or Solution)

Double Excitation Monochromator

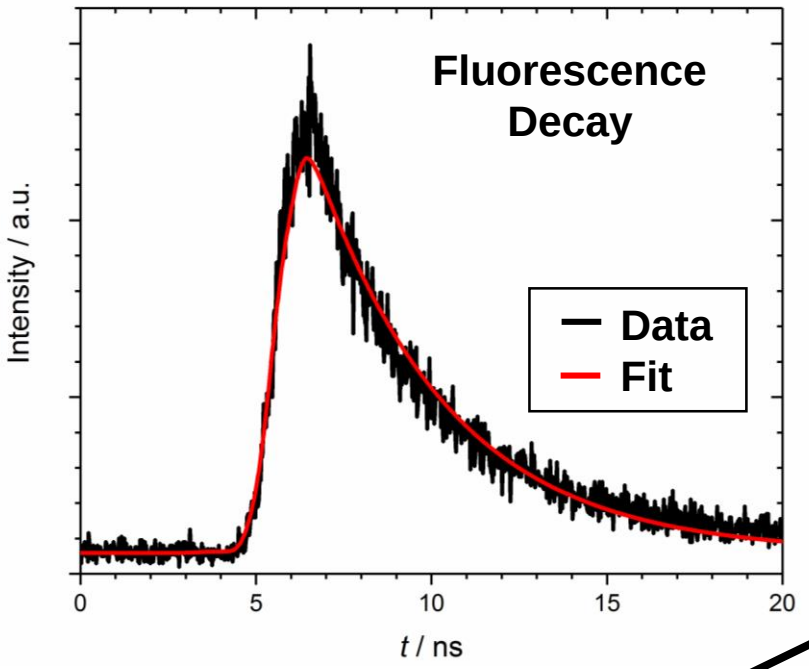

Lifetime Detector

Double Excitation
Monochromator

Flip
Prism

Sample Chamber

Supercontinuum
White Light Laser
(λ = 410 – 3000 nm)

Sample (Powder,
Cluster or Solution)

Double Excitation
Monochromator

Pulsed Picosecond
Laser (λ = 357.6 nm)

Raman Spectroscopy

- **Observe vibrational, rotational and other low frequency modes**

- **Common features in Raman spectroscopy:**
  - **< 200 cm^{-1} = lattice vibrations**
  - **200 – 1200 cm^{-1} = most transitions**
  - **1630-1680 cm^{-1} = water bending mode, $\delta(H_2O)$[1]**
  - **3000 – 3800 cm^{-1} = OH vibrations (from water)[2]**

- **Spectra scan at one point**

- **Raman mapping across surface**

[1] A.F. Bell, *J. Am. Chem. Soc.*, 1997, 119, 6006
[2] S.M. Pershin, *Optics Spectrosc.*, 2005, 98, 543

Raman Spectroscopy

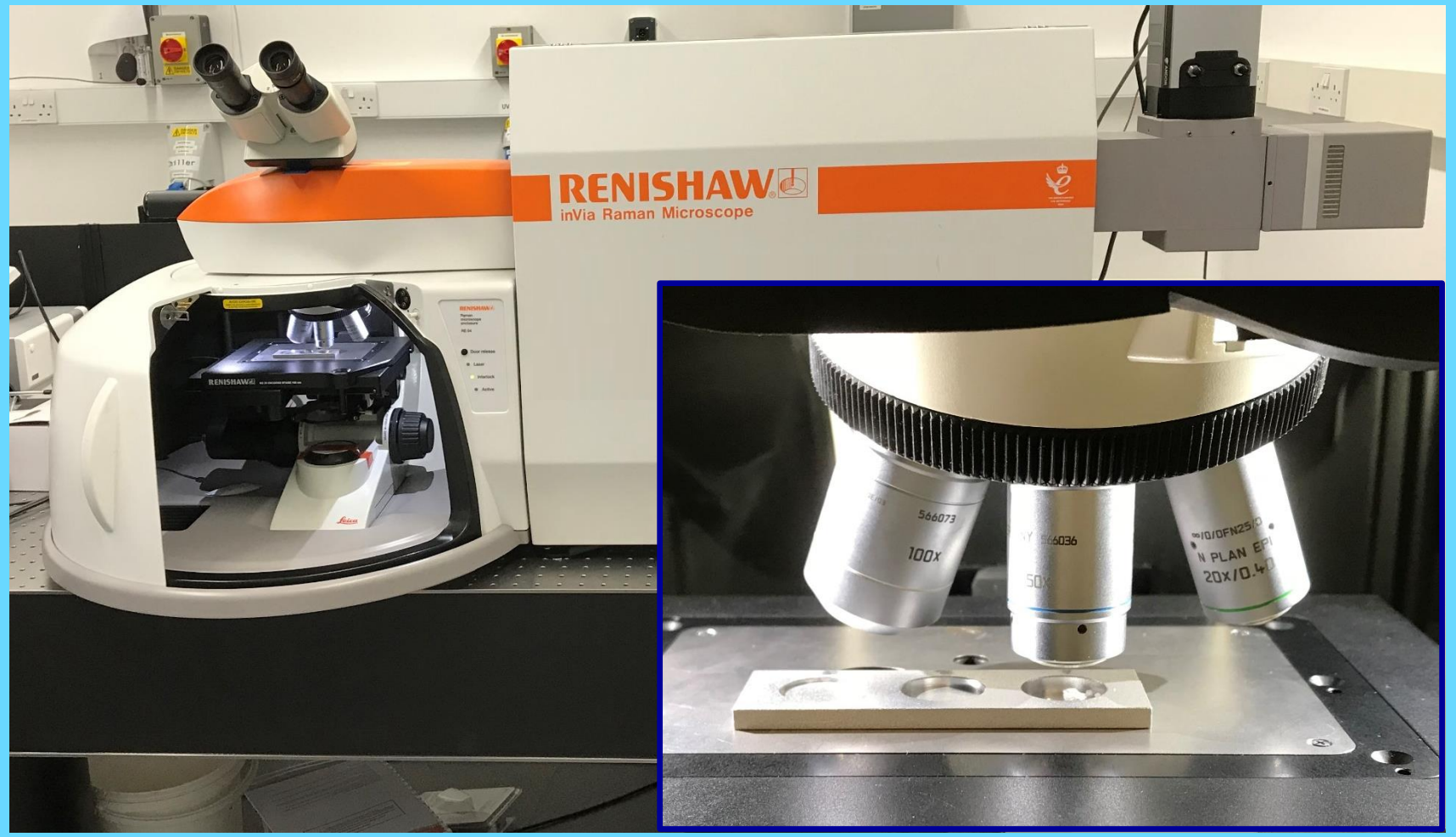

- 5 Lasers:
  - 244 nm (UV)
  - 457 nm (blue)
  - 532 nm (green)
  - 633 nm (red)
  - 785 nm (IR)
- Powders and Clusters
- Alternative stage for solutions

Preliminary Characterisation Results

TRLFS:
Eu_2O_3, $Eu(NO_3)_3$ and $EuCl_3$

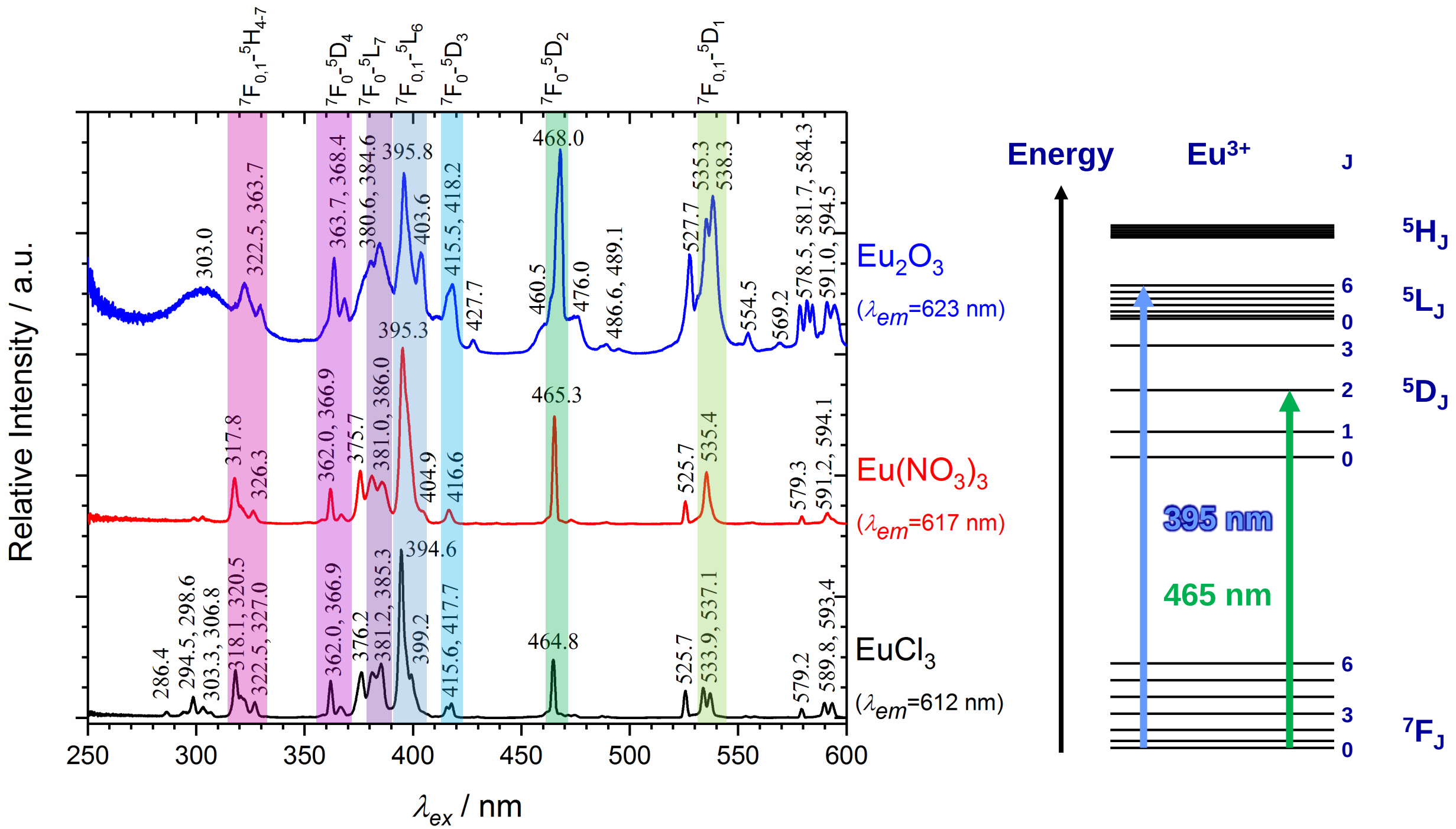
$^7F_{0,1}$-$^5H_{4-7}$
$^7F_0$-$^5D_4$
$^7F_0$-$^5L_7$
$^7F_{0,1}$-$^5L_6$
$^7F_0$-$^5D_3$
$^7F_0$-$^5D_2$
$^7F_{0,1}$-$^5D_1$
Relative Intensity / a.u.
λ_{ex} / nm
250
300
350
400
450
500
550
600
303.0
322.5, 363.7
363.7, 368.4
380.6, 384.6
395.8
403.6
415.5, 418.2
427.7
460.5
468.0
476.0
486.6, 489.1
527.7
535.3
538.3
554.5
569.2
578.5, 581.7, 584.3
591.0, 594.5
Eu_2O_3
(λ_{em}=623 nm)
317.8
326.3
362.0, 366.9
375.7
381.0, 386.0
395.3
404.9
416.6
465.3
525.7
535.4
579.3
591.2, 594.1
$Eu(NO_3)_3$
(λ_{em}=617 nm)
286.4
294.5, 298.6
303.3, 306.8
318.1, 320.5
322.5, 327.0
362.0, 366.9
376.2
381.2, 385.3
394.6
399.2
415.6, 417.7
464.8
525.7
533.9, 537.1
579.2
589.8, 593.4
$EuCl_3$
(λ_{em}=612 nm)
Energy
Eu^{3+}
J
^5H_J
^5L_J
^5D_J
^7F_J
6
0
3
2
1
0
6
3
0
395 nm
465 nm

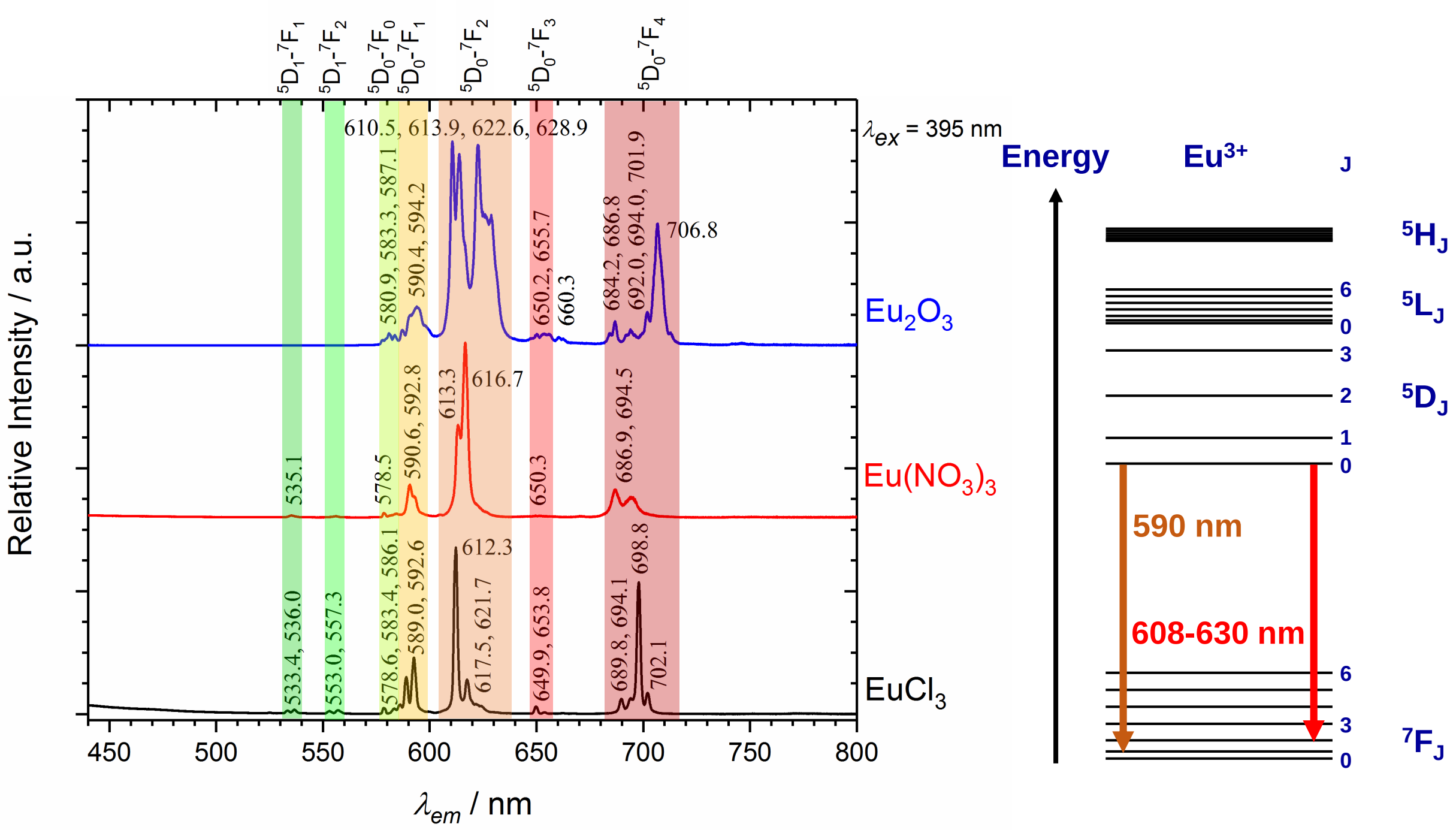
$^5D_1$-$^7F_1$
$^5D_1$-$^7F_2$
$^5D_0$-$^7F_0$
$^5D_0$-$^7F_1$
$^5D_0$-$^7F_2$
$^5D_0$-$^7F_3$
$^5D_0$-$^7F_4$
λ_{ex} = 395 nm
610.5, 613.9, 622.6, 628.9
580.9, 583.3, 587.1
590.4, 594.2
650.2, 655.7
660.3
684.2, 686.8
692.0, 694.0, 701.9
706.8
Eu_2O_3
535.1
578.5
590.6, 592.8
613.3
616.7
650.3
686.9, 694.5
$Eu(NO_3)_3$
533.4, 536.0
553.0, 557.3
578.6, 583.4, 586.1
589.0, 592.6
612.3
617.5, 621.7
649.9, 653.8
689.8, 694.1
698.8
702.1
$EuCl_3$
Relative Intensity / a.u.
450
500
550
600
650
700
750
800
λ_{em} / nm
Energy
Eu^{3+}
J
^5H_J
^5L_J
^5D_J
^7F_J
6
0
3
2
1
0
590 nm
608-630 nm
6
3
0

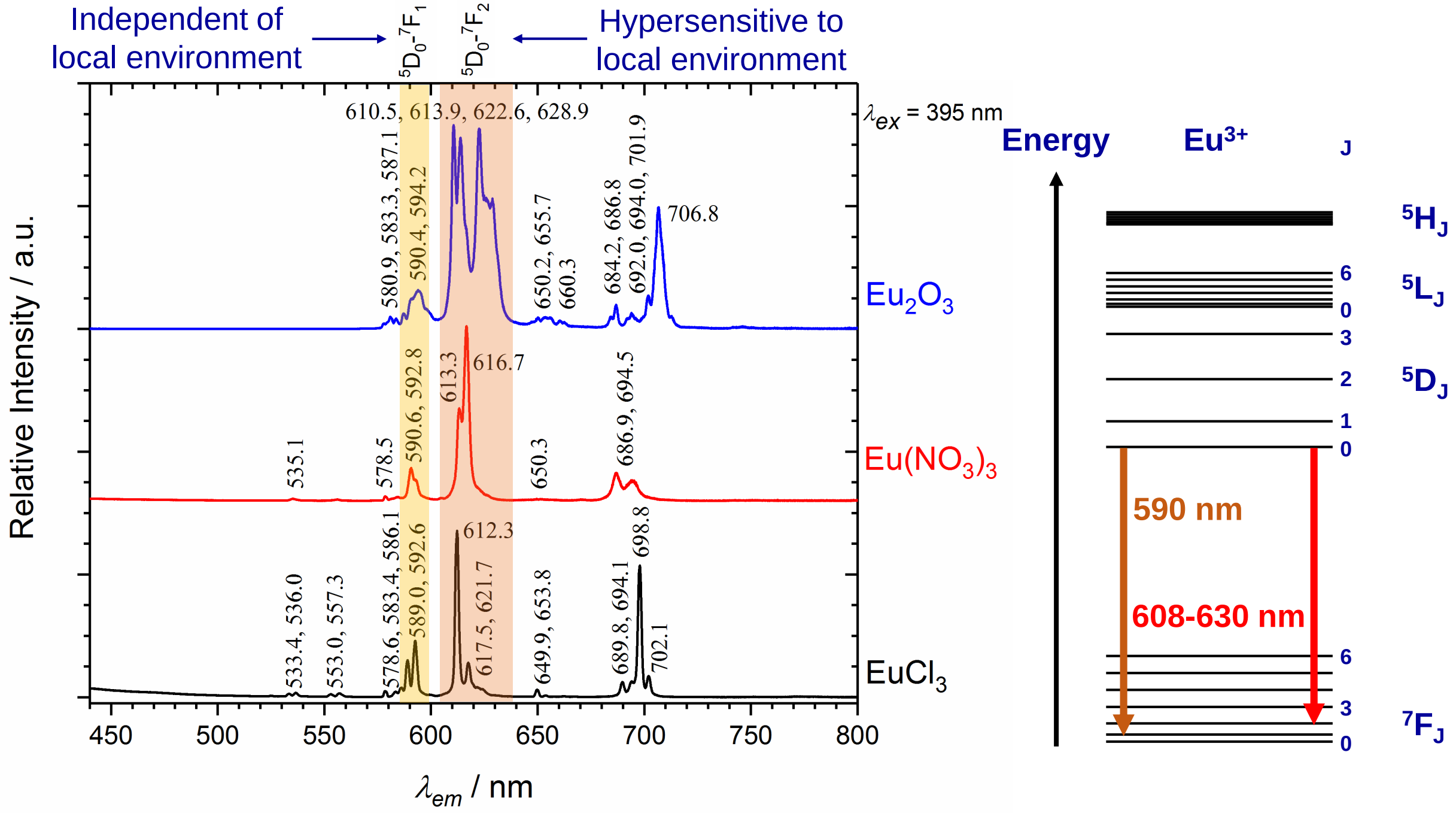
Independent of local environment
$^5D_0$-$^7F_1$
$^5D_0$-$^7F_2$
Hypersensitive to local environment
λ_{ex} = 395 nm
610.5, 613.9, 622.6, 628.9
580.9, 583.3, 587.1
590.4, 594.2
650.2, 655.7
660.3
684.2, 686.8
692.0, 694.0, 701.9
706.8
Eu_2O_3
535.1
578.5
590.6, 592.8
613.3
616.7
650.3
686.9, 694.5
$Eu(NO_3)_3$
533.4, 536.0
553.0, 557.3
578.6, 583.4, 586.1
589.0, 592.6
612.3
617.5, 621.7
649.9, 653.8
689.8, 694.1
698.8
702.1
$EuCl_3$
Relative Intensity / a.u.
450
500
550
600
650
700
750
800
λ_{em} / nm
Energy
Eu^{3+}
J
^5H_J
^5L_J
^5D_J
^7F_J
6
0
3
2
1
0
590 nm
608-630 nm
6
3
0

Hypersensitive $^5D_0 \rightarrow {}^7F_2$ Peak

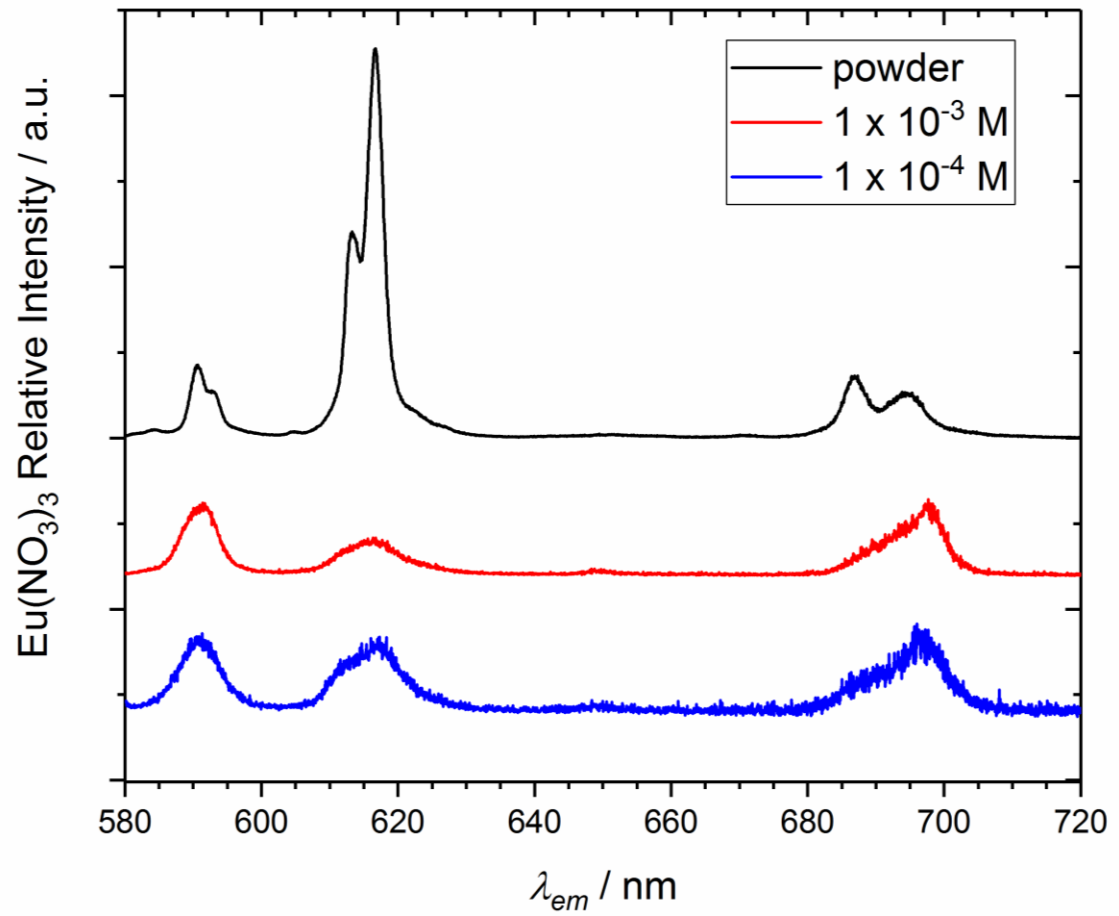

- Changes in the position and intensity of $^5D_0 \rightarrow {}^7F_2$ peak
- $^5D_0 \rightarrow {}^7F_2$: $^5D_0 \rightarrow {}^7F_1$ gives indication of ligand strength
- Fluorescence decay lifetime, τ, and number of H_2O molecules in 1st sphere, $n[H_2O]$,[1-2]

$$n[H_2O] = \frac{1.07 \times 10^{-3}}{\tau[Eu^{3+}]} - 0.62$$

[1] P.P. Barthelemy and G.R. Choppin, *Inorg. Chem.*, 1989, 28, 3354

[2] T. Kimura, *et al.*, *Radiochim. Acta*, 1996, 72, 61

Preliminary Characterisation Results

Raman:
Eu_2O_3, $Eu(NO_3)_3$ and $EuCl_3$

Eu_2O_3 Peaks

Cubic only[1-2]:
337 and 557 cm^{-1}

Monoclinic only[3]:
258, 395, 465 and 580 cm^{-1}

Both phases[1-4]:
110, 175, 285 and 424 cm^{-1}

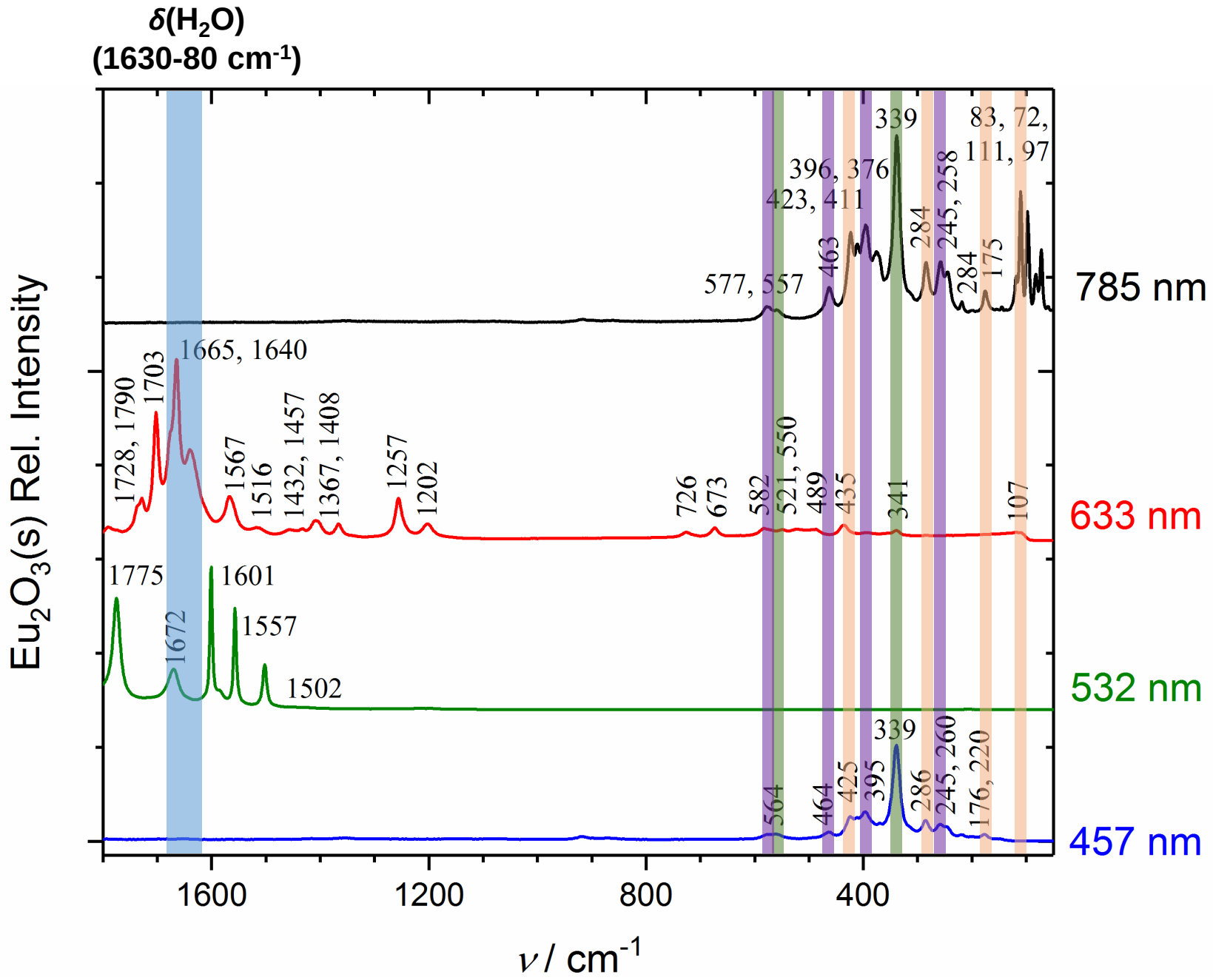

[1] L.A. Tucker, *et al.*, *Appl. Spectrosc.*, 1984, 38, 857
[2] Z.H. Yu, *et al.*, *J. Alloy. Compd.*, 2017, 701, 542
[3] J. Gouteron, *et al.*, *J. Solid State Chem.*, 1981, 38, 288
[4] K.W. Chae, *et al.*, *J. Lumin.*, 2012, 132, 2293

$Eu(NO_3)_3$ Peaks

< 200 cm^{-1} = lattice vibrations

~ 1045 cm^{-1} = $\nu_2(NO_3^-)$ [1]

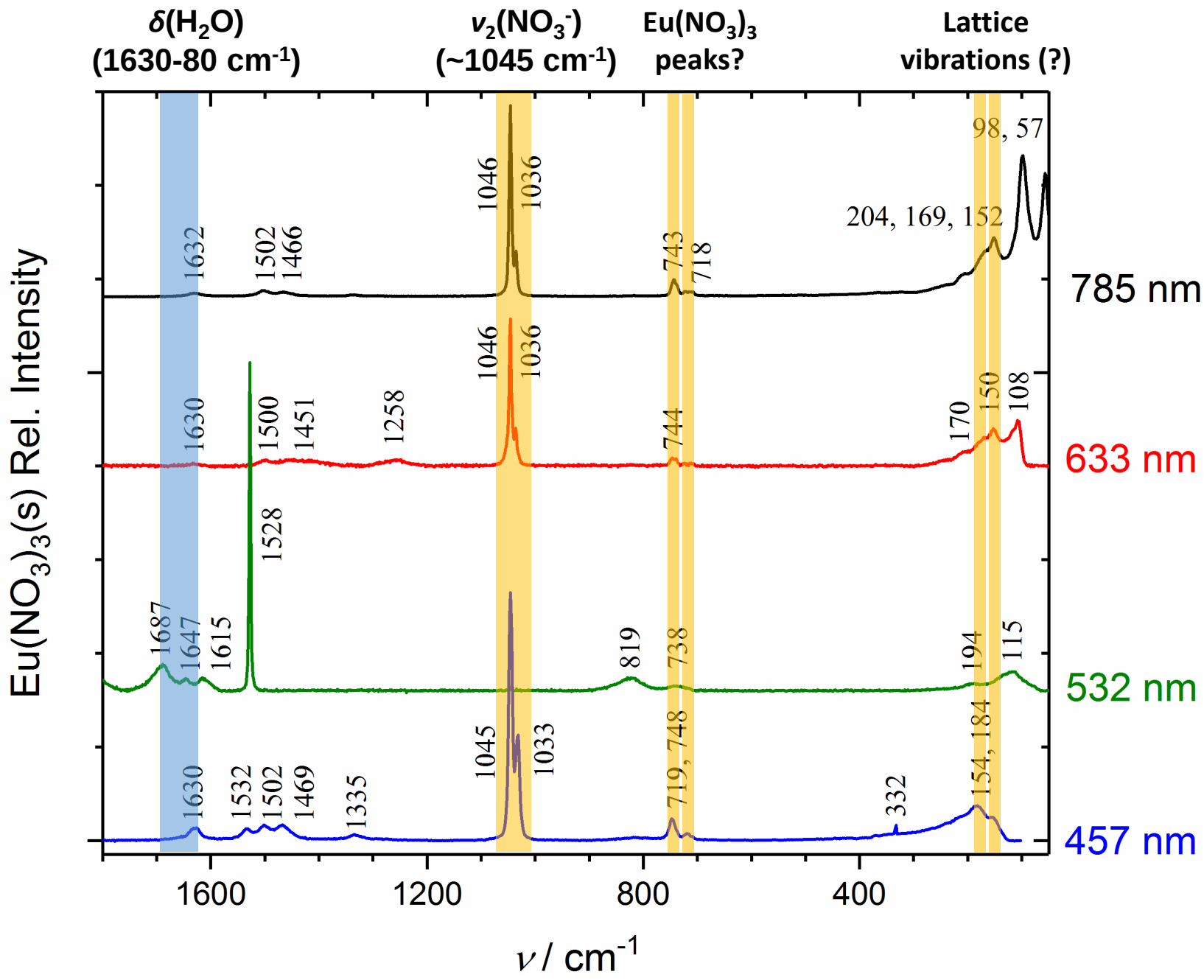

[1] V. Tsaryuk, *et al.*, *Spectrochim. Acta A*, 2005, 61, 185

$EuCl_3$ Peaks

< 200 cm^{-1} = lattice vibrations

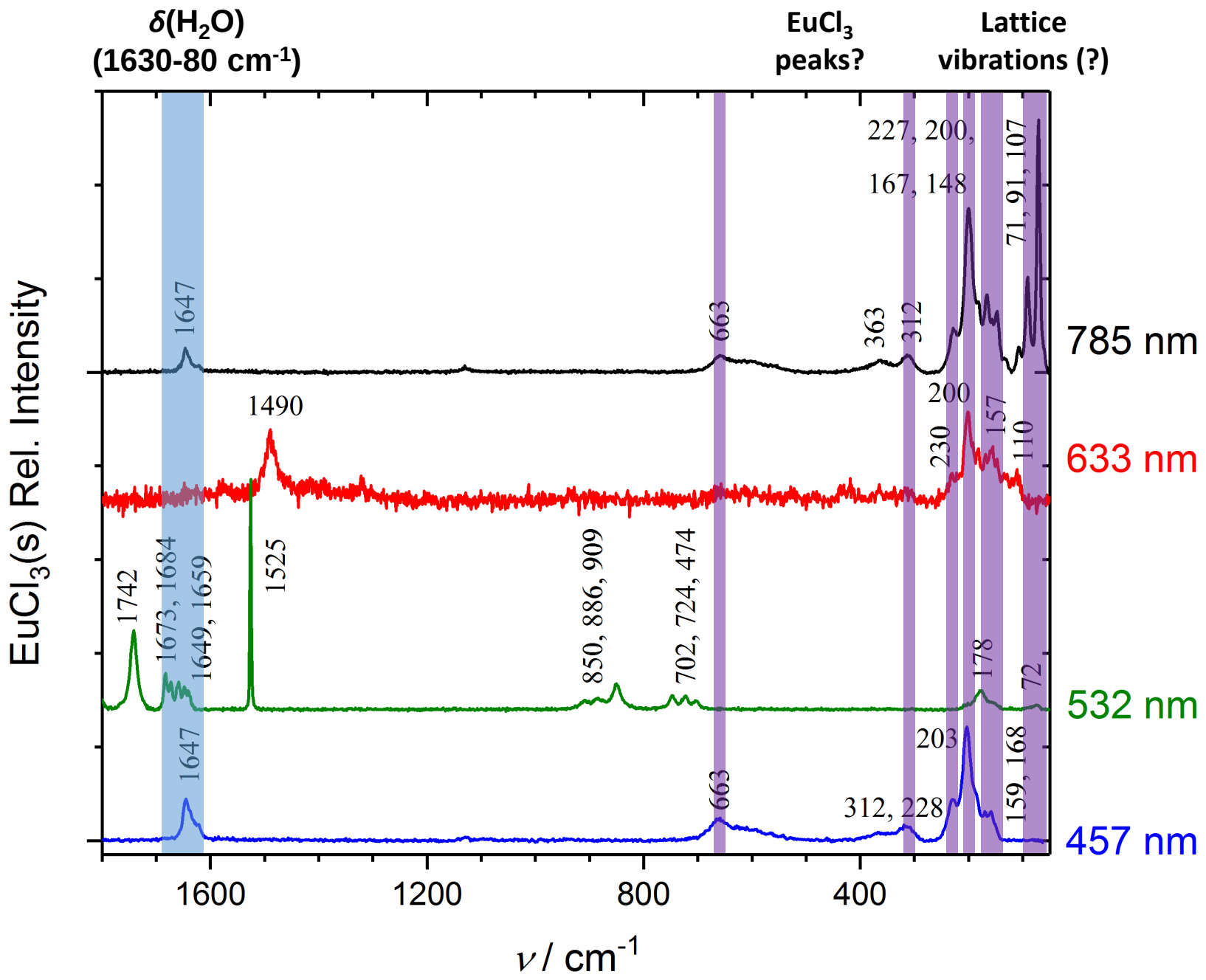

Characterisation Database

For this project and literature results:

- **Fluorescence peak positions**
- **Fluorescence decay lifetimes**
- **Raman features (at which wavelengths)**
- **Resource for project partners and the wider community**

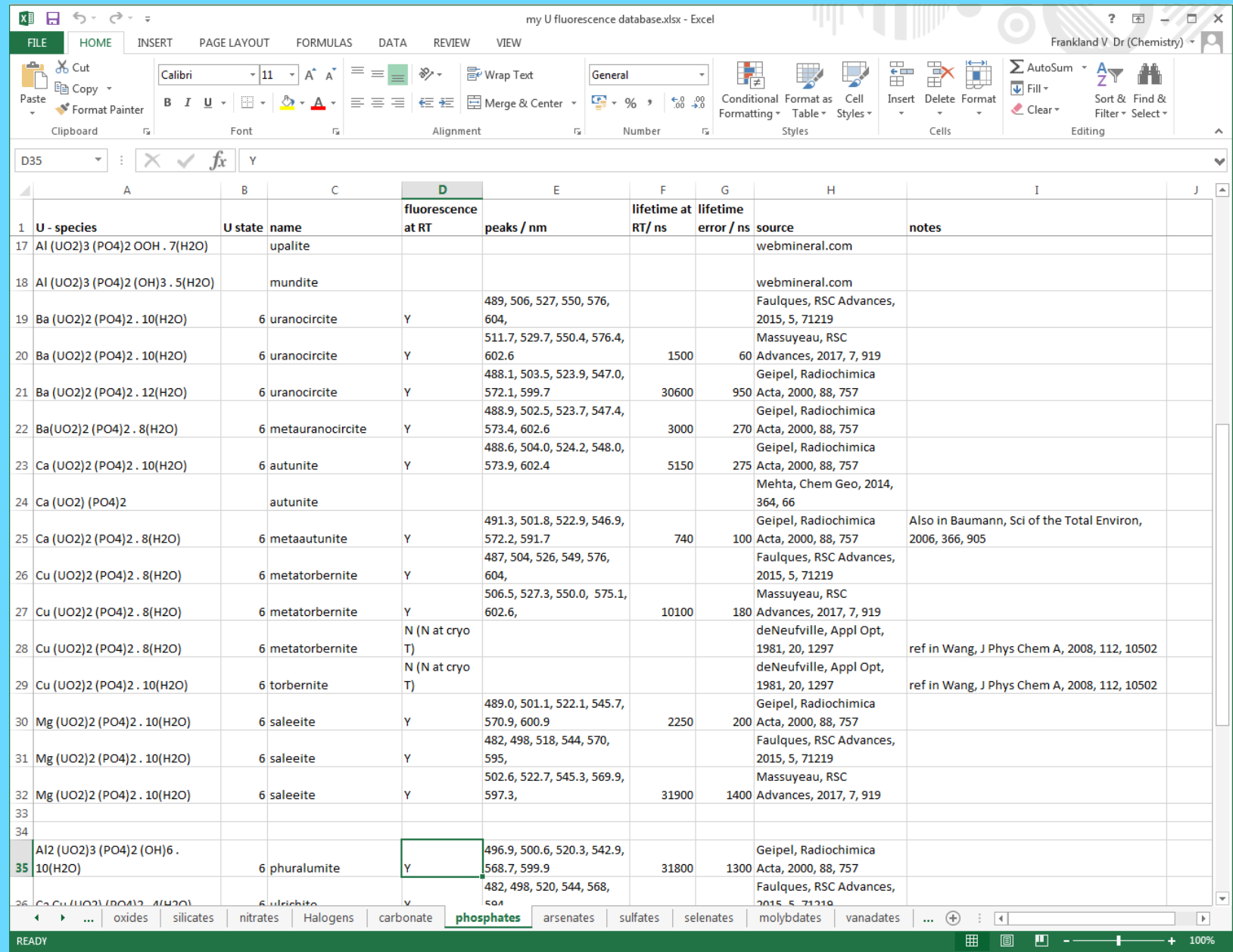

	A	B	C	D	E	F	G	H	I	J
1	U - species	U state	name	fluorescence at RT	peaks / nm	lifetime at RT/ ns	lifetime error / ns	source	notes	
17	Al (UO2)3 (PO4)2 OOH . 7(H2O)		upalite					webmineral.com		
18	Al (UO2)3 (PO4)2 (OH)3 . 5(H2O)		mundite					webmineral.com		
19	Ba (UO2)2 (PO4)2 . 10(H2O)	6	uranocircite	Y	489, 506, 527, 550, 576, 604,			Faulques, RSC Advances, 2015, 5, 71219		
20	Ba (UO2)2 (PO4)2 . 10(H2O)	6	uranocircite	Y	511.7, 529.7, 550.4, 576.4, 602.6	1500	60	Massuyeau, RSC Advances, 2017, 7, 919		
21	Ba (UO2)2 (PO4)2 . 12(H2O)	6	uranocircite	Y	488.1, 503.5, 523.9, 547.0, 572.1, 599.7	30600	950	Geipel, Radiochimica Acta, 2000, 88, 757		
22	Ba(UO2)2 (PO4)2 . 8(H2O)	6	metauranocircite	Y	488.9, 502.5, 523.7, 547.4, 573.4, 602.6	3000	270	Geipel, Radiochimica Acta, 2000, 88, 757		
23	Ca (UO2)2 (PO4)2 . 10(H2O)	6	autunite	Y	488.6, 504.0, 524.2, 548.0, 573.9, 602.4	5150	275	Geipel, Radiochimica Acta, 2000, 88, 757		
24	Ca (UO2) (PO4)2		autunite					Mehta, Chem Geo, 2014, 364, 66		
25	Ca (UO2)2 (PO4)2 . 8(H2O)	6	metaautunite	Y	491.3, 501.8, 522.9, 546.9, 572.2, 591.7	740	100	Geipel, Radiochimica Acta, 2000, 88, 757	Also in Baumann, Sci of the Total Environ, 2006, 366, 905	
26	Cu (UO2)2 (PO4)2 . 8(H2O)	6	metatorbernite	Y	487, 504, 526, 549, 576, 604,			Faulques, RSC Advances, 2015, 5, 71219		
27	Cu (UO2)2 (PO4)2 . 8(H2O)	6	metatorbernite	Y	506.5, 527.3, 550.0, 575.1, 602.6,	10100	180	Massuyeau, RSC Advances, 2017, 7, 919		
28	Cu (UO2)2 (PO4)2 . 8(H2O)	6	metatorbernite	N (N at cryo T)				deNeufville, Appl Opt, 1981, 20, 1297	ref in Wang, J Phys Chem A, 2008, 112, 10502	
29	Cu (UO2)2 (PO4)2 . 10(H2O)	6	torbernite	N (N at cryo T)				deNeufville, Appl Opt, 1981, 20, 1297	ref in Wang, J Phys Chem A, 2008, 112, 10502	
30	Mg (UO2)2 (PO4)2 . 10(H2O)	6	saleeite	Y	489.0, 501.1, 522.1, 545.7, 570.9, 600.9	2250	200	Geipel, Radiochimica Acta, 2000, 88, 757		
31	Mg (UO2)2 (PO4)2 . 10(H2O)	6	saleeite	Y	482, 498, 518, 544, 570, 595,			Faulques, RSC Advances, 2015, 5, 71219		
32	Mg (UO2)2 (PO4)2 . 10(H2O)	6	saleeite	Y	502.6, 522.7, 545.3, 569.9, 597.3,	31900	1400	Massuyeau, RSC Advances, 2017, 7, 919		
33										
34										
35	Al2 (UO2)3 (PO4)2 (OH)6 . 10(H2O)	6	phuralumite	Y	496.9, 500.6, 520.3, 542.9, 568.7, 599.9	31800	1300	Geipel, Radiochimica Acta, 2000, 88, 757		
36	Ca Cu (UO2) (PO4)2 . 4(H2O)	6	ulrichite	Y	482, 498, 520, 544, 568, 594			Faulques, RSC Advances, 2015, 5, 71219		

Future Work

- TRLFS and Raman spectroscopy characterisation of uranium-bearing minerals
  - Samples from: - British Geological Survey Reference Collection
    - Natural History Museum collection - tbc
- XRD characterisation to confirm phase pure
- TRLFS and Raman spectroscopy characterisation of uranium-bearing solutions

Acknowledgements

Prof David Read, Dr Carol Crean, Dr Rachida Bance-Soualhi and Emily Rastrick

Thank you all for listening